REPORT DOCUMENTATION PAGE

Form Approved
OMB No. 0704-0188

1. AGENCY USE ONLY *(Leave blank)*	2. REPORT DATE	3. REPORT TYPE AND DATES COVERED
	19 Aug 00	Final Report, 1 Jan 98 - 31 May 00

4. TITLE AND SUBTITLE

A Knowledge-Based Diagnosis and Treatment Display Unit

5. FUNDING NUMBERS

DAAG55-98-C-0002

6. AUTHOR(S)

Frank T. Djuth[1], John H. Elder[1], Paula M. Johnston[2],
Paul P. Woodward[2], Jackie A. Hahn[2]

7. PERFORMING ORGANIZATION NAME(S) AND ADDRESS(ES)

[1] Geospace Research, Inc.
550 N. Continental Boulevard, Suite 110, El Segundo, CA 90245
[2] Loma Linda University Medical Center
11234 Anderson Street, Loma Linda, CA 92354

8. PERFORMING ORGANIZATION REPORT NUMBER

GRI-ST-00-7430

9. SPONSORING/MONITORING AGENCY NAME(S) AND ADDRESS(ES)

U.S. Army Research Office
P. O. Box 12211
Research Triangle Park, NC 27709-2211

10. SPONSORING/MONITORING AGENCY REPORT NUMBER

11. SUPPLEMENTARY NOTES

The views, opinions and/or findings contained in this report are those of the author(s) and should not be construed as an official Department of the Army position, policy or decision, unless so designated by other documentation.

12a. DISTRIBUTION/AVAILABILITY STATEMENT

Approved for public release; distribution unlimited.

12b. DISTRIBUTION CODE

13. ABSTRACT *(Maximum 200 words)*

The objective of this project was to develop a high-performance diagnostic and treatment display unit that is optimized for a user equivalent to a physician's assistant. A key aspect of the system is the decision-making software which monitors the patient's physiological status and anticipates downturns in medical condition. Data from physiological sensors are combined with a knowledge base that includes treatments for penetrating and blunt trauma. The unit is optimized to monitor trauma victims that are not in need of immediate surgery at a Battalion Aid Station. This makes it possible to provide significantly improved medical care to wounded soldiers while reducing the number of attending medical personnel. The primary application in civilian medical care is in intensive care units. Here, patients are often hemodynamically stable but not hemodynamically normal.

The diagnosis and treatment display software runs on a laptop computer and is linked to medical sensors via serial and PCMCIA ports. A variety of real-time displays are available during the patient monitoring period. These include displays of patient status, parsed and processed sensor data, and fully analyzed sensor values and trends. Sensor data are automatically checked by the analysis algorithm for validity, and commonly occurring artifacts are identified and eliminated.

14. SUBJECT TERMS

Knowledge-Based System, Trauma, Medical Treatment, STTR Report, Medical Diagnosis, Gunshot Wounds, Combat Casualty

15. NUMBER OF PAGES

103

16. PRICE CODE

17. SECURITY CLASSIFICATION OF REPORT	18. SECURITY CLASSIFICATION OF THIS PAGE	19. SECURITY CLASSIFICATION OF ABSTRACT	20. LIMITATION OF ABSTRACT
Unclassified	Unclassified	Unclassified	UL

Report Date: August 19, 2000 GRI-ST-00-7430

FINAL REPORT

CONTRACT NO. DAAG55-98-C-0002

Report Period: January 1, 1998 through May 31, 2000

A KNOWLEDGE-BASED DIAGNOSIS AND TREATMENT DISPLAY UNIT

Submitted by

Dr. Frank T. Djuth

Geospace Research, Inc.
550 N. Continental Blvd., Suite 110
El Segundo, CA 90245

Voice: (310) 322-1160
FAX: (310) 322-2596
E mail: Djuth@ix.netcom.com

Prepared for

U.S. Army Research Office
Attention: AMXRO-ICA (Sylvia Hall)
4300 South Miami Boulevard
P. O. Box 12211
Research Triangle Park, NC 27709-2211

TABLE OF CONTENTS

1. Introduction

The project was undertaken at a time when the trauma needs of the Army were rapidly evolving and the Army's combat casualty care program was undergoing reorganization. A general program meeting was held at the Institute of Surgical Research (ISR), Brooke Army Medical Center (BAMC), San Antonio, Texas on May 5, 1998. The meeting at the ISR was attended by approximately 12 representatives of various elements of the Army's medical program along with members of the small business technology transfer (STTR) project team (Frank T. Djuth, principal investigator, Geospace Research, Inc., and Paula Johnston, Director of Adult Trauma Support Services, Loma Linda University Medical Center). The Army participants included Colonel Cleon Goodwin (director of the ISR, BAMC) and Colonels Vandre, Gouge, Jaffin, and Zolock. Major Omar Hottenstein (MCMR), Lieutenant Colonel John Holcomb (Chief, MTR, ISR), Major Flaherty (Chief of Trauma Surgery, BAMC), and Major Frank De Lorenzo (emergency physician, Center for Health Education Studies) were also present.

A general consensus among many of the meeting participants appeared to emerge concerning diagnostic sensors for future Army medical support. It was agreed that the most important diagnostic sensors are: 1) a pulse oximeter, 2) a non-invasive lactate sensor, 3) a non-invasive intracranial pressure (ICP) sensor, and 4) a "bio-threat" sensor. Of the four sensors suggested, only the pulse oximeter is FDA-approved and in commercial production. Non-invasive (or minimally invasive) lactate sensors, non-invasive ICP sensors, and bio-threat sensors are in various stages of development. None of these sensors are currently available for test purposes or otherwise. Other FDA-approved sensors discussed below were added to the STTR project diagnostics to improve the monitoring of trauma victims.

With increasing time, the Army's combat casualty care began to focus on the resuscitation of combat casualties in hypovolemic shock. The aim is to determine when it is necessary for a medic on the battlefield to resuscitate a trauma victim, how the effectiveness of the resuscitation effort can be measured, and what is the desired end point of resuscitation. This entails the evaluation of available resuscitative fluid, investigations to improve resuscitative therapies, and investigations of novel markers indicating the need to resuscitate.

After extensive discussions with personnel at Army's Medical Research Materials Command (MRMC) as well as members of several Army medical laboratories, medical

institutes, and research organizations, it was concluded that the current diagnosis and treatment display unit should be initially developed for a battalion aid station. In the future, adjustments could be made to make the unit compatible with resuscitative strategies in more forward positions.

1.1 Knowledge-Based Systems and Trauma Care

The knowledge-based system that has been developed provides important decision-making support currently unavailable at the Battalion Aid Station or in an intensive care unit for trauma victims. Data from several physiological sensors can be combined with a knowledge-based system to greatly enhance the oversight of a patient. In essence, the system serves as a computerized trauma support team. The system monitors commonly occurring trauma conditions, pays particular attention to the classification of acute hemorrhagic shock, and incorporates an early detection algorithm for rapid downturns in patient status. The utility of the knowledge-based diagnosis and treatment unit is very great in situations where the number of trauma cases overwhelm the medical delivery system. The computerized unit facilitates the triage process subsequent to a major natural disaster (e.g., a large earthquake) or in the event of mass casualties on the battlefield.

In general, gunshot wounds (GSWs) represent the most prevalent source of serious penetrating trauma in the civilian arena. Handguns, shotguns, rifles, and, to a lesser extent, knives account for the majority of penetrating and perforating wounds. In military combat, penetrating and perforating wounds make up the majority of battlefield wounds. Most are produced by metal fragments from explosive devices such as aerial bombs, artillery and mortar shells, and mines. In modern mechanized warfare, only 15-20% of such wounds result from rifle and machine gun fire [*Wiener and Barrett*, 1986]. Although the civilian mix of penetrating trauma is not identical to that of military combat, the pathophysiology was similar enough to justify the use of GSWs in the Phase II study.

The current work addresses the Army's medical needs at the Battalion Aid Station, that is, in Echelon 2 of the Army's medical treatment and transport areas. Figure 1 illustrates the Army's four areas of treatment for casualties [*F. J. Pearce*, private communication, 1999]. The forward area (Echelon 1) involves on-the-spot treatment of casualties by medics. Casualties are subsequently transported to Echelon 2 for further treatment. Individuals who have sustained severe trauma undergo surgery on and are later transported with the Life Support for Trauma and

Medical Treatment and Transport Areas

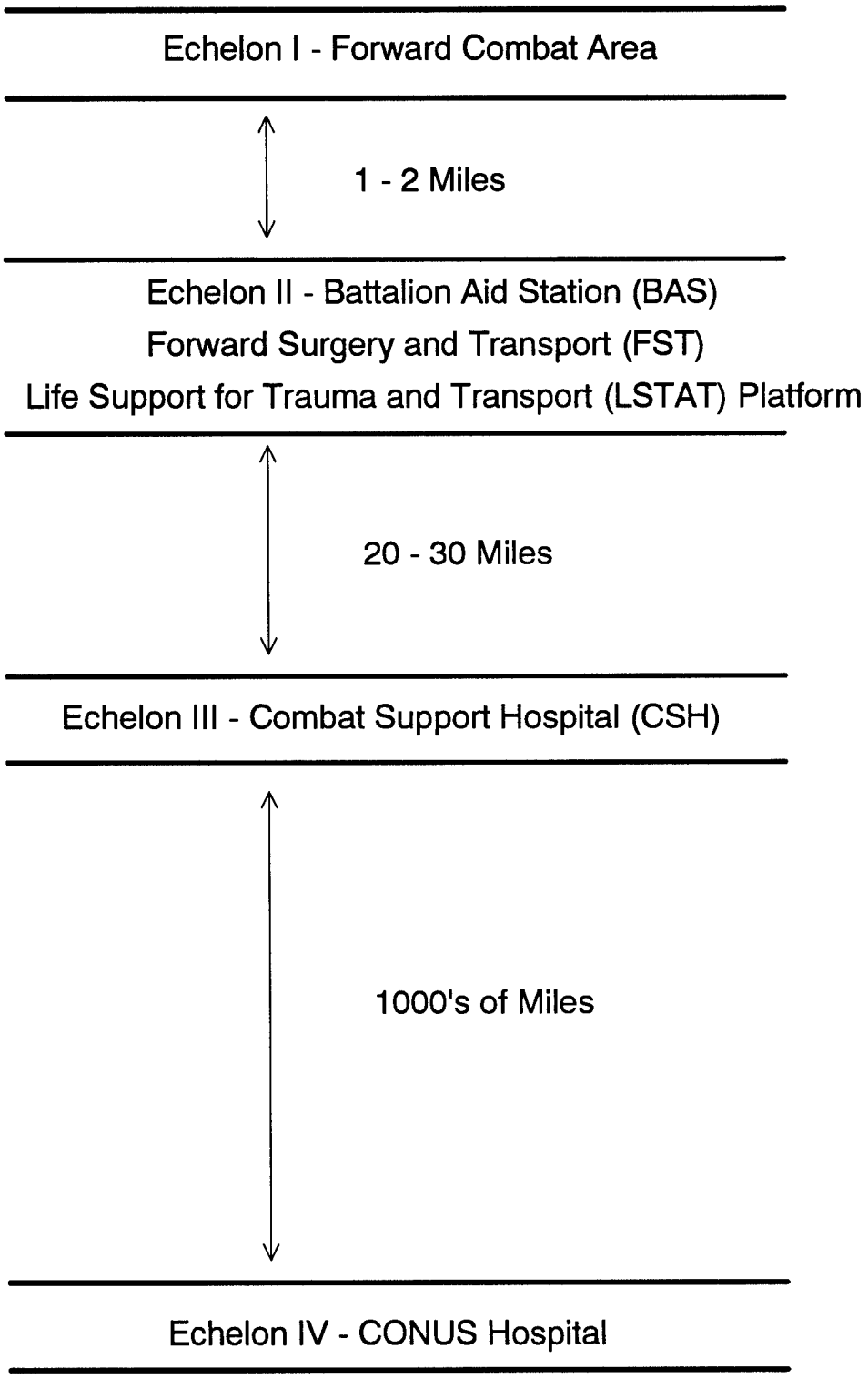

Figure 1

Transport (LSTAT) platform [e.g., *Pearce et al.*, 1998]. The Phase II diagnosis and treatment display unit satisfies the requirement for oversight of triaged patients who do not require immediate surgery in the forward area. This is approximately 80% of the trauma victims in Echelon 2. By definition, the unit includes knowledge-based software with decision-making capability. In general, the individuals to be monitored are in shock states 0 (no shock), 1, or marginally 2. The objective of the knowledge-based system is to record and monitor the physiological sensor data of these patients and use it in conjunction with other observational data to anticipate potential downturns in patient status. When this is the case, the system sounds an alarm so that a physician's assistant (PA), or equivalent, can reassess the victims need for surgical intervention and/or more intensive care in the forward area. Typically, the knowledge-based system will provide oversight of a trauma victim for 5 hours or longer depending on the logistics of patient transport to Echelon 3.

Overall, the knowledge-based system described below provides important decision-making support currently unavailable for on-the-spot trauma care. Data from several physiological sensors are combined with a knowledge-based system to greatly enhance the emergency treatment of trauma victims. In essence, the system serves as a computerized trauma support team.

The primary application in civilian medical care centers is in intensive care units (ICUs). Here, patients are often hemodynamically stable but not hemodynamically normal. It is therefore not surprising that data were gathered for knowledge-based system simulations in the trauma ICU at Loma Linda University Medical Center (LLUMC). As in the case of the Battalion Aid Station, the unit serves as a constant intelligent monitor of the patient status; it constantly watches the patient when trained medical personnel are absent. Many of the protocols for the knowledge-based software originate in the Advanced Trauma Life Support Manual issued by the Committee on Trauma, American College of Surgeons.

In general, the mechanism and details of the injury are distinct in the two trauma environments. In part, this arises because of the higher average speed of projectiles in the military environment. However, the distribution of injuries by anatomic site is comparable for civilian and Army trauma. For example, in a battlefield/wartime situation (e.g., Korea, Vietnam, Northern Ireland), the distribution of severe trauma by anatomic site tends to follow the ordering: limbs (most common), head and neck, chest and abdomen (least common) [e.g., *Wiener and*

Barrett, 1986]. In the civilian sector, the ordering is similar. However, other important differences exist. For example, knowledge of the patient's prior medical history can be programmed in advance in a Personal Information Carrier (PIC) for most military applications, whereas such information is much more limited in the civilian arena. The medical history data available to a hospital is usually restricted to information on Medic Alert I.D. emblems. In general, the Army is more likely to require shorter term trauma support in Echelon 2 (~5 hours) than in a civilian ICU. In the latter case, the monitoring typically goes on for days.

1.2 Project Overview

The objective of the study was to add "intelligence" to the processing and display of trauma sensor data streams. This entails the acquisition of "raw voltage data" from medical sensors as well as the reading of preprocessed sensor measurements across serial data lines. Additional observational data (e.g. pupil/verbal/motor responses used to develop the Glascow Coma Scale (GCS) score) are fused with the sensor data in an effort to provide an accurate representation of the patient's pathophysiology. The data are subsequently analyzed in real-time to determine the trends of sensor values over three distinct time scales and to assign confidence intervals to the results. The analyzed results are then examined by decision-making software which takes into account the diagnosis, analyzed sensor results, and other medical inputs to provide early warning of an impending downturn in patient status. Warnings are also generated when the sensor trends do not match those expected for a particular diagnosis.

The system architecture outlined above has five main elements. These are the physiologic sensors, the non-sensor data interface (i.e. observational data), a data acquisition and processing module (DAPM), a real-time analysis module (RTAM), and a decision-making module (DMM). The latter three programs run in parallel. Three Graphical User Interfaces (GUIs) are provided for the input of observational data, for the display of the real-time sensor data and processed results, and for messages and alarms issued by the knowledge-based program.

2. Medical Sensors and Trauma

To satisfy the Army's needs, trauma sensors used by the diagnosis and treatment display unit had to be either non-invasive or minimally invasive. In part, the current research program was limited by the FDA-approved trauma sensors available for developing patient data bases. Such data were necessary for the testing of the diagnostic and display unit software. Data were

secured from trauma patients by personnel at LLUMC, and sensors were limited to those approved by the LLUMC Institution Review Board (IRB). Advance informed consent was obtained from all trauma patients consistent with Title 10 U.S.C. 980. Data acquisition, processing, and storage of the patient data were accomplished with the aid of a laptop computer system programmed by Geospace Research, Inc. (GRI). A single element of the final software system (DAPM) was used for this purpose. This program helped guide the treatment of patients in the LLUMC ICU by making the temporal histories of all medical sensors available to medical personnel in a single unified graphical display.

2.1 Sensors Used in the Current Project

Noninvasive sensors integrated into the Colin Pilot 9200 medical suite were used along with a supplementary (invasive) arterial line blood pressure monitor. The Colin Pilot provides continuous non-invasive blood pressure (arterial tonometer calibrated with a cuff), pulse oximetry (SpO_2), end-tidal CO_2 ($EtCO_2$) via the side stream method, core body temperature, and 3 or 5 lead electrocardiograms (ECGs) as required. Two serial lines connect the Colin Pilot to the computer unit. Serial line #1 is used for weighted average values of all sensor outputs (including the tonometer) as they appear on the real-time display of the Colin Pilot. The temporal resolution of this data is two seconds. Serial line #2 provides the beat-to-beat systolic and diastolic blood pressures and pulse rate measured with the tonometer with no weighting. The tonometer pulse waveform is available as an analog output on the Colin Pilot, but it is typically not sampled. The temporal resolution of the tonometer data on line #2 is equal to the pulse rate.

Invasive arterial blood pressure and the pulse waveform are measured with an HP M1006B pressure module. The analog output of this unit contains the pulse waveform. This signal is digitized at a rate of 300 Hz with 12-bit precision and stored in a data file. In addition, the systolic and diastolic blood pressures are calculated periodically in real-time (once every two seconds). Pulse-to-pulse blood pressure measurements are obtained after the fact as part of the analysis of the A-line data. Within the context of the current sensor data acquisition system, beat-to-beat blood pressure calculations in software require too much of the computer's resources. Typically, such real-time calculations are performed in firmware within the medical instrument.

The DAPM acquires, stores, sorts, and screens data sent by the Colin Pilot across serial lines #1 and #2. This portion of the software was written in National Instruments' LabVIEW programming language. Data screening is necessary because two errors exist in the firmware used to send information to the serial ports. These errors were encountered by Geospace Research, Inc. during the course of its testing of DAPM. One firmware error exists on each of the two serial lines. It is unlikely that Colin will correct this problem until a new Pilot model is put into production, and this will probably not occur for at least two years. The Colin Pilot firmware errors were mitigated with the aid of a parser routine. As noted above, there are two types of data: the two-second weighted data, and the beat-to-beat tonometer blood pressure readings. All sensor data are stored for later processing at the maximum temporal resolution available with the measuring instrumentation. In addition, all sensor data, including redundant sensor measurements, are displayed in real-time. The DMM uses only one sensor for a given measured quantity and has certain default priorities for the selection of redundant sensor measurements. For example, the pulse rate is available from unweighted tonometer data (serial line #2), from the weighted-average tonometer data (serial line #1), from the pulse oximeter, and from the ECG when used. The order of selection in this case is: pulse oximeter, ECG, serial line #1, and serial line #2. A similar situation occurs with systolic and diastolic blood pressures, which are obtained from the weighted-average tonometer data, the unweighted tonometer data, and the invasive arterial line data. In this case, the selection priority is serial line #1, serial line #2, and arterial line.

2.2 Emergence of New Trauma Sensors

The system architecture allows new sensors to be added as they become available. A list of present and emerging trauma sensors is presented in Table 1. By far, the best combination of sensors for hemorrhagic shock and airway obstruction is tissue serum lactate (and/or tissue P_{CO_2}) and end-tidal P_{CO_2}. Because of the much wider range of pressures that develop with CO_2, the sensitivity of CO_2 measurements of ischemia tends to be much greater than that obtained with O_2 techniques. Thus, tissue P_{CO_2} measurements provide important input for triage decisions and serve as a precise indicator of the success of resuscitation efforts. The simultaneous monitoring of tissue P_{CO_2} and end-tidal P_{CO_2} allows airway obstructions and early states of shock to be readily identified.

Table 1. Present and Future Trauma Sensors for a Battalion Aid Station

Non-Invasive Sensor	Sensor Developer/ Manufacturer	Sensor Status	Measured Quantities	Trauma Examples	Effective Range of Measured Quantities
Tissue P_{CO_2}	Walter Reed Army Institute of Research/USC School of Medicine/others Institute of Critical Care Medicine, Palm Springs, CA/Optical Sensors, Inc.	Under development or in prototype form First units commercially available in March 2000	Transcutaneous measurement of P_{CO_2} tension Mucosal fluid P_{CO_2}	Hemorrhagic shock Airway obstruction	Large increase (20-150 mm Hg) Moderate increase (up to 80-90 mm Hg)
Lactate	Under study by the Army	Currently unavailable	Tissue serum lactate		
End-Tidal P_{CO_2} (lightweight mask)	HP, SIMS BCI, Novametrix, many others	Commercially available	Expired P_{CO_2}	Hemorrhagic shock Airway obstruction	Decrease (0 - 100 mm Hg) Decrease (0 - 100 mm Hg)
Sensor Combination Tissue P_{CO_2} with End-Tidal P_{CO_2}	Listed above	Listed above	End-Tidal P_{CO_2} minus Tissue P_{CO_2}	Hemorrhagic shock Airway obstruction	Strongly negative Moderately negative
Pulse Oximeter	Nellcor, HP, Criticare, Novametrix, Ohmeda, many others	Commercially available	$\%SaO_2$	Hemorrhagic shock Airway obstruction	Erratic measurements for high shock states 80-100%
Noninvasive ICP (absolute intracranial pressure)	A direct and reliable sensor is not available.	Currently unavailable			
Beat-to-Beat Blood Pressure/Pulse Rate **BP and Pulse Rate with a Standard Cuff**	Colin Medical Instruments HP, Colin, Nellcor, Omron, Nellcor, many others	Commercially available Commercially available	Beat-to-beat BP - arterial tonometry BP with oscillometric technique	Hemorrhagic shock Airway obstruction	Decreasing BP, Increasing pulse Incr. then Decr. BP, Incr. then Decr. pulse
Bio-Threat Sensors	Under development at Oak Ridge National Laboratory	Currently unavailable			

2.2.1 Minimally Invasive Lactate Sensors

At present there are no known research programs aimed at developing a non-invasive lactate sensor. However, a minimally invasive sensor is under development [*J. B. Holcomb*, private communication, 1999]. The lactate sensor and several other minimally invasive sensors are expected to emerge from MicroFluidic Molecular Systems (MicroFlumes) research. MicroFlumes make it possible to continuously sample and test subcutaneous body fluids *in vivo*. This is done with the aid of extremely small (~100 μm) sensor/control submodules. MicroFlumes have computer chip-scale fluid handling capability and are intended to replace macroscale fluidic components such as pumps, valves, reservoirs, and tubing. All aspects of microfluidics are automated. This includes sample acquisition and preparation, analysis/detection, and digital data input and output. A lactate MicroFlumes sensor could readily be incorporated into the knowledge-based system discussed herein.

2.2.2 Non-invasive P_{CO_2} Sensors

Extensive studies have been conducted in the past concerning the diagnostic benefits of P_{CO_2}. End-tidal P_{CO_2} has been examined as a measure of cardiac output, and therefore pulmonary blood flow, during cardiopulmonary resuscitation [e.g., *Weil et al.*, 1985; *Trevino et al.*, 1985]. Under conditions of constant ventilation, end-tidal P_{CO_2} reflects the status of the circulatory system [e.g., *Gudipati et al.*, 1988; *Falk et al.*, 1988]. When cardiac output is critically reduced, end-tidal P_{CO_2} is linearly correlated with pulmonary blood flow. In addition, it serves as a good predictor for successful resuscitation, particularly in regard to resuscitation by extracorporeal circulation [*von Planta et al.*, 1989; *Gazmuri et al.*, 1991]. A similar relationship holds in the case of hemorrhagic shock [e.g., *Nakagawa, et al.*, 1998]. In general, end-tidal P_{CO_2} is an effective diagnostic for pulmonary blood flow when cardiac output is low. However, it is also responsive to changes in ventilation.

As noted by *Johnson and Weil* [1991], shock and ischemia have been traditionally viewed as a simple deficit of oxygen supply alone. However, profound increases in venous and tissue P_{CO_2} values are quantitatively related to the severity of perfusion failure. Thus, hypovolemic shock involves a circulatory failure with the dual defects of an oxygen deficit and a carbon dioxide excess. Because of the loss of oxygenated blood, the metabolism of carbohydrates and the formation of adenosine triphosphate is severely restricted. By far, the most important means

by which energy is released from a glucose molecule is glycolysis. The end products of glycolysis are mainly oxidized to provide energy. Glycolysis refers to the splitting of a glucose molecule to form two molecules of pyruvic acid. This takes place in ten successive steps of chemical reactions. The net reaction per molecule is:

$$\text{Glucose} + 2\text{ADP} + 2\text{PO}_4^{---} \rightarrow 2\ \text{Pyruvic acid} + 2\text{ATP} + 4\text{H}$$

Ordinarily the pyruvic acid is processed through the Krebs cycle (an intermediate metabolic process). However, this is curtailed by the absence of an adequate oxygen supply, and the production of adenosine 5′-triphosphate (ATP) is commensurately reduced. Because pyruvate is no longer cleared by the Krebs cycle, anaerobic glycolysis accelerates leading to the production and accumulation of lactic acid. In this situation, a major portion of the pyruvic acid generated during glycolysis is converted into lactic acid, which quickly diffuses out of cells involved in metabolic processes. Lactic acid enters extracellular fluids and intracellular fluids of other less active cells as well as the blood. Thus, measurements of anaerobically generated lactic acid provide an excellent basis for characterizing hypovolemic shock. However, the shortcoming of this approach lies in the long lactate time constant for clearing after a rapid restoration of effective circulation. As a result, some researchers believe that venous hypercarbia detected with a CO_2 sensor is clinically a more useful predictor of shock state. This is because hypercarbia exhibits a rapid reversal within 1-2 min of circulation restoration whereas lactic acidosis requires ~4 hours or more [see e.g., *Johnson and Weil.*, 1991]. In general, both lactate production and tissue hypercarbia are associated with a low blood flow state [*Desai et al.*, 1995].

Over the past five years, invasive measurements of gastric wall P_{CO_2} have emerged as an option for estimating gastrointestinal ischemia during circulatory shock [*Desai et al.*, 1993; *Tang et al.*, 1994]. However, adverse effects such as nosocomial pneumonia prompted other approaches. *Sato et al.* [1997] show that a non-invasive esophageal sensor can be used to monitor perfusion failure during hemorrhagic shock. Measurements are made with an ion-sensitive field-effect transistor (ISFET) P_{CO_2} sensor. Initial trials in pigs demonstrated that there were significant increases in esophageal wall P_{CO_2} during hemorrhagic shock. The more decisive study of *Sato et al.* [1997] reveals that shock-related increases in esophageal P_{CO_2} were as great as those in the gastric wall. Thus, increases in tissue P_{CO_2} and decreases in blood flow were approximately the same in the stomach and the esophagus. Subsequently, a hypothesis was

put forth that hypercarbia, being a universal phenomenon associated with critically reduced tissue perfusion, would also involve the very proximal gastrointestinal tract, namely the sublingual mucosa. Preliminary trials showed that measurements of P_{CO_2} under the tongue provide a quantitative indicator of the severity of circulatory shock in a manner very similar to that of gastric and esophageal P_{CO_2}. The decisive investigation of *Nakagawa et al.* [1998] focused on systemic comparisons of sublingual P_{CO_2} with gastric P_{CO_2} and hemodynamic and metabolic indicators for the severity and prognosis of shock state. This included direct measurements of sublingual P_{CO_2}, end-tidal P_{CO_2}, mean aortic pressure, cardiac index, gastric P_{CO_2}, and arterial lactate. A close correlation between sublingual P_{CO_2} and gastric P_{CO_2} was demonstrated. In addition, increases in sublingual P_{CO_2} compared favorably with those of arterial lactate. However, it is noteworthy that sublingual P_{CO_2} exhibited a significantly shorter response time following resuscitation than arterial lactate. The short time constant is of significant benefit in determining the effectiveness of therapy. The study showed that sublingual P_{CO_2} was extremely useful for triage, diagnosis, and estimation of the severity of hemorrhagic shock. The strength of the sublingual P_{CO_2} sensor is that it provides a simple, noninvasive, real-time monitor of shock state.

In a recent clinical study involving five normal human volunteers and 46 patients with acute life-threatening illnesses or injuries, sublingual P_{CO_2} proved to be a good estimator of severity of circulatory shock state [*Weil et al.*, 1998]. It was found that when sublingual P_{CO_2} exceeded a well-defined threshold of 70 mm Hg, its positive predictive value for the presence of physical signs of circulatory shock was 1.00. When it was less than 70 mm Hg, it predicted survival with a predictive value of 0.93. A majority of patients in whom sublingual P_{CO_2} exceeded 70 mm Hg on admission, died in the hospital. Overall, this investigation illustrates the feasibility of using sublingual P_{CO_2} to diagnose hemorrhagic shock, make reasonable decisions regarding triage, and monitor the response of the patient to a treatment regimen in real-time.

3. Trauma Conditions Addressed in the Current Study

In the prototype system that was developed for this program, the medical conditions tracked by the knowledge-based software are limited to the following: hypovolemic shock, neurogenic shock, hemo-pneumothorax, respiratory failure, cardiac tamponade, head injury, and Acute Respiratory Distress Syndrome (ARDS). Additional injuries and syndromes can be

readily added to the software package in the future. The pathophysiology of each of the trauma conditions addressed by the current project is described below.

3.1 Shock

At the cellular physiology level, shock is the clinical manifestation of cellular disorganization. The cell maintains order through biosynthesis of high energy compounds, which are used to make cell components and allow the cell to function efficiently. Most human cells have a delicate thermodynamic economy; any perturbation in delivery of substrates, or removal of cellular waste products quickly produces chemical and physical disequilibrium. From this perspective, shock is the condition produced by the inability of the circulatory system to adequately nourish tissues or remove toxic metabolites.

During shock, virtually any index of biosynthesis: metabolism, ion homeostasis, structure, or electrical or mechanical function is altered. The cellular response to shock can be dynamic and complex. For example, one can selectively consider the effect of hypoperfusion on cardiac muscle pH and interactions with Ca^{++} homeostasis. With severe hypoperfusion, cellular adenosine triphosphate (ATP) is depleted, thus weakening contractile force. Hypoxia also generates lactate and H^+, the latter exerting a negative inotropic effect. Intracellular CO_2 arises from several sources, including H^+ buffering by HCO_3^-, decarboxylation of pyruvate and α ketoglutarate, and decreased CO_2 removal from the cell as a result of low-flow hemodynamics. Hence shock exhibits the dual defects of an oxygen deficit and a carbon dioxide excess.

Cytosolic H^+ antagonizes Ca^{++} entry through the sarcolemmal voltage-sensitive calcium channels, and antagonizes Ca^{++} binding to contractile proteins. Intracellular H^+ accumulation also initiates a sequence of ion exchanges that increases cytosolic Ca^{++} independently of the voltage-channels. Eventually, Ca^{++} overload develops followed by myofilament dysfunction.

Because penetrating and blunt trauma is of central interest to the present study, attention is focussed on hemorrhagic shock and neurogenic shock

3.1.1 Hemorrhagic Shock

Hemorrhage that acutely decreases intravascular volume by ~20% unloads arterial baroreceptors in the carotid artery, aorta, and pulmonary artery. This information travels to the medulla, where the nucleus ambiguous is inhibited and vasomotor centers are activated, increasing sympathetic outflow to the heart, blood vessels, and adrenal medulla. With

hemorrhage, autonomic reflexes increase heart rate, myocardial contraction and ejection fraction, whereas smooth muscle constriction increases vascular resistance leading to high total peripheral resistance. The peripheral resistance gives rise to increased diastolic blood pressure, but this does little to increase organ perfusion. In progressive hemorrhage where blood loss is greater than ~35%, stroke volume decreases, and pulse pressure narrows concomitantly. Eventually, tachycardia alone cannot compensate for diminishing stroke volume and decreases in cardiac output and mean arterial blood pressure. The degree of hemorrhage roughly corresponds to heart rate. A heart rate greater than 150 beats per minute in trauma victims with hemorrhagic shock is associated with blood loss greater than ~40% and high mortality.

At the cellular level, inadequately perfused and oxygenated cells are deprived of essential substrates for normal aerobic metabolism and energy generation. Initially, compensation occurs by shifting to anaerobic metabolism, which results in the formation of lactic acid and the development of metabolic acidosis. If shock is prolonged and the substrate delivery for the generation of ATP is inadequate, the cellular membrane loses the ability to maintain its integrity and the normal electrical gradient is lost.

Cellular and interstitial swelling occurs in nearly every tissue after injury. Edema of the endoplasmic reticulum is the first ultrastructural evidence of cellular hypoxia. Mitochondrial damage soon follows. Lysosomes rupture and release enzymes that digest other intracellular structural elements. Sodium and water enter the cell, and cellular edema occurs. Intracellular calcium deposition also arises. If the process is not reversed, progressive cellular damage, additional tissue swelling, and cellular death ensues.

From a clinical standpoint, shock is a syndrome in which the peripheral blood flow is inadequate to return sufficient blood to the heart for normal function. This abnormality of the circulatory system results in inadequate organ perfusion and tissue oxygenation. The identification and classification of shock is an operative tool for the diagnosis and treatment display.

Proper assessment of acute hemorrhage plays an essential role in both the diagnosis and treatment of trauma associated with penetrating wounds. Shock is often ranked as mild, moderate, or severe. However, in the case where acute hemorrhagic shock is involved, it is more appropriate to adopt the classification put forth by the *American College of Surgeons* [1981,

1994]. A table adapted from the recommendations of the American College of Surgeons is presented on p. 68 of *Copass et al.*, [1991]. This table was initially augmented by LLUMC/GRI to include neck veins, skin color, skin moisture, and skin temperature as shock diagnostics. Additionally, CNS mental status was made more quantitative by referencing the Glascow Coma Scale. We have further expanded this table to include estimates of parameter importance and certainty. The final GRI/LLUMC revisions are displayed in Table 2.

The classification emphasizes the early signs and physiology of the shock state. Class I is uncomplicated shock characterized by the potential need for crystalloid fluid. Class II is also uncomplicated, but requires crystalloid fluid to effect resuscitation. Class III is a complicated state in which at least crystalloid fluid and perhaps blood replacement is required. Finally, Class IV can be considered a preterminal event. Unless very aggressive measures are taken, the patient dies within minutes. For the most part, a patient in Class III shock has a fairly good chance of full recovery, but complete recovery from Class IV shock is very unlikely.

In general, sole reliance on systolic blood pressure as an indicator of shock results in delayed recognition of the shock state. Compensatory mechanisms among Army combat troops may preclude a measurable fall in systolic pressure until 30% or more of the victim's blood volume is lost. Within the context of current medical sensors, the ATLS [Advanced Trauma Life Support for Doctors, American College of Surgeons, sixth edition, 1997] recommends that special attention be paid to pulse rate, respiratory rate, skin circulation, and pulse pressure. The ATLS course suggests that tachycardia and cutaneous vasoconstriction are usually the early physiologic responses to volume loss in most adults. Adult tachycardia is defined as a heart rate greater than ~100 beats per minute.

The inability of the heart to respond to shock with tachycardia is often described as relative bradycardia, paradoxical bradycardia, or the absence of tachycardic response [Johnsen, 1978; Barriot and Riou, 1987; Adams and Greene, 1986]. *Demetriades et al.* [1998] observe that relative bradycardia is a common finding in hypotensive trauma. Quantitatively *Demetriades et al.* [1998] define relative bradycardia as a systolic pressure $\leq$ 90 mm Hg and a pulse rate of $\leq$ 90 beats per minute. Approximately 29% of all hypotensive patients in this study exhibited relative bradycardia. Patients 55 years of age and less exhibited relative bradycardia 26% of the time whereas patients older than 55 displayed relative bradycardia 52% of the time.

Table 2.

Classes of Acute Hemorrhagic Shock* Revised by LLUMC/GRI for Knowledge-Based System

Imp.†	Cert.‡		Class I	Class II	Class III	Class IV
0.7	0.4	Blood loss in ml	up to 750 ml	1000 to 1250 ml	1500 to 1800 ml	2000 to 2500 ml
0.0	0.2	~~Blood loss in %[1]~~	~~up to 15%~~	~~20 to 25%~~	~~30 to 35%~~	~~40 to 50%~~
0.9	1.0	Pulse rate[2]	72 to 84 beats/min	100 beats/min	120 beats/min	140 beats/min, or greater
1.0	0.9	Blood pressure[3]	118/82 mm Hg	110/80 mm Hg	70-90/50-60 mm Hg	50-60 mm Hg
0.4	0.9	Pulse pressure (mm Hg)	36 mm Hg	30 mm Hg	20 to 30 mm Hg	10 to 20 mm Hg
0.3	0.2	Capillary blanch test	Normal	Delayed or None	Delayed or None	Delayed or None
0.2	0.7	Respiratory rate	14 to 20	20 to 30	30 to 40	≥ 35
0.8	0.8	CNS mental status			Confused	Confused and lethargic
					From GCS Verbal (1-3).	From GCS Verbal (1-3). Query for lethargic if Class IV is in doubt.
0.1	0.0	~~Neck Veins~~	~~Flat while supine~~			~~Apparently absent neck veins while supine~~
0.6	0.6	Skin Color	Normal	Pale	Pale	Pale or cyonotoic
0.5	0.3	Skin Moisture	Normal	Moist	Moist	Profuse
0.4	0.5	Skin Temperature	Normal	Cool	Cool	Cold

*Adapted from Committee on Trauma, American College of Surgeons: *Advanced Trauma Life Support Course,* 1981, p. 45.
†Weighting factor for importance of measurement in determining hemorrhage classification.
‡Assessed confidence factor for field determination of measured quantity.
[1]% of blood volume in an average 70-kg male.
[2]Assume normal of 72 beats/min.
[3]Assume normal of 120/80 mm Hg.

The overall average is 29% because there were few trauma patients in the study that were over 55 years old. Although there are many hypotheses, the overall cause of relative bradycardia is not known. Moreover, as noted by *Demetriades et al.*, the prognostic significance of relative bradycardia is not clear. In the past, several authors have indicated that the absence of tachycardic response is a bad prognostic sign [*Mannix*, 1988; *Millikan et al.*, 1980]. No difference between bradycardic and tachycardic hypotensive patients was noted by *Thompson* [1990] in reference to penetrating abdominal and isolated extremity injuries. *Barriot and Riou* [1987] report that fluid resuscitation corrected the bradycardic response.

The *Demetriades et al.* [1998] study shows that overall crude mortality in hypotensive patients with relative bradycardia was lower than that in tachycardic patients (21.7% versus 29.2%). The authors speculate that the lower pulse rate in relative bradycardia patients may be beneficial because it increases the diastolic ventricular filling and cardiac output as suggested by *Oberg and Thoren* [1970]. In this case, the increased parasympathetic activity in bradycardia may be associated with better tissue perfusion attributable to peripheral vasodilation. *Demetriades et al.* [1998] emphasize that the better survival of their bradycardic patients is the result of less severe trauma in this group. They conclude that while the cause and significance of the relative bradycardia is not clear, some subgroups of bradycardic patients may have a better outcome than tachycardic patients.

The results of the *Demetriades et al.* [1998] study indicate that hypovolemic shock can be complex. Although ATLS emphasized tachycardia as one of the early indicators for hemorrhagic shock, this particular sign may not be valid in a significant portion of the trauma population.

3.1.2 Neurogenic Shock

As noted by *Kline* [1998] central neurogenic hypotension (spinal shock) usually results from spinal cord injury and interrupts sympathetic efferent fibers. Sympathetic out flow originates in the hypothalamus and nucleus tractus solitarus of the medulla and descends in the intermediolateral column of the spinal cord, exiting to synapse on paired ganglia on either side of the spinal column, or in larger regional ganglia. The heart chambers and thoracic blood vessels receive fibers from T1 to T8. Other more distal ganglia provide sympathetic tone to the vasculature below the diaphram. The vagi, on the other hand, exit the skull and descend in the carotid sheath. Cervical spinal cord damage can selectively interrupt sympathetic, but not vagal outflow. The result is bradycardia and hypotension, the hallmarks of central neurogenic

hypotension [e.g., *Arrowood et al.*, 1987]. Spinal cord lesions distal to T4 are unlikely to cause bradycardia, but complete cord transection at this level can cause enough vasodilation to produce hypotension in a supine trauma victim with marginal intravascular volume.

In summary, the classic picture of neurogenic shock is hypotension without tachycardia or cutaneous vasoconstriction. This contrasts with hemorrhagic shock discussed above. In addition, a narrowed pulse pressure is not seen in neurogenic shock. It is likely that patients who sustain spinal injury will have concurrent torso trauma. As a result, patients suspected of neurogenic shock in the current study are also considered at risk for hypovolemia.

3.1.3 Noninvasive Diagnostic Sensors for Shock

At present, routine monitoring of suspected shock with FDA approved, noninvasive sensors consists of cardiovascular and pulse oximetry monitoring of the trauma victim. It is often recommended that arterial blood pressure be determined with a cuff sphygmomanometer every 2 to 5 minutes. In the current project, we made use of the Colin Pilot 9200, which incorporates FDA-approved arterial tonometry. Systolic and diastolic blood is provided in two forms: pulse-to-pulse and two-second output values that are a weighted average of six pulses. When shock is suspected in a trauma victim, attention is usually focussed on the trends in heart rate, mean arterial blood pressure, and pulse pressure width. (In a hospital setting urine production is also monitored.) Under conditions of shock, cuff sphygmomanometry (as well as tonometry) usually overestimates aortic blood pressure and inaccurately predicts tissue perfusion. Similarly, if pulse oximetry is monitored on a distal extremity, the readings will quickly become erratic and unusable as the patient enters shock state 2.

End tidal CO_2 monitoring can provide a noninvasive estimate of cardiac output during shock. Carbon dioxide is transported from cells in venous blood to the lungs where it diffuses out and can be measured during expiration with capnometry. End-tidal CO_2 is decreased by alveolar dead space expansion. Dead space is increased when enough alveoli are ventilated more than perfused. Significant decreases in end-tidal CO_2 occur with low flow to the lungs, such as occurs with low cardiac output. The primary use of capnography is monitoring the success of resuscitation from high-level shock. Most patients in shock will show an initially low end-tidal CO_2 because of low flow and hyperventilation [*Weil et al.*, 1985]. With effective resuscitation, end-tidal CO_2 is expected to increase.

New sensors such as the sublingual P_{CO_2} device or the serum lactate MicroFlumes device described in Sections 2.2.1 and 2.2.2 offer significant advantages in monitoring shock state. Lactate measurements are useful semiquantitative measures of shock. Regardless of the cause of inadequate perfusion, anerobic metabolism will lead to increased lactate production and blood lactate concentrations. Studies have been performed to set guidelines for lactate concentrations associated with poor outcomes, even in patients with reasons for abnormal baseline lactate concentrations [e.g., *Kruse et al.,* 1987]. Normal lactate measurements are below 2.0 millimole. Lactate concentrations above 4.0 millimole are pathologic and are taken as evidence of advanced systemic hypoperfusion [*Stacpoole et al.*, 1994]. Lactate levels in excess of 4.0 millimoles are associated with mortality in excess of 50% in heterogenous populations of patients in shock [*Aduen et al.*, 1994]. As noted in Section 2.2.2, the slow response time of arterial lactate is a shortcoming when lactate measurements are being used to determine the effectiveness of resuscitative efforts. It is noteworthy that tissue P_{CO_2} exhibits a significantly shorter response time following resuscitation. The short time constant is of significant benefit in determining the effectiveness of therapy.

3.2 Cardiac Tamponade

Cardiac tamponade is a pathological condition resulting from accumulation of excess fluid in the pericardium. It can arise from injuries to the heart or the great blood vessels involving the accumulation of blood. Cardiac tamponade is characterized by abnormalities of diastolic filling, resulting in increased ventricular end-diastolic pressures, decreased ventricular volumes, reduced ventricular compliance, and impaired cardiac output [e.g., *Shabetal*, 1990]. Most commonly, cardiac tamponade is associated with penetrating injuries. However, blunt injury may also cause the pericardium to fill with blood from the heart, great vessels, or pericardial vessels. The pericardial sac is a fixed fibrous structure, and only a relatively small amount of blood is required to restrict cardiac activity and interfere with cardiac filling. Removal of small amounts of blood or fluid, often as little as 15 - 20 mL, by pericardiocentesis may result in immediate hemodynamic improvement if tamponade exists.

The diagnosis of cardiac tamponade can be difficult. The classic diagnostic "Beck's triad" consists of venous pressure elevation, decline in arterial pressure, and muffled heart tones. Muffled heart tones are difficult to assess, distended neck veins may be absent because of hypovolemia. Pulsus paradoxus is a normal physiologic decrease in systolic bood pressure that

occurs during spontaneous inspiration. When this change is exaggerated and exceeds 10 mm Hg, it is another indicator of cardiac tamponade. Kussmaul's sign (a rise in venous pressure with inspiration when breathing spontaneously) is the true paradoxical venous pressure abnormality associated with tamponade. It is also difficult to measure noninvasively. Pulseless Electrical Activity (PEA) in the absence of hypovolemia and tension pneumothorax suggests cardiac tamponade.

3.3 Hemo-pneumothorax

Pneumothorax, or the accumulation of air in the pleural space, is a common complication of chest trauma. Pneumothorax can be divided into three classifications: simple, communicating (or open), and tension. Only the first two are directly relevant to this project.

Pneumothorax results from air entering the potential space between the visceral and parietal pleura. Both penetrating and nonpenetrating trauma may cause this injury. Thoracic spine fracture dislocations also may be associated with a pneumothorax. Lung laceration with air leakage is the most common cause of pneumothorax resulting from blunt trauma.

Normally, the thorax is completely filled by the lung, which is held to the chest wall by surface tension between the pleural surfaces. Air in the pleural space collapses lung tissue. A ventilation/perfusion defect occurs because the blood perfusing the nonventilated area is not oxygenated. Simple pneumothorax occurs when there is no communication with the atmosphere or any shift of the mediastinum or hemidiaphragm resulting from the accumulation of air. It is normally graded by the degree of collapse. A small pneumothorax occupies 15% or less of the pleural cavity, a moderate one 15% to 60%, and a large pneumothorax more than 60%. Traumatic pneumothorax is often caused by a fractured rib that is driven inward, lacerating the pleura. It may also occur without a fracture when the impact is delivered at full inspiration with the glottis closed. A penetrating injury such as a gunshot or stab wound may also produce a simple pneumothorax if there is no free communication with the atmosphere.

Open pneumothorax, which is associated with a defect in the chest wall, is a common combat injury. Air can sometimes be heard flowing sonorously in and out of the chest wound, prompting the term "sucking chest wound." Paradoxically, the loss of chest wall integrity causes the involved lung to collapse on inspiration and expand slightly on expiration, forcing air in and out of the wound. This results in a large functional dead space for the normal lung, and together with the loss of ventilation of the involved lung, produces a severe ventilatory perturbation.

Tension pneumothorax occurs when the injury acts like a one-way valve. This prevents free bilateral communication with the atmosphere, and leads to a progressive increase in intrapleural pressure. Air enters on inspiration but cannot exit with expiration. The increased thoracic pressure compresses the vena cava and distorts the cavoatrial junction, leading to decreased diastolic filling of the heart and subsequent decrease in cardiac output [e.g., *Ballinger et al.*, 1968]. In addition, the compression of the contralateral lung causes a shunting of the blood to nonventilated areas and gives rise to a severe respiratory disturbance. These developments result in rapid onset of hypoxia, acidosis, and shock. If a needle thoracostomy is not performed within a few minutes, death will ensue.

In the civilian population, the primary cause of hemothorax is lung laceration or laceration of an intercostal vessel or internal mammary artery due to either penetrating or blunt trauma. The accumulation of blood in the pleural space after blunt or penetrating chest trauma is a common complication that may produce hypovolemic shock and dangerously reduce vital capacity. It usually occurs in conjunction with pneumothorax and extrathoracic injuries. In the civilian population, hemorrhage from injured lung parenchyma is most common but tends to be self-limiting unless there is a major laceration. Also, the intercostal and internal mamary arteries tend to cause hemothorax more often than hilar or great vessels [e.g. Cohn, 1972]. The compression effect of the lost blood, the high concentration of thromboplastin in the lung, low pulmonary artery pressure, and pulmonary collapse produce early clotting and usually hemostasis. Bleeding from the intercostal arteries may be brisk, however, because they branch directly from the aorta [e.g., *Rosen and Murphy*, 1983]. Thoracic spine fracture dislocations may also be associated with a hemothorax. However, in this case bleeding tends to be self-limiting and does not require operative intervention.

3.4 Head Trauma

Head trauma within the environment of the Battalion Aid Station (BAS) is somewhat problematic because the treatment options are limited. At present, a non-invasive intracranial pressure (ICP) sensor does not exist and neither a neurosurgeon nor CT scan capability is present at the BAS. As a result, the options for diagnosis and treatment are limited. The focus on a non-invasive intracranial pressure sensor lies in the fact that several pathologic processes that affect the brain give rise to elevated ICP. In turn, intracranial hypertension can have consequences that adversely affect brain function and hence the trauma patient's outcome. Thus, elevated ICP not

not only indicates the presence of a problem, but can often contribute to the problem. "Normal" ICP in the resting state is approximately 10 mm Hg. Pressures greater than 20 mm Hg are considered clearly abnormal and pressures greater than ~40 mm Hg are categorized as severe elevations. In general, the higher the ICP following head injury, the worse the outcome.

In the civilian population, more than two million patients in the U.S. undergo emergency evaluation for acute head trauma [e.g., *White and Likavec*, 1992; *Waxweiler et al.*, 1995]. Eighty percent sustain minor head trauma defined as a presenting Glasgow Coma Scale (GCS) of 13 to 15. Ten percent have moderate head injuries (GCS of 9 to 12), and 10% have severe head injuries (GCS of 8 or less). Almost 25% of these patients are hospitalized and approximately 200,000 die or are permanently disabled because of their injury. In addition, as many as 50,000 patients with severe head trauma die each year before reaching an emergency department.

Civilian gun shot wounds (GSWs) to the head account for about 33,000 deaths per year and up to 76% of all patients who sustain a GSW to the head are dead at the scene [*Ward et al.*, 1994; *Kaufman et al.*, 1986]. Overall, the mortality caused by a GSW to the head in patients who arrive at the hospital for emergency resuscitation is estimated to be greater than 60% [*Benzel et al.*, 1991; *Hernesniemi*, 1979]. If the patient is hemodynamically stable, has not sustained secondary systemic insults such as hypoxia or hypotension, has no expanding mass lesions from the missile injury, and has not ingested intoxicants that may interfere with assessment, the prognosis after a GSW to the head can be predicted by the presenting GCS and pupillary responsiveness [*Ward et al.*, 1994]. If the presenting GCS is less than 5, mortality approaches 100%. If the presenting GCS is greater than 8 and the pupils are reactive, survival approaches 75% [*Ward et al.*, 1994]. Survivors of GSW to the head tend to do well, with up to 60% returning to their former employment [*Kaufman et al.*, 1986; *Nagib et al.*, 1986].

At the BAS, the monitoring of vital signs and neurologic examinations are available for trauma support. Vital sign monitoring is essential to insure that the trauma victim has adequate oxygenation and ventilation. Both are essential to the head-injured patient because hypoxia and hypercarbia can convert reversible brain trauma into irreversible injury. Moderate hypercarbia can cause profound cerebral vasodilation, resulting in increased ICP with further ventilation deterioration. A vicious cycle can ensue in which the secondary brain injury becomes more profound than the initial primary impact injury.

An elevated systolic blood pressure can reflect a rise in ICP and be part of the Cushing reflex (i.e., hypertension and bradycardia). Hypertension reflects the brain's attempt to maintain cerebral perfusion pressure (mean systemic arterial blood pressure minus mean intracranial pressure). Hypotension is rarely due to head injury except as a terminal event with medullary collapse. An exception is the case of serious blood loss from scalp lacerations. Because hypotension in a severely head-injured patient can greatly impair neurologic function, blood pressure must be restored before an accurate neurologic assessment can be made.

Neurological assessments with GCS offers an essential method for establishing the severity of head injury and charting a clinical course. In the present project, the GCS are viewed as observational data inputs. Repeat examinations are required to determine if the trauma victim is stable, improving, or deteriorating. Level of consciousness is the most important factor in assessing head injury.

GCS evaluates three aspects of the patient's responsiveness: (1) eye opening, (2) best verbal response, and (3) best motor response. Spontaneous eye opening suggests that the reticular activating centers are functioning. However, this does not imply awareness. If spontaneous eye opening is not present, verbal stimuli or commands must be used next, followed by vigorous pinching or pressure on the nail bed. Verbal response (speech) suggests a relatively intact central nervous system. Oriented speech implies awareness of oneself and one's environment. Orientation implies awareness of name, place, and date. A trauma patient may be well-articulated and organized but disoriented. Inappropriate words refer to those that are exclamatory or random only. Incomprehensible speech consists of moaning or groaning but no recognizable words.

Motor responses are the most important and reproducible portion of the GCS. Obeying verbal commands means that the trauma victim has the ability to move his limbs readily and without the need for painful stimulation. Localizing pain means that the patient moves a limb sequentially to the location of the painful stimulus in an effort to remove it. Flexion-withdrawal implies that the patient pulls in flexion away from a pain stimulus. Abnormal flexion means a decorticate response is consistently apparent. An extensor response is decerebration, with abduction and internal rotation of the shoulder and pronation of the forearm. No response is hypotonia or flaccidity, which strongly suggests loss of medullary function. A head-injured patient who exhibits flaccidity often has experienced a spinal cord injury.

The maximum GCS score is 15 and the minimum is 3. Severe head injury is defined as a GCS of 8 or less persisting for 6 hours or longer. Moderate head injury implies a GCS of 9 to 12, and mild head injury is 13 to 15.

Pupil size and reactivity to light also assist in the neurologic assessment and are used in conjunction with GCS. For example, an enlarging pupil in the face of a decreasing level of consciousness is strongly suggestive of uncal herniation with associated oculomotor nerve compression.

Head trauma is commonly classified by mechanism, severity, and morphology [e.g., *Valadka and Narayan*, 1996]. The mechanism is either blunt [high velocity (automobile collision), low velocity (fall, assault)] or penetrating [e.g., gunshot wounds]. The GCS scale described above establishes the mild (GCS 14-15), moderate (GCS 9-13), and serious (GCS 3-8) levels of severity. Morphology is divided into skull fractures [Vault (linear versus stellate, depressed or nondepressed, open or closed) or Basilar (with or without cerebrospinal fluid leakage, with or without VIIth nerve palsy] or intracranial lesions [focal (epidural, subdural, intracerebral) or diffuse (mild concussion, classic concussion, diffuse axonal injury)].

Many of the specific injuries sustained in head trauma cannot be diagnosed at the BAS. Exceptions include injuries such as basilar skull fracture which is primarily a clinical diagnosis. Symptoms include hemotympanum or bloody discharge from the ear, rhinorrhea or otorrhea, retroauricular ecchymosis (Battle sign), periorbital ecchymosis (raccoon's eyes), and first-, second-, seventh-, and eighth-cranial nerve deficits. Within the scope of the current project, we rely on observational data (e.g., GCS, pupil status, etc.) along with measurements of physiologic sensor data to signal a downturn in patient state. This approach is appropriate for mild and possibly moderate head injury.

3.5 Respiratory Failure

Wilson [1996] indicates that, within the civilian population, thoracic trauma directly causes at least 25% of trauma deaths and is a contributing factor in another 25%. About 80% of patients with chest trauma do not have hypotension or severe respiratory distress when first seen in the emergency department. Such patients will generally do very well, and if no other injuries are present, will have a mortality rate of less than 1%. However, if the patient with chest trauma has a systolic blood pressure less than 80 mm Hg on admission and/or requires urgent endotracheal intubation, the mortality rate will generally exceed 10-20%.

Patients with chest trauma who develop acute, severe respiratory distress have a high mortality rate. In the study of *Wilson et al.* [1977], 11% of patients admitted with chest trauma required endotrachial intubation almost immediately upon entrance to the emergency department. Of these, 58% died. If shock accompanied the respiratory distress, the mortality rate rose to 73%. In patients with blunt chest trauma, the most frequent factors associated with acute respiratory distress include shock, coma, multiple rib fractures, and hemo-pneumothorax. In patients with penetrating trauma, respiratory distress is usually due to severe shock or hemo-pneumothorax.

3.6 Acute Respiratory Distress Syndrome (ARDS)

ARDS is a form a noncardiogenic pulmonary edema that is a result of the nonspecific response of the lung to a variety of insults. Respiratory failure results from damage to the region of alveolar-capillary oxygen exchange with increased permeability of plasma fluid and protein. ARDS can be caused by either a direct injury to the lungs (e.g., aspiration of liquids or inhaled toxins) or may result from circulating inflammatory mediators associated with multisystem trauma, sepsis or drugs. Trauma, sepsis, shock, burns, and radiation injury are prominently associated with ARDS. A variety of mediators have been implicated in the development of ARDS, including neutrophil production of proteases and oxygen radicals, thromboxanes, kallikrein, and complement factors. The concept of global microcirculatory injury has won the favor of many ARDS investigators. Patients with ARDS develop progressive respiratory failure associated with diffuse bilateral infiltrates. In the situation of trauma and sepsis, ARDS affects capillary beds throughout the body concurrently. When increased microvascular permeability presents itself in the lung, alveolar flooding occurs, causing dyspnea and hypoxemia. The appearance of ARDS varies from within minutes to hours of the onset of sepsis. Although there are no specific and sensitive markers for ARDS, common physiologic criteria include bilateral pulmonary infiltrates, pulmonary capillary wedge pressure < 18 mm Hg, the ratio of arterial to alveolar pressure $P_{aO_2}/P_{AO_2} < 0.2$, and static compliance < 40 ml/cm H_2O.

3.7 Multiple Trauma

As the current project progressed, it became clear that the overall software architecture should provide for the expansion of trauma conditions covered and allow for the introduction of new sensors. Beyond this, it is clear that multiple trauma conditions cannot at present be reliably

handled given the current medical knowledge base and the existing noninvasive medical sensors. Thus, the present software is geared to track a single, dominant trauma condition.

Even in the absence of decision-making software, the management of patients with multiple trauma by an emergency physician is a complex undertaking that requires broad knowledge and considerable experience. Vital signs must be recorded frequently in this situation, and the current program is capable of recording and analyzing such data. Unstable patients require continuous pulse oximetry and end-tidal CO_2 monitoring where applicable. As noted above, a measurement of blood lactate or tissue P_{CO_2} would contribute greatly to the assessment of shock state and aid in determining the effectiveness of the resuscitative efforts. The addition of these and other sensors would pave the way for the implementation of more advanced decision-making software.

3.8 Model Profiles for Trauma Conditions

In order to be effective, the knowledge-based system must have information concerning the response of medical sensors to the trauma conditions described above. Sensor profiles for the "nominal" response of a healthy person in good physical condition were developed for each of the conditions addressed by this program. These profiles are illustrated in Figures 2-8. In general, the temporal scales shown in the figures are only nominal, because the time history is a variable dependent on many elements including the severity of injury. For example, rapidly increasing intracranial pressure will greatly compress the temporal scale in Figure 6. ARDS shown in Figure 8 can develop over very long time scales many times the 60-minute interval used in the figure. Delayed hemo-pneumothorax can have onset times ranging from minutes to tens of minutes, and the development of spinal shock can be influenced by swelling in the spinal column. The profiles for hypovolemic shock (Figure 2) have a strong tachycardia component. However, as noted previously *Demetriades et al.* [1998] indicate that relative bradycardia in hypotensive trauma patients is a common hemodynamic finding. In their study, 71% of the trauma victims were tachycardic and 29% were bradycardic.

Obviously, the expansion and contraction of the temporal scale determines the magnitude of the trends of the various sensor values, and the absolute magnitude of the trends will be quite variable. We recognize that all individuals will not exhibit the general trends illustrated in the figures. Nevertheless, a general framework must be laid for the initial program development. To first order, the signs of the trend values (positive or negative) provide important diagnostic

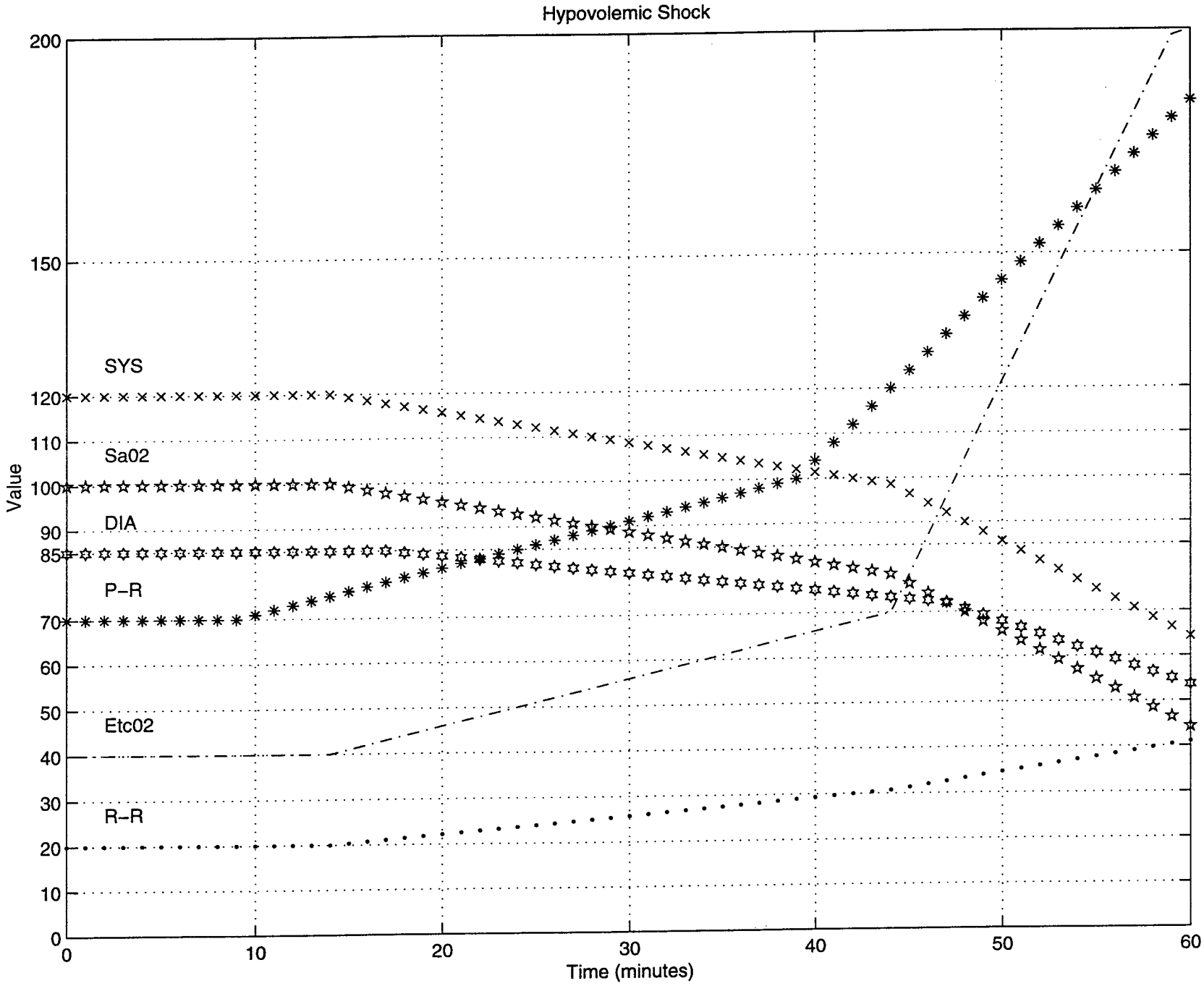
Hypovolemic Shock
SYS
Sa02
DIA
P-R
Etc02
R-R
Value
Time (minutes)
0
10
20
30
40
50
60
70
85
90
100
110
120
150
200

Figure 2

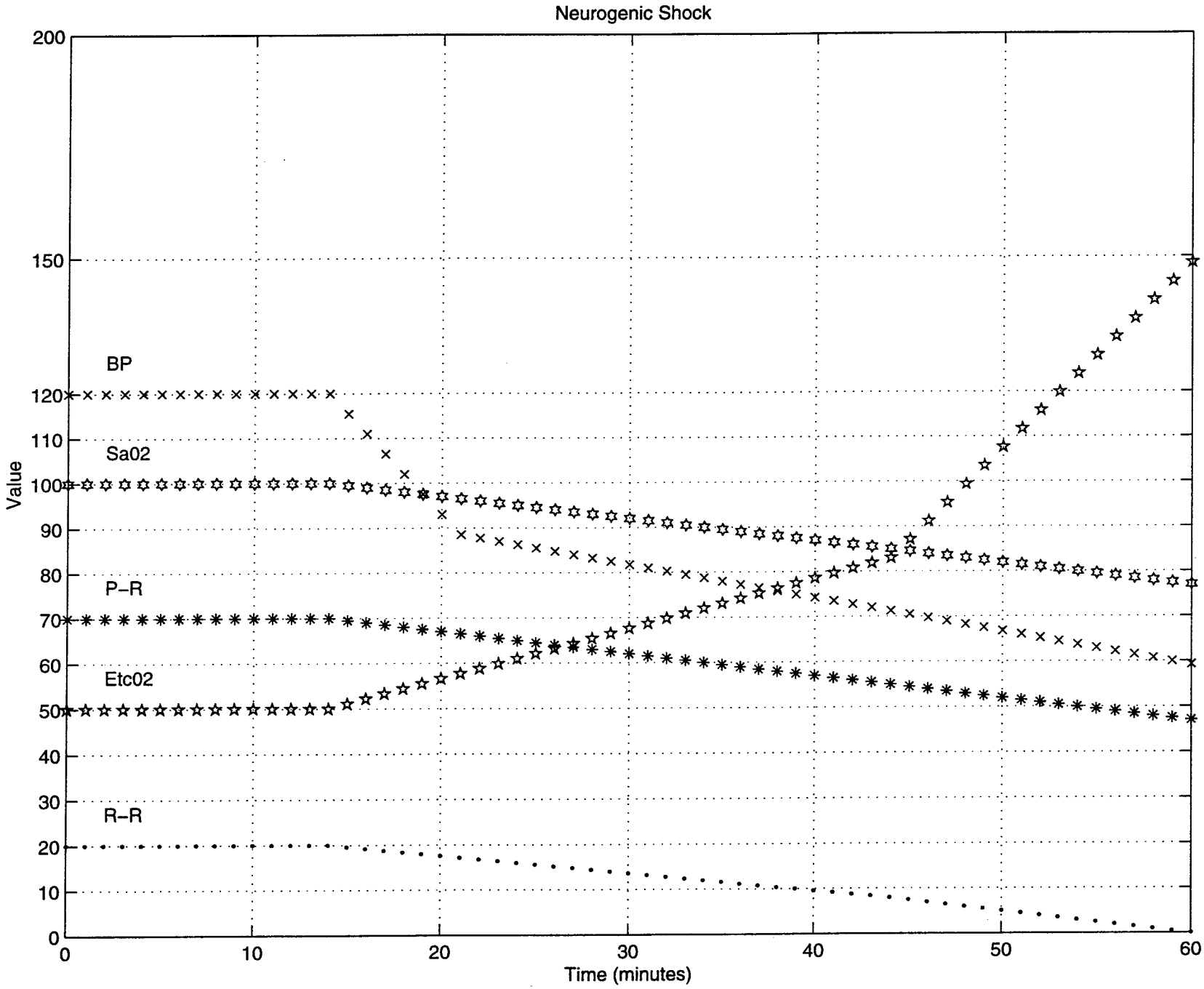
Neurogenic Shock
BP
Sa02
P–R
Etc02
R–R
Value
Time (minutes)
0
10
20
30
40
50
60
0
10
20
30
40
50
60
70
80
90
100
110
120
150
200

Figure 3

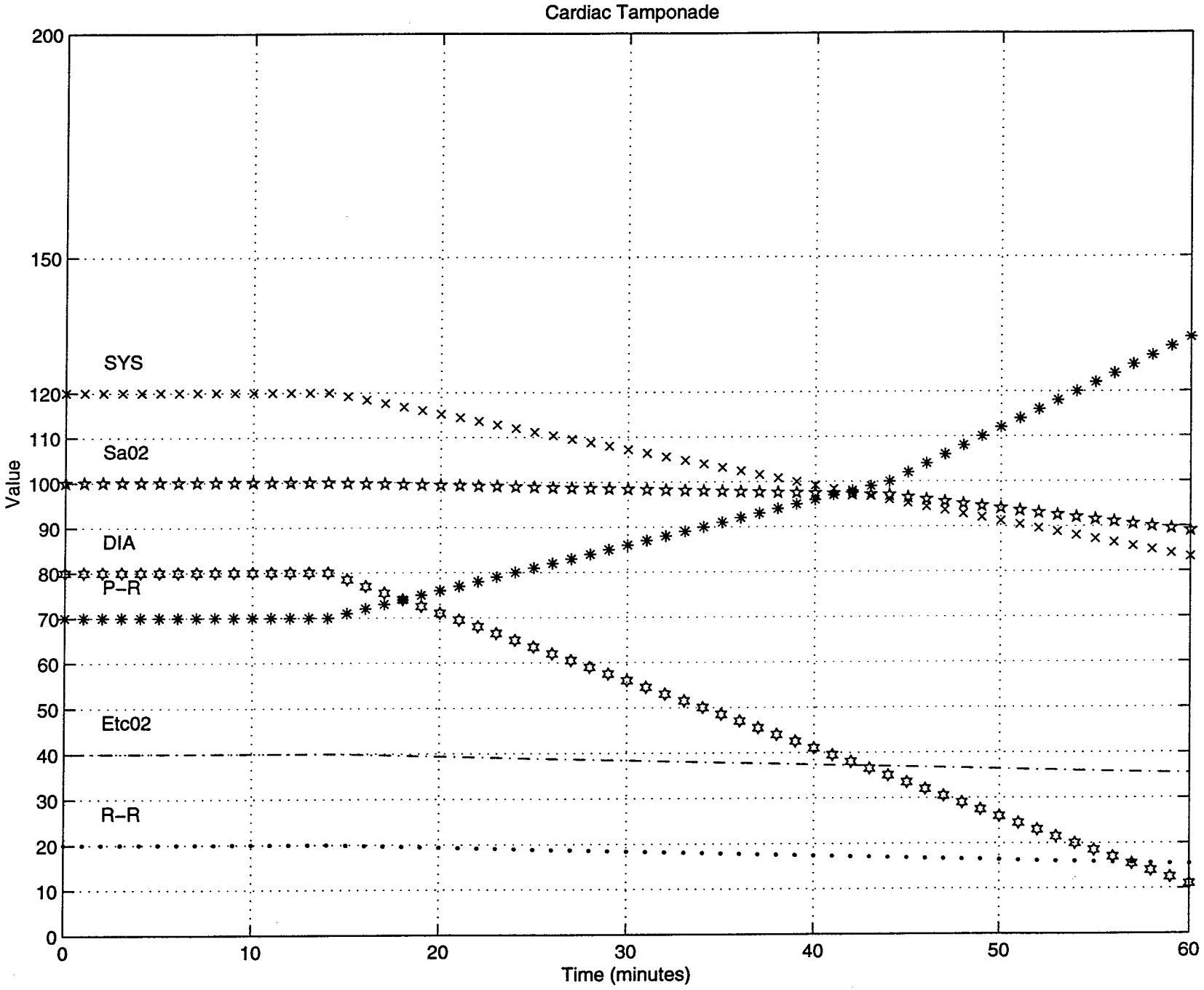
Cardiac Tamponade
200
150
120
110
100
90
80
70
60
50
40
30
20
10
0
Value
SYS
Sa02
DIA
P–R
Etc02
R–R
0
10
20
30
40
50
60
Time (minutes)

Figure 4

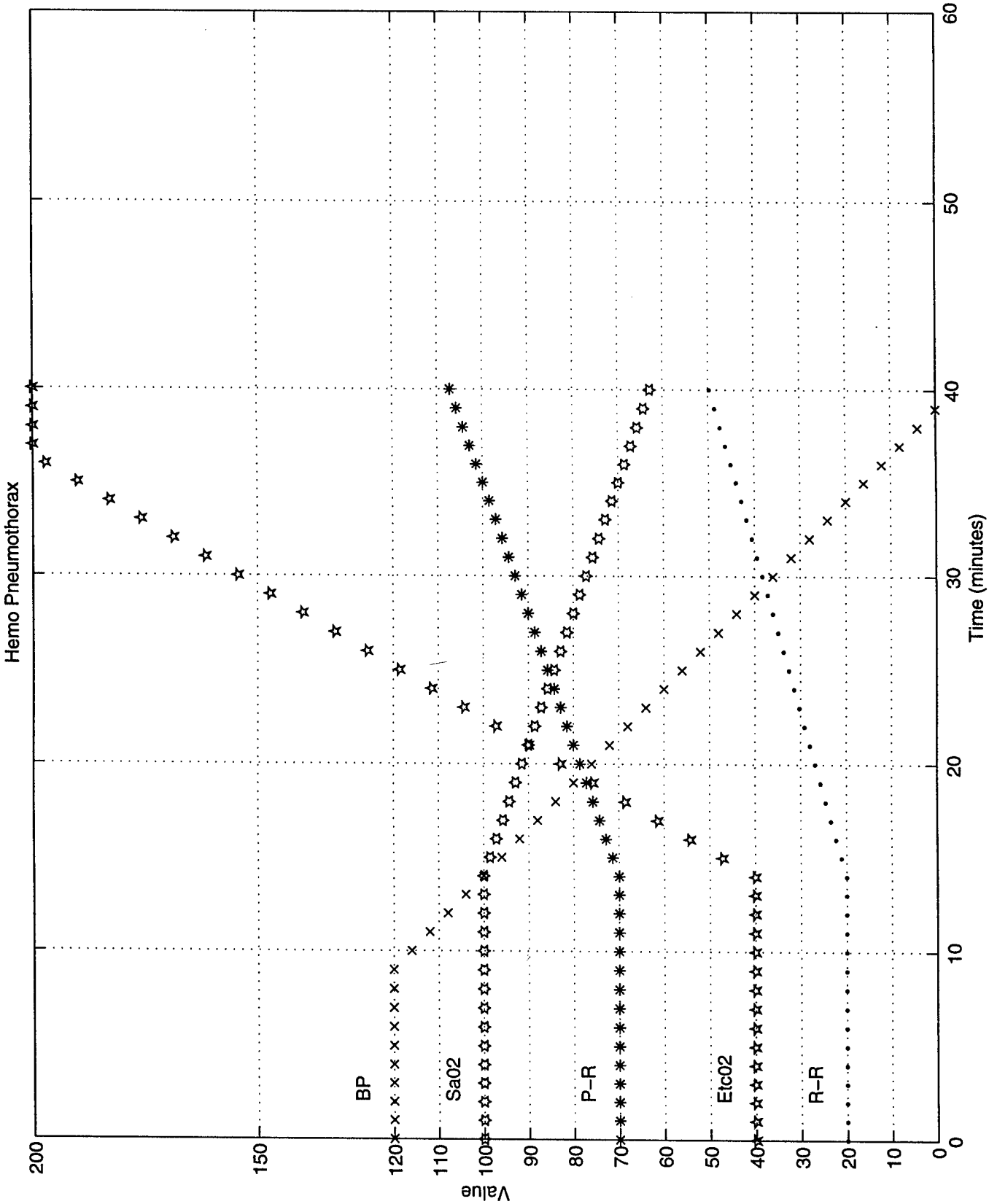
Hemo Pneumothorax
Value
Time (minutes)
BP
Sa02
P-R
Etc02
R-R
200
150
120
110
100
90
80
70
60
50
40
30
20
10
0
10
20
30
40
50
60

Figure 5

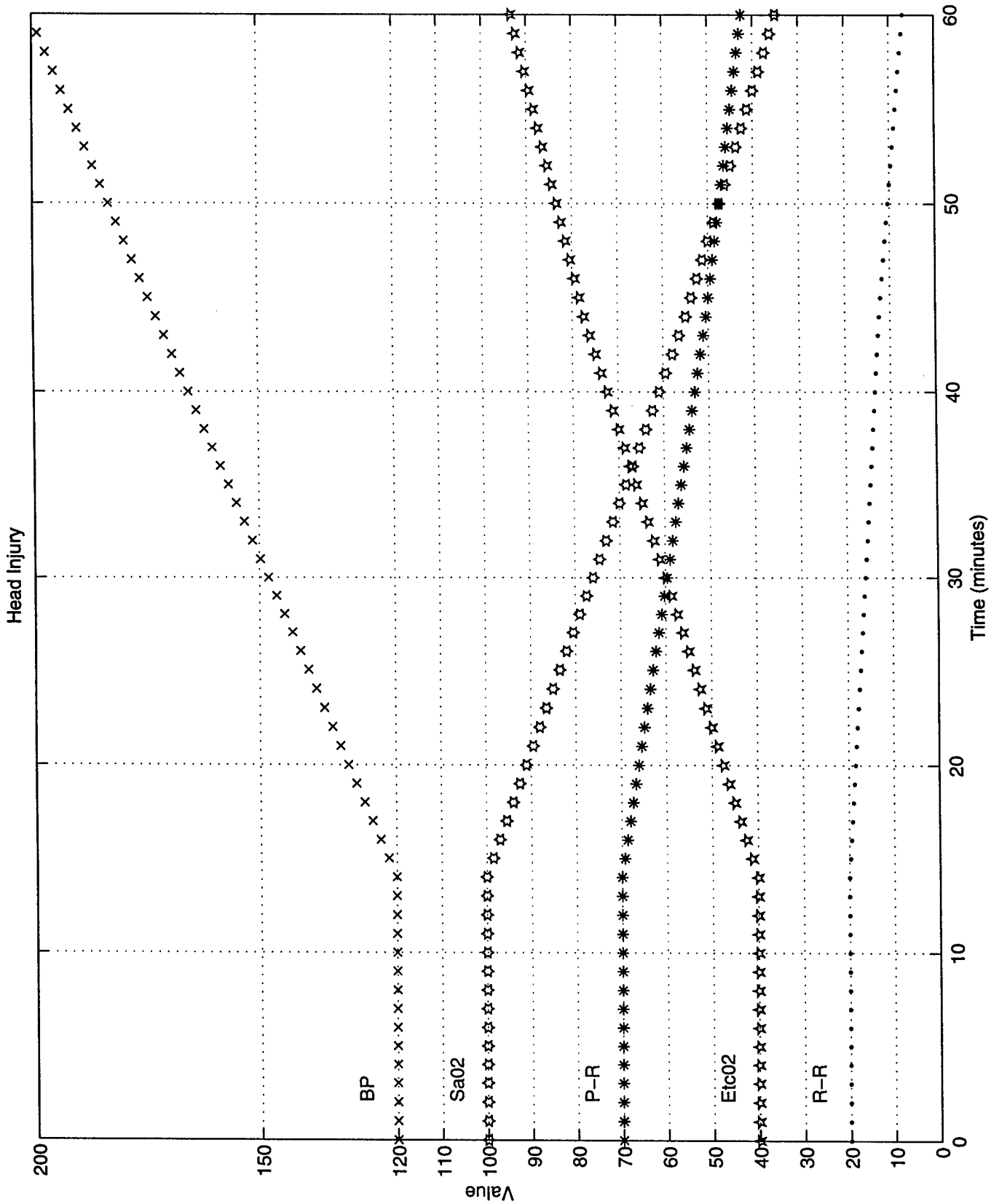
Head Injury
Value
Time (minutes)
BP
Sa02
P–R
Etc02
R–R
200
150
120
110
100
90
80
70
60
50
40
30
20
10
0
0
10
20
30
40
50
60

Figure 6

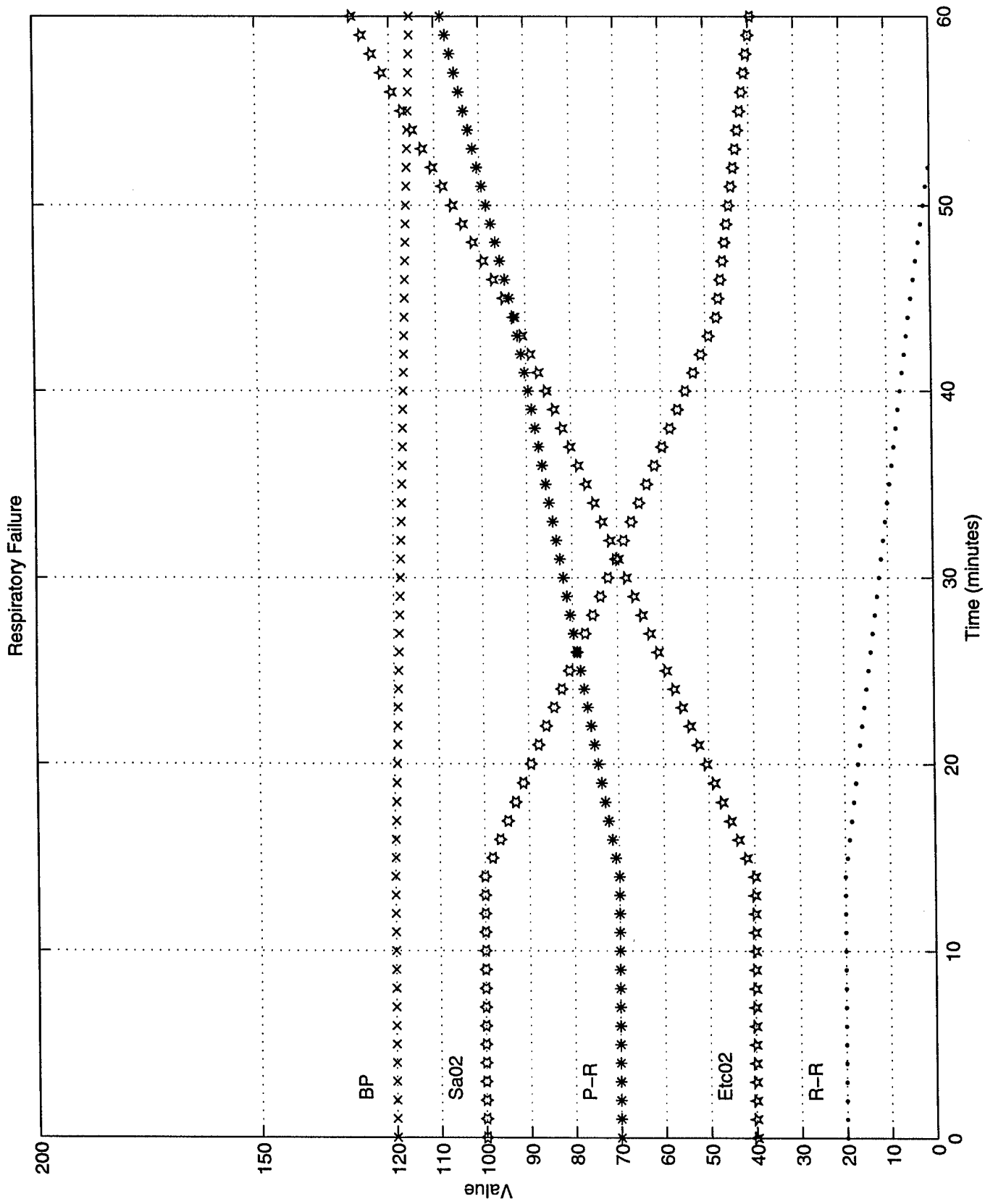
Respiratory Failure
Value
Time (minutes)
BP
Sa02
P–R
Etc02
R–R
200
150
120
110
100
90
80
70
60
50
40
30
20
10
0
0
10
20
30
40
50
60

Figure 7

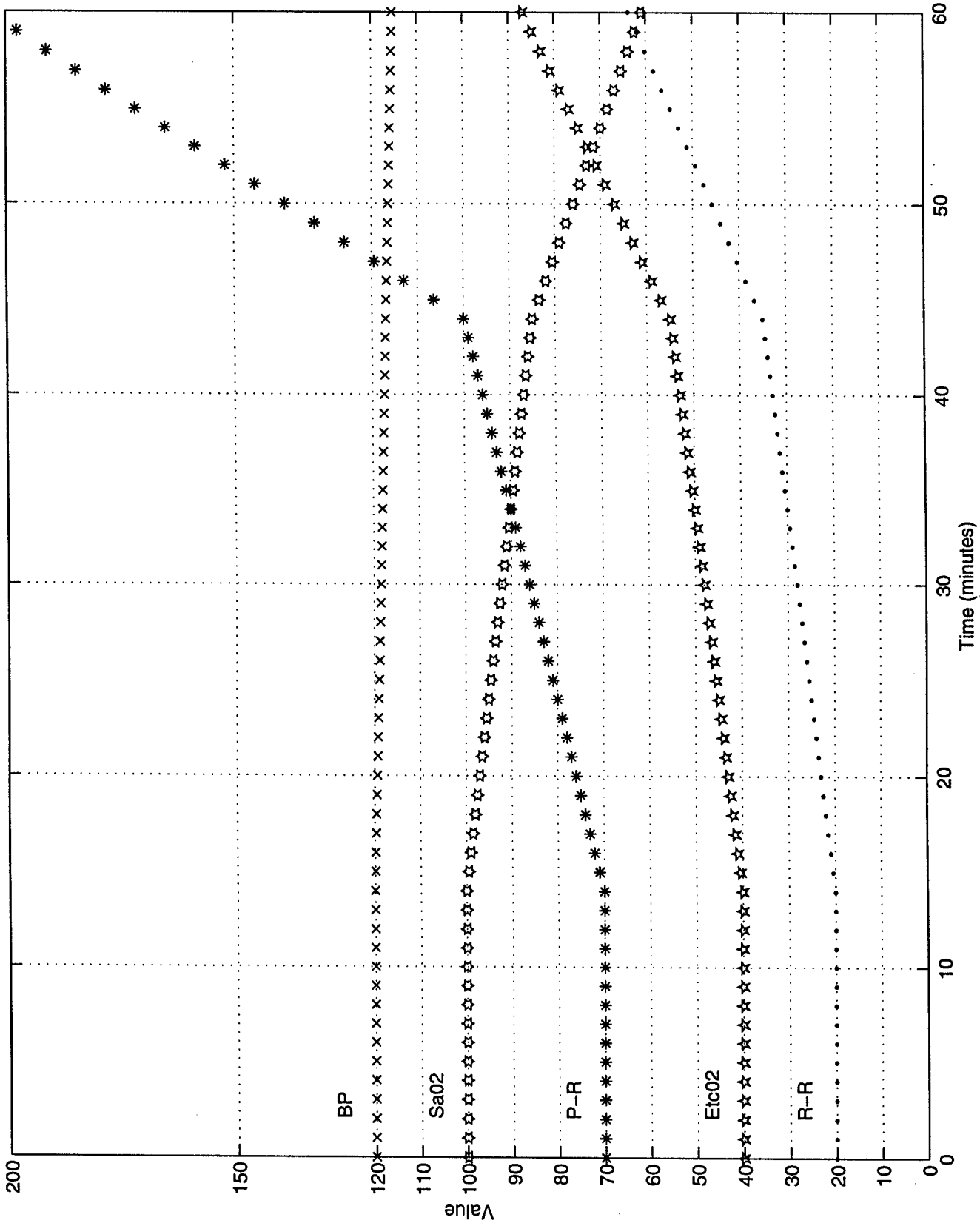
ARDS
BP
Sa02
P–R
Etc02
R–R
Value
Time (minutes)
200
150
120
110
100
90
80
70
60
50
40
30
20
10
0
10
20
30
40
50
60

Figure 8

information to the program. The magnitudes of the trends represent "fuzzy" variables that are given great latitude in the program.

4. Basic System Architecture and Implementation Strategy

Implementation of the system software on a compact computer unit is necessary to establish system feasibility and utility in the prototype stage. Two laptop computers are used in this project: a Toshiba Tecra 8000 and a Toshiba Satellite 6030. Both make use of Windows NT as the operating system. The former is the central computer of the diagnostic and treatment display unit, whereas the latter is used to collect trauma patient data at LLUMC. These laptops were selected because of their built-in stability and networking capabilities.

In a combat situation, ease of use is important and the number of menus should ideally be kept to a minimum. The software illustrated in this report is the complete developmental system assembled under this program. Consequently, the menu system presented here is quite general and all inclusive. The software can be readily tailored to a particular application. This reduces the number of menus necessary for trauma support and in certain cases simplifies many of the menu screens. A user-friendly graphical user interface was developed so that the entry of non-sensor observational data, wound location, preliminary diagnoses, and tracking information would be intuitive and efficient. An overview of this system is provided below. A more detailed description of the menu choices is provided in Section 10.2.

4.1 Observational Data

To enhance the amount of information available to the decision-making modules, we have made provisions for the entry of standard non-sensor data. These data help quantify routine observations made during the primary examination of the trauma victim. The parameters are similar to those obtained and recorded by a paramedic/EMT II in the civilian arena. In many instances observational data are essential for an adequate assessment of patient status. For example, accurate estimates of blood loss aid in shock evaluation and neurological assessments rely heavily on the results of physical determinations of pupil response, verbal response, motor response, and pupil status. Items that can currently be entered in a non-sensor submenu are listed in Table 3 below.

Table 3. Non-Sensor Parameters Available for Entry

Parameter	Values
Pupil Response	1. spontaneous, 2. to voice, 3. to pain, 4. none
Verbal Response	1. oriented, 2. confused, 3. inappropriate, 4. incomprehensible, 5. none
Motor Response	1. obedient, 2. purposeful, 3. withdrawal, 4. flexion, extension, 5. none
Pupil Status	Left Eye: 1. normal, 2. constricted, 3. dilated
	Right Eye: 1. normal, 2. constricted, 3. dilated
Skin Color	1. normal, 2. pale/ashen, 3. cyanotic, 4. flushed
Skin Moisture	1. normal, 2. dry, 3. moist, 4. profuse
Skin Temperature	1. warm, 2. hot, 3. cool, 4. cold
Respiratory Effort	1. normal, 2. shallow, 3. retracted, 4. labored, 5. intubated, 6. chest tube, 7. tracheotomy
Capillary Refill	1. immediate, 2. delayed, 3. none
Blood Loss	750 mL (default value)

4.2 Wound Location/Diagnosis

In addition to the observational data discussed above, the program must be informed as to the location of the injuries and their nature. The entry is performed in a separate menu that divides the body into five key areas: head, thorax (front and back), abdomen (front and back), upper extremities, and lower extremities. If one clicks the mouse on a particular region of the body, a submenu with an injury selection automatically appears. If "Penetrating Wound" is selected in any injury category, another menu item requests information as to whether single or multiple wounds are involved. This menu is currently used for documentation only, and can readily be eliminated to reduce the number of mouse clicks required for data input.

4.3 Injury Tracking

As noted in Section 3.7 above, multiple severe trauma conditions cannot at present be reliably handled. In part, this is due to the limited data available concerning the status of the trauma victim. In addition, the current collection of FDA-approved, non-invasive sensors are somewhat limited in their ability to diagnose many trauma conditions. This situation is likely to improve in the future. However, at present we found it necessary to restrict the use of the decision-making software to dominant injuries in one area of the body, that is, either the thorax anterior, thorax posterior, abdomen anterior, abdomen posterior, head, upper extremity, or lower extremity. Each condition selected in the wound location section shows up in the tracking menu and the user is asked to select the area to track.

The system architecture allows new sensors to be added as they become available. A list of present and emerging trauma sensors was presented earlier in Table 1. A good combination of sensors for hemorrhagic shock and airway obstruction is tissue serum lactate (and/or tissue P_{CO_2}) and end-tidal P_{CO_2}. Because of the much wider range of pressures that develop with CO_2, the sensitivity of CO_2 measurements of ischemia tends to be much greater than that obtained with O_2 techniques. Thus, tissue P_{CO_2} measurements provide important input for triage decisions and serve as a precise indicator of the success of resuscitation efforts. The simultaneous monitoring of tissue P_{CO_2} and end-tidal P_{CO_2} allows airway obstructions and early states of shock to be readily identified. When this project was initiated, it was thought that a FDA-approved tissue P_{CO_2} sensor would be available for diagnoses, but this sensor has yet to appear in the commercial marketplace.

4.4 Displays and Indicators During the Monitoring Period

A host of real-time displays are available during the patient monitoring period. These are described in detail in Section 10.2. The primary displays show results from the decision-making module and have associated alarms and patient status windows. In addition, parsed and processed sensor data are graphically displayed along with fully analyzed sensor values and trends. During the monitoring period, data from all active sensors are acquired at the maximum rate possible. The sensor data, combined with rule-based medical protocols, time dependent sensor profiles, and fuzzy logic, enable the decision-making software to monitor the patient. However, the user does not have to use the decision-making software. Options exist for monitoring only the processed and analyzed data in graphical and/or tabular formats. Sensor data are analyzed for validity, and commonly occurring artifacts are identified. For example, the analysis algorithm examines the data streams to determine whether a sensor is disconnected or improperly applied. Problems of this nature are reported to the user, and the data are automatically corrected.

5. Patient Data Acquired for Software Simulations

Data for simulations involving the knowledge-based software are obtained from trauma victims in intensive care units (ICUs) at LLUMC. Advance informed consent is obtained consistent with Title 10 U.S.C. 980. Patient data acquisition began in May 1999 and ended in April 2000. In general, Title 10 greatly limited the number of patient histories available to the

project. Over the course of a year, eight patient histories were obtained. As always, the adopted procedures for sensor data acquisition and the conditions for use of the patient records must be approved by the Institution Review Board. In addition, the medical equipment/computers must undergo instrument review by the hospital. LLUMC supplements the physiologic sensor measurements with other relevant hospital records

The data acquisition and display portion of the Knowledge-Based Diagnosis and Treatment Display Unit was developed first so that patient data could be obtained. The real-time display and appropriate trending algorithms proved beneficial for the physicians and nurses overseeing the patient in the ICU. In general, program participants obtained somewhat better care than they would have under ordinary circumstances. We found that the display unit with its trending capability materially assists the medical staff in determining the patient's current status and short-term prognosis. The length of observations for a given patient ranged from 2-4 hours. Complete patient records were obtained from LLUMC including admission records, physician notes, pharmaceutical records, invasive test results, surgical procedures performed, diagnosis, and discharge summary.

5.1 Colin Tonometer and Invasive Blood Pressure Measurements with the HP M1006B Arterial Pressure Module

An HP M1006B arterial-line (A-line) module was originally purchased so that invasive arterial pressure could be simultaneously monitored along with the noninvasive Colin tonometer measurements. Both units provide beat-to-beat blood pressure.

Arterial tonometry is an old technique first suggested in 1963 [*Pressman and Newgard*, 1963]; a comprehensive review of arterial tonometry is provided by *Drzewiecki et al.* [1983]. Early tests of the prototype for the Colin 9200 tonometer are described by *Sato et al.* [1993]. (The prototype was named JENTOW, which is an amalgamation the first letter of the last names of each of the inventors.) A validation study for the Colin tonometer is presented by *Zorn et al.* [1997]. The Colin tonometer overcomes the major problem of placing the transducer precisely on the radial artery with an array of 31 micro-piezoresistive transducers mounted on a silicon substrate. Each array element monitors the magnitude and shape of the arterial waveform and the best waveform is subsequently selected. An automatic mechanical sensor-positioning system is used to determine the best location for the array. A chronic problem with the tonometer arises from the need to immobilize the wrist during a period of continuous measurement. The reason

for this is that the instrument is highly susceptible to motion artifacts. Because of its sensitivity to motion, the tonometer worked best on trauma patients that were sedated or unconscious at the time of the measurement.

The tonometer requires an absolute calibration which is accomplished with the aid of an oscillometric cuff. Typically cuff measurements are recorded every 5 min to provide an "absolute calibration" of the tonometer. However, this calibration technique is not without error. Under ideal conditions (which are never realized in trauma care) random errors in systolic blood pressure measurement are commonly determined by the instrument exhaust rate during a single interpulse interval. Generally, this translates into systolic pressure error bars of ±1-3 mm for a given measurement.

During the course of tests conducted with the tonometer, the systolic blood pressure appeared to undergo a small secular drift between cuff calibrations on healthy volunteer subjects. This was evident when the systolic tonometer pressures were recalibrated by periodic cuff measurements. The apparent drift typically exceeded the estimated error bars of ±1-3 mm for the cuff measurements. At present, the drift is not well understood.

A-line measurements were introduced in part because of the high sensitivity of the tonometer to motion, general difficulties in properly positioning the tonometer on a patient, and uncertainties in the origin of the drift described above. In addition, the acquisition of the A-line data was prompted by an unresolved situation with a trauma victim wherein the A-line blood pressures on the right side of the body were significantly lower (20 mm Hg) than the cuff and tonometer on the left side. Obviously, a vascular blockage could have given rise to such a pressure differential. However, it is also possible that an instrument calibration error or some other systematic error existed which gave rise to an incorrect result. A key reason for acquiring the A-line data is to help eliminate uncertainties in the measurement process. Unfortunately, because the A-line data was added late in the program and the number of trauma patients involved in the study was limited, decisive tests of the tonometer versus the A-line pressure measurements could not be performed.

It should noted that other beat-to-beat blood pressure techniques were considered at the beginning of this program but only the Colin tonometer had FDA approval. A promising technique that is pending FDA approval is pulse wave velocity. This technique utilizes the measured wave velocity with the theoretical pulse propagation relation to determine arterial

pulsatile pressure [*Weltman*, 1959]. This simple technique is complicated by the fact that the pulse cannot be treated as a single frequency: wave propagation considerations must also include reflected waves from the periphery [*Noordergraaf*, 1978]. PWV Medical sells several pulse wave velocity units under the name SphygmoCor; it claims to be able to derive the pressure at the ascending aorta using mathematical models of hemodynamics.

5.2 Tests with the HP M1006B Arterial Pressure Module

This unit has an analog output that provides the pulse waveform from which systolic and diastolic pressures can be deduced. It also has a serial port for digitally processed data. The digital data generated by the HP M1006B is used exclusively by the hospital as part of its normal operations. Because each data stream is completely separate from the other, no activities on the part of GRI can affect the hospital readings. The use of the HP M1006B required approval by the LLUMC IRB. Ultimately, the tonometer was replaced by the HP M1006B unit.

The diagnostic and treatment display unit employs a small 12-bit analog-to-digital converter to sample the pulse waveform provided by the HP M1006B. The digitization rate is set at 300 samples/s. The complete digitized pulse waveform is archived in a data file for later use. In addition, the acquisition unit computes the systolic and diastolic pressures periodically (once every 1.08 s) and displays the measurements in real-time for use by attending physicians and nurses. A single calibration process is used to determine absolute blood pressures for the analog and digital outputs.

5.3 Arterial-Line Data Analysis

A-line data obtained from a trauma patient was analyzed in detail to verify data quality and integrity and determine reasonable averaging/fitting parameters for the calculation of trends. Figure 9 illustrates the methodology for systolic and diastolic blood pressures and pulse rate. The top panel shows the calibrated raw data that is acquired with the acquisition system. These data are subsequently low-pass filtered to generate a baseline having a period that closely corresponds to the respiration rate. In addition, pulse waveform data are also low-pass filtered at a higher cutoff frequency to eliminate random noise from the signal. The intersection of the baseline with the pulse waveform determines the locations of zero crossings from which the pulse period is determined. This is illustrated in the third panel from the top. The maximum and minimum between the zero crossings are by definition the systolic and diastolic blood pressures.

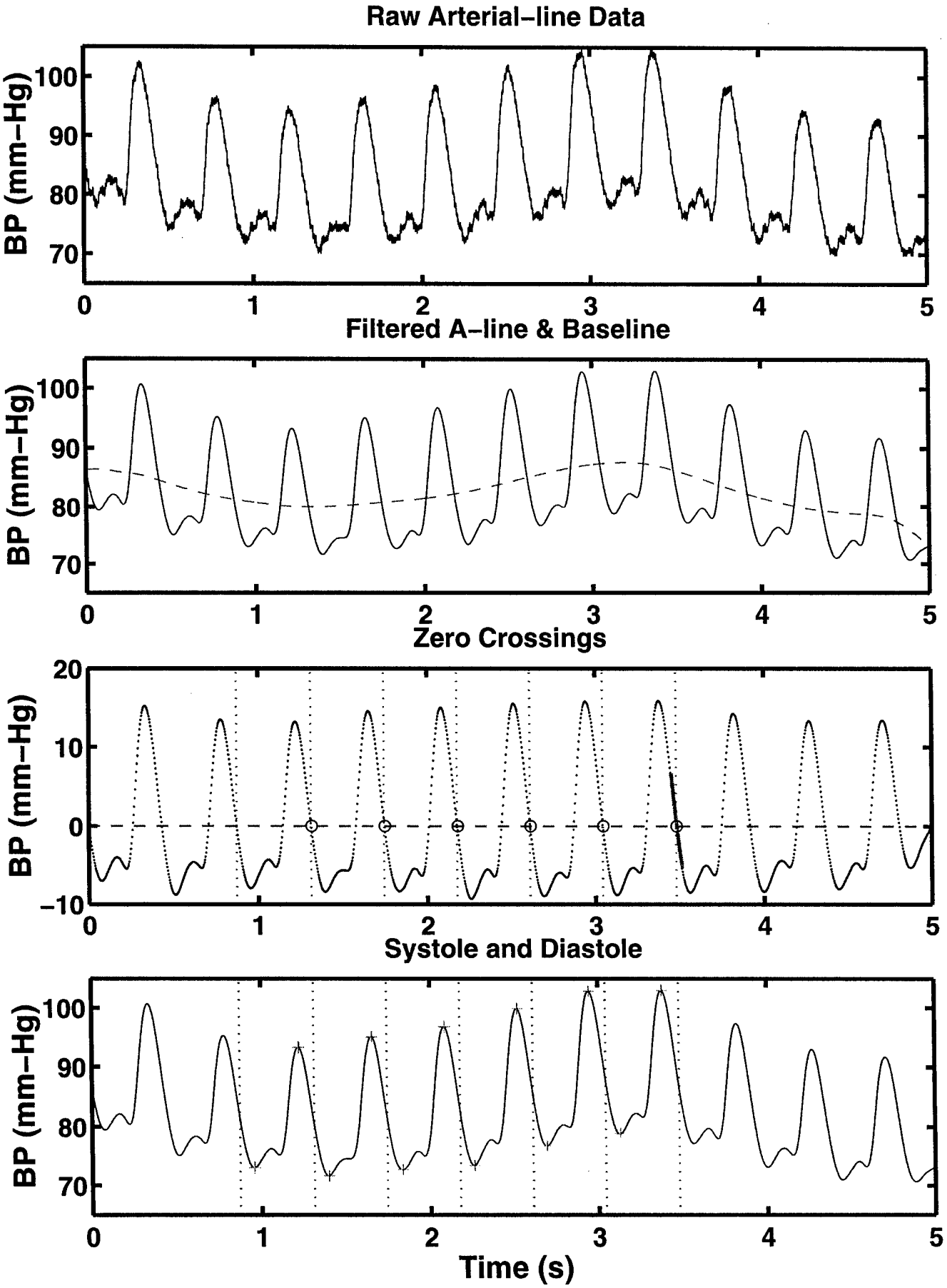
Raw Arterial-line Data
BP (mm-Hg)
100
90
80
70
0
1
2
3
4
5
Filtered A-line & Baseline
BP (mm-Hg)
100
90
80
70
0
1
2
3
4
5
Zero Crossings
BP (mm-Hg)
20
10
0
-10
0
1
2
3
4
5
Systole and Diastole
BP (mm-Hg)
100
90
80
70
0
1
2
3
4
5
Time (s)

Figure 9

In Figure 10, the pulse rate determined from the A-line is compared with the heart rate simultaneously measured via ECG. The A-line data was averaged over ten points to make it consistent with the processing performed by the Colin firmware on the ECG signal. The two pulse rates match up very well. Slight differences arise because the Colin firmware rounds off the pulse rate to an integer value whereas this is not done for the A-line observations. A line fit to the A-line pulse to pulse measurements shows that the average pulse rate increased from an initial value of 138.9 beats/min at a rate of one beat every 7 min: 55 s (Figure 11).

One can also deduce the respiration rate from the temporal modulation of the pulse waveform. Figure 12 illustrates how this was done. The calibrated raw data was low-pass filtered to remove the pulse waveform (second panel from the top). The raw data is then filtered to remove both the pulse and respiration signatures (third panel from the top). The subtraction of panel 3 from panel 2 yields the respiration signature shown in panel 4. This signal can now be processed to obtain the magnitude of the respiration modulations and respiration rate. These are shown in Figure 13. The respiration rate is virtually constant at 18.2 breaths/min because the patient was attached to a ventilator. Figure 14 shows the residual pulse pressure associated with the respiratory cycle.

An autoregressive analysis of the beat-to-beat systolic and diastolic blood pressures is presented in Figure 15. The most prominent spectral features are the respiration rate peak (3.32 s, 18.1 breaths/min) and its second and third harmonics at 1.68 s and 0.84 s.

The temporal history of the pulse waveform shape is analyzed in two different ways in Figures 16 and 17. Figure 16 shows blood pressure versus time at various locations within the pulse cycle, whereas Figure 17 depicts the steepness of the pulse waveform at positive and negative going zero crossings. In Figure 17, the correlation of the two slopes with time is shown along with the average deduced correlation coefficient, which yields a probability of linear correlation of greater than 99.99%.

For completeness, all parameters measured simultaneously with the Colin 9200 instrumentation suite are shown in Figure 18. Dropouts in the data are caused by problems with the Colin firmware used to drive its serial data line.

Overall, the vital signs deduced from the A-line measurements are consistent with the parameters measured by other sensors on the Colin instrumentation suite. The analyses also

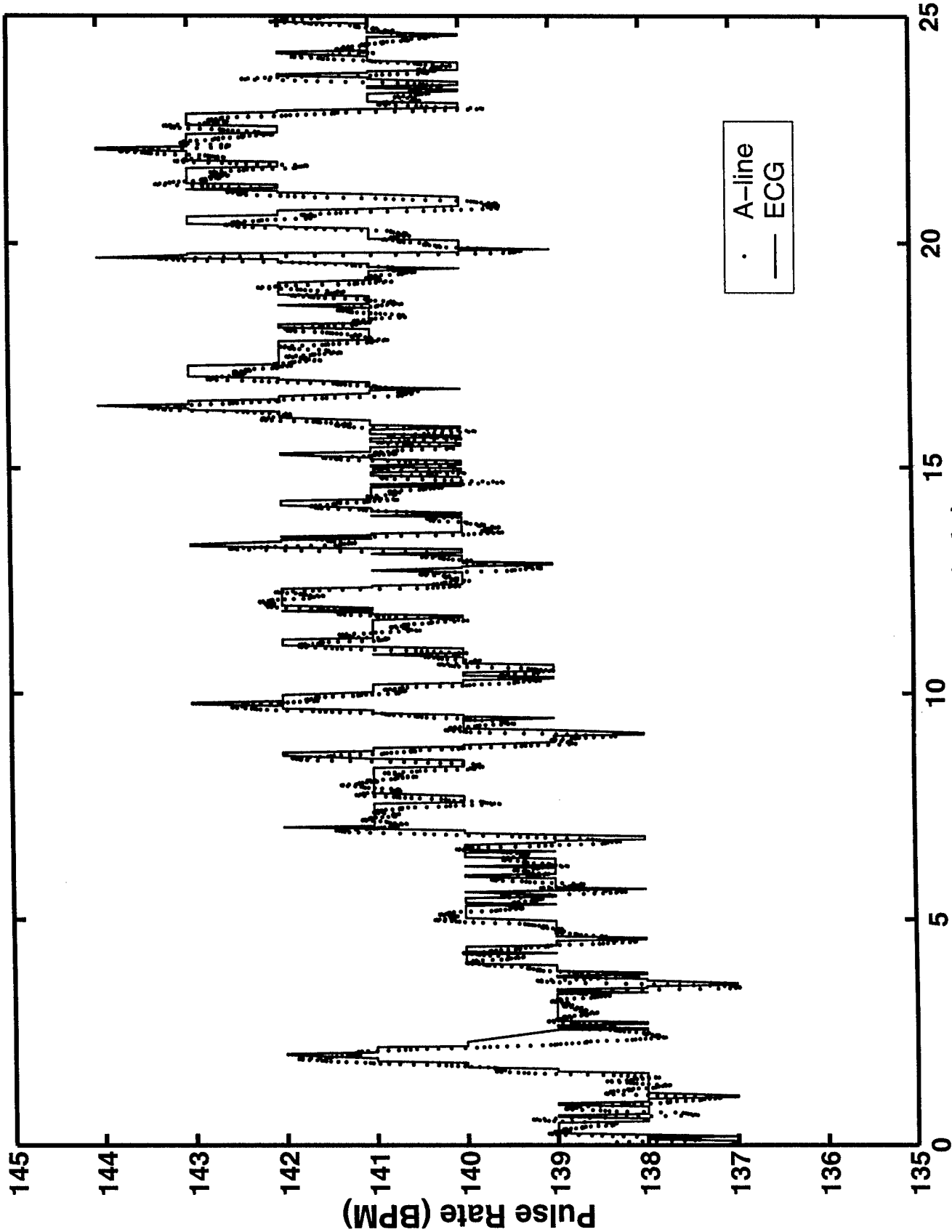
Pulse Rate
Pulse Rate (BPM)
Time (min)
A–line
ECG
145
144
143
142
141
140
139
138
137
136
135
0
5
10
15
20
25

Figure 10

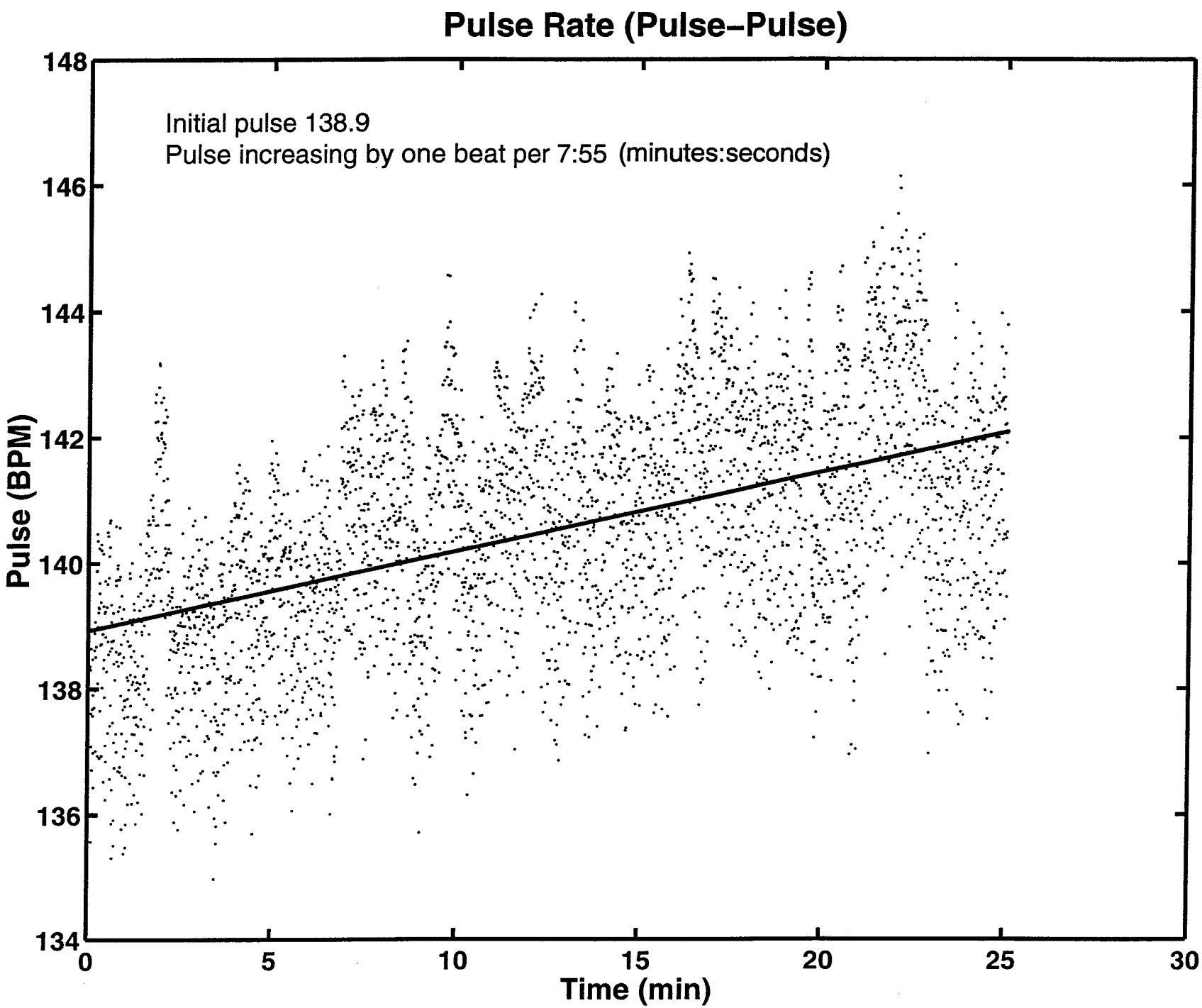
Pulse Rate (Pulse–Pulse)
Initial pulse 138.9
Pulse increasing by one beat per 7:55 (minutes:seconds)
Pulse (BPM)
148
146
144
142
140
138
136
134
0
5
10
15
20
25
30
Time (min)

Figure 11

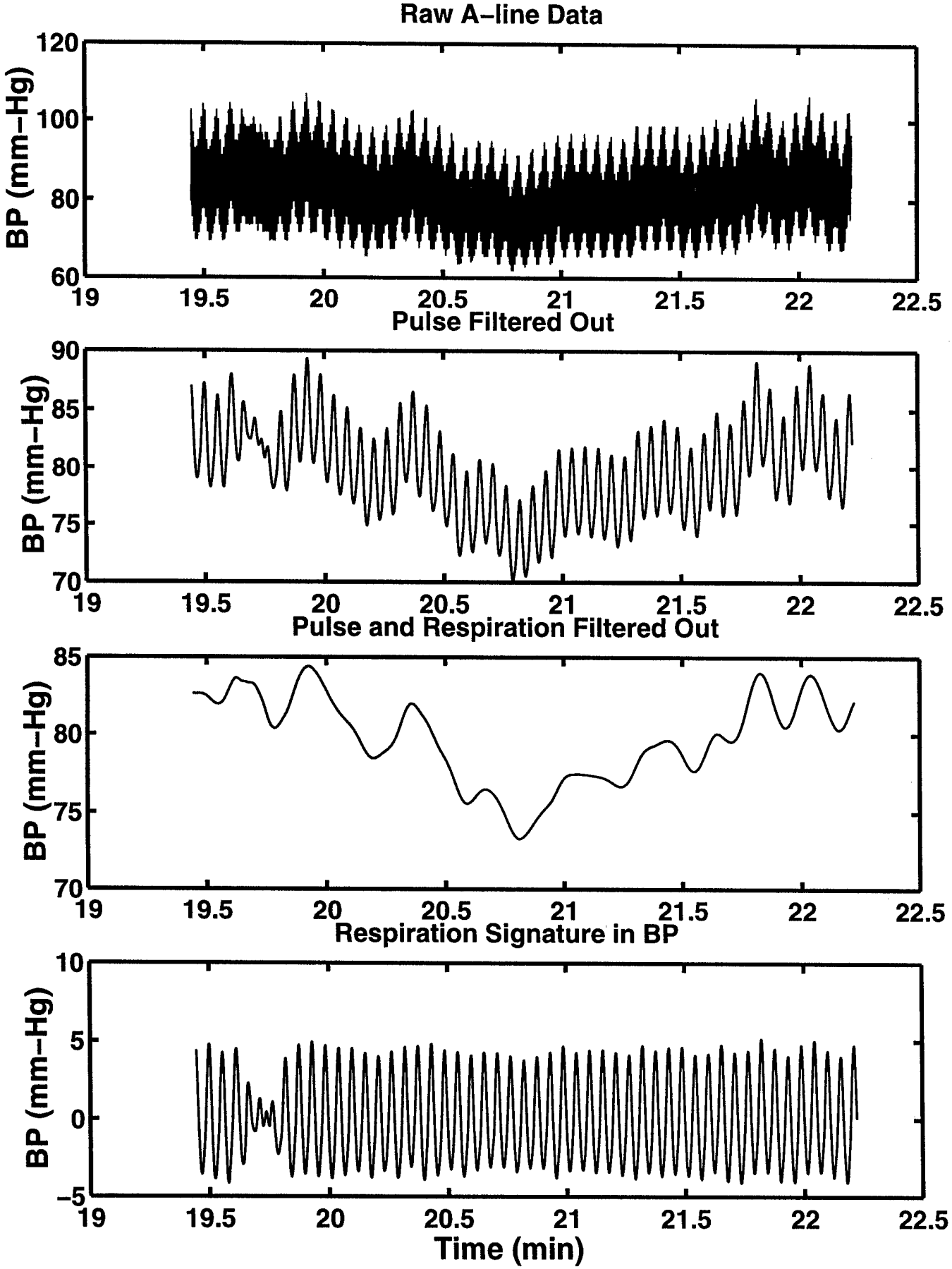
Raw A-line Data
BP (mm-Hg)
120
100
80
60
19
19.5
20
20.5
21
21.5
22
22.5
Pulse Filtered Out
BP (mm-Hg)
90
85
80
75
70
19
19.5
20
20.5
21
21.5
22
22.5
Pulse and Respiration Filtered Out
BP (mm-Hg)
85
80
75
70
19
19.5
20
20.5
21
21.5
22
22.5
Respiration Signature in BP
BP (mm-Hg)
10
5
0
-5
19
19.5
20
20.5
21
21.5
22
22.5
Time (min)

Figure 12

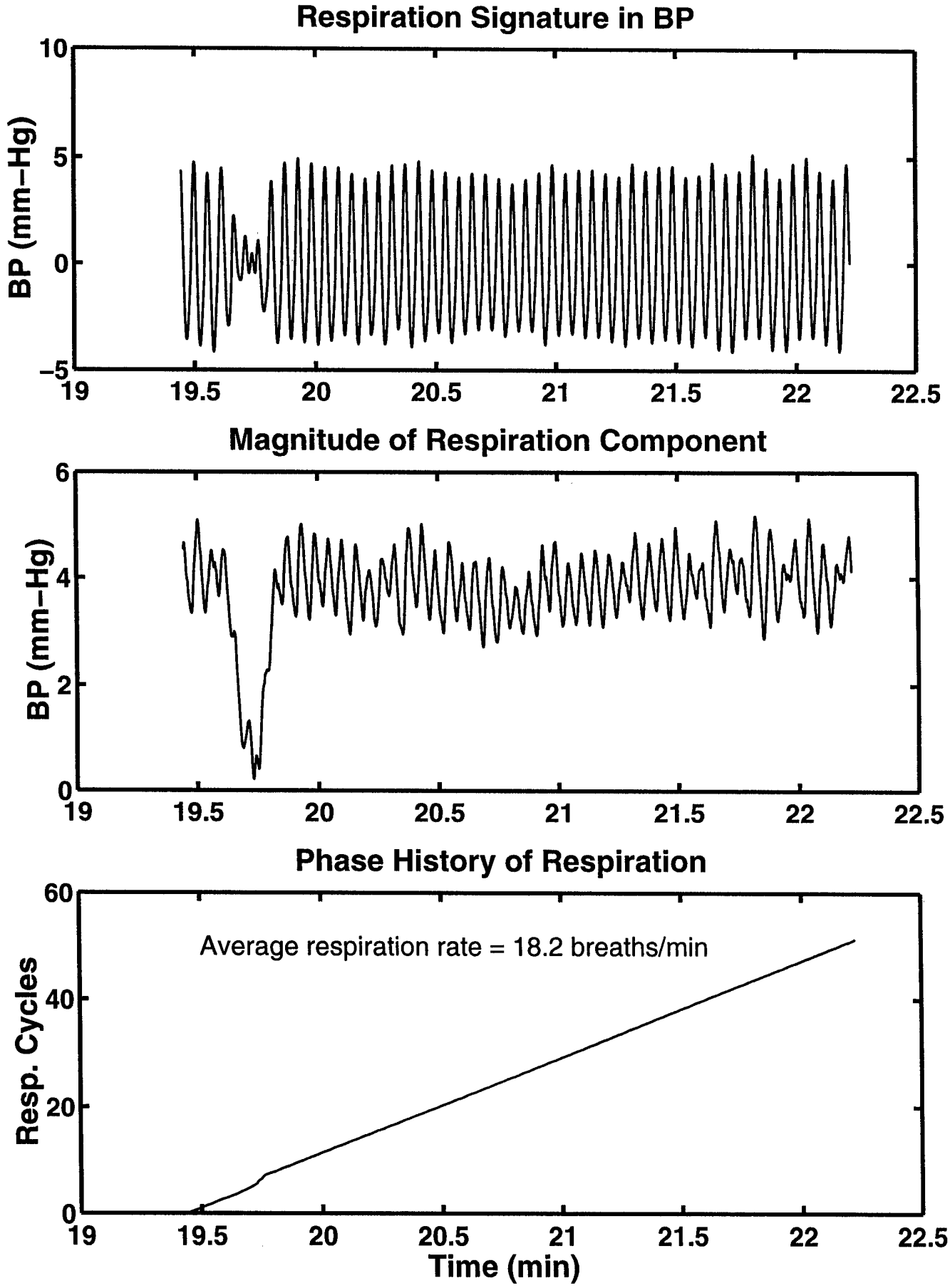
Respiration Signature in BP
BP (mm–Hg)
10
5
0
–5
19
19.5
20
20.5
21
21.5
22
22.5
Magnitude of Respiration Component
BP (mm–Hg)
6
4
2
0
19
19.5
20
20.5
21
21.5
22
22.5
Phase History of Respiration
Average respiration rate = 18.2 breaths/min
Resp. Cycles
60
40
20
0
19
19.5
20
20.5
21
21.5
22
22.5
Time (min)

Figure 13

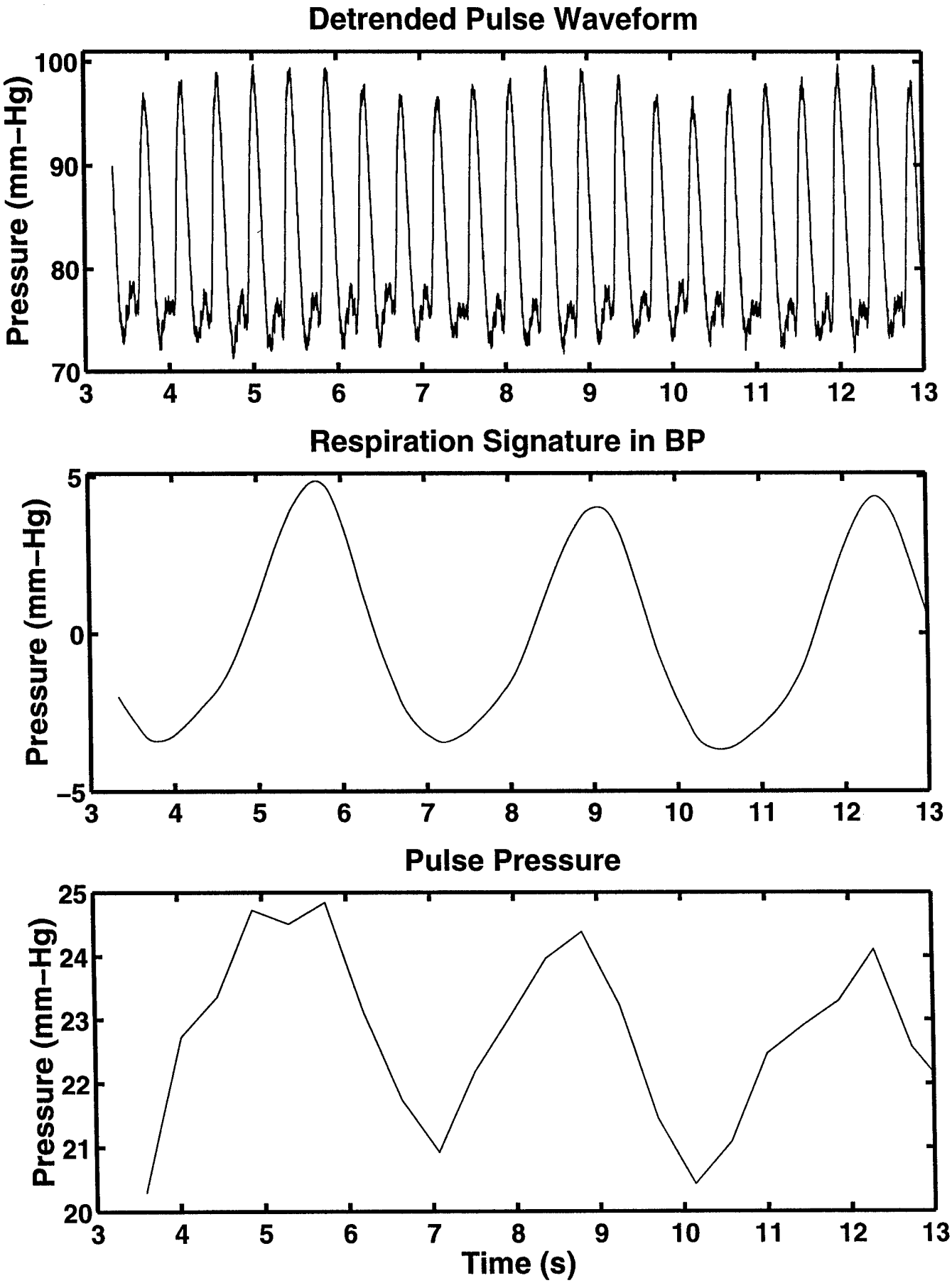
Detrended Pulse Waveform
Pressure (mm–Hg)
100
90
80
70
3
4
5
6
7
8
9
10
11
12
13
Respiration Signature in BP
Pressure (mm–Hg)
5
0
–5
3
4
5
6
7
8
9
10
11
12
13
Pulse Pressure
Pressure (mm–Hg)
25
24
23
22
21
20
3
4
5
6
7
8
9
10
11
12
13
Time (s)

Figure 14

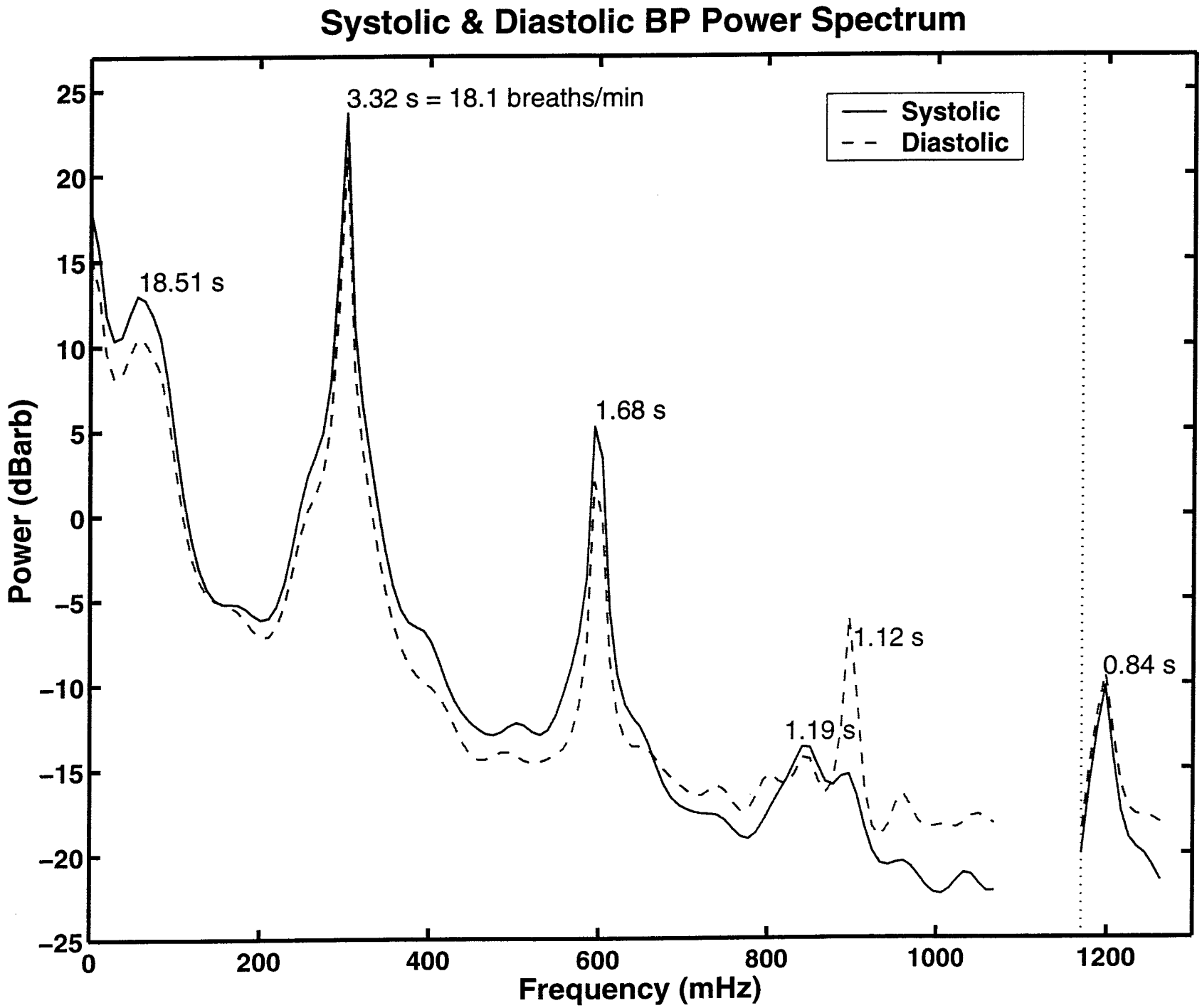
Systolic & Diastolic BP Power Spectrum
3.32 s = 18.1 breaths/min
Systolic
Diastolic
18.51 s
1.68 s
1.12 s
1.19 s
0.84 s
Power (dBarb)
Frequency (mHz)
25
20
15
10
5
0
−5
−10
−15
−20
−25
0
200
400
600
800
1000
1200

Figure 15

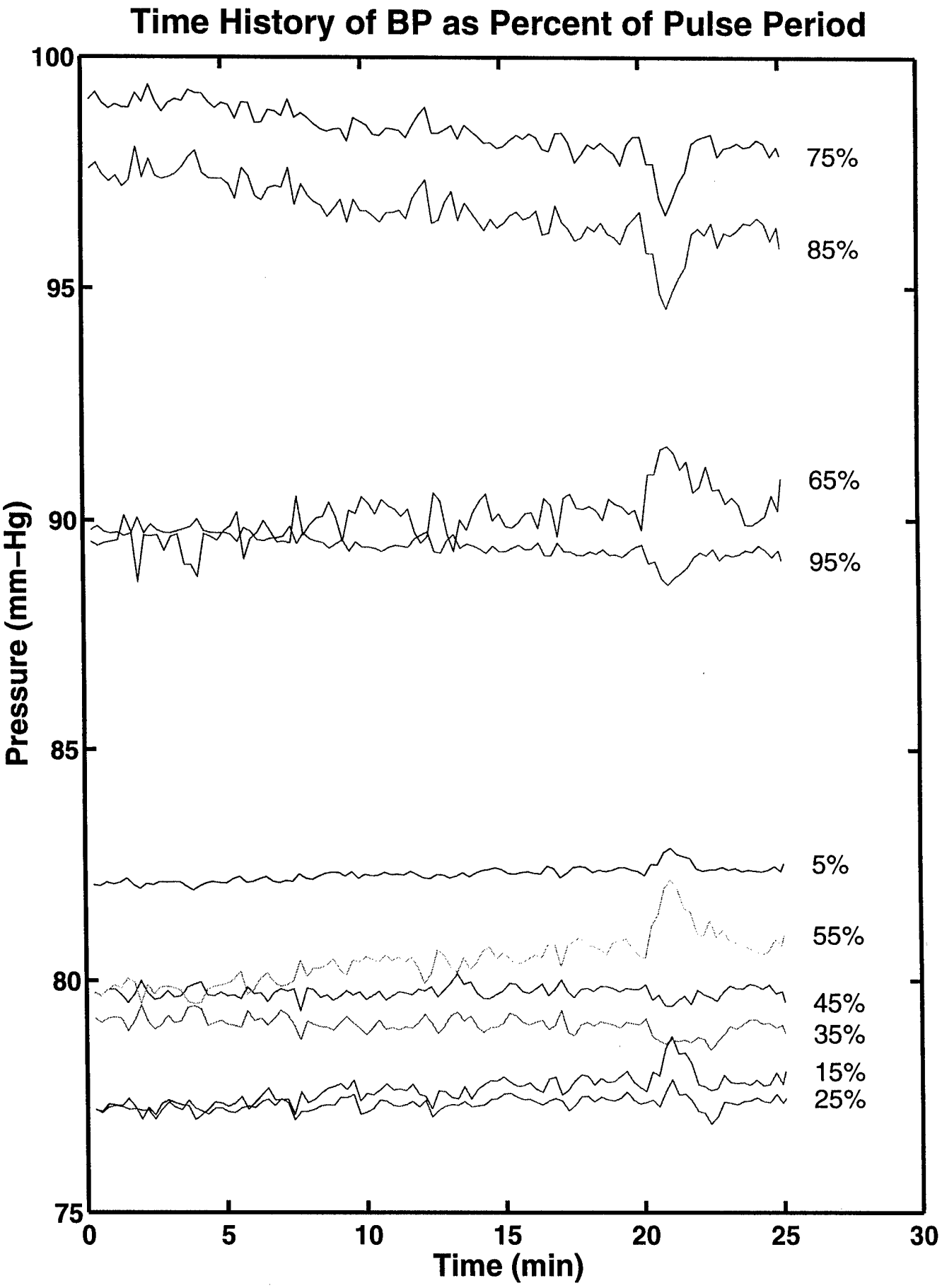
Time History of BP as Percent of Pulse Period
100
95
90
85
80
75
Pressure (mm-Hg)
0
5
10
15
20
25
30
Time (min)
75%
85%
65%
95%
5%
55%
45%
35%
15%
25%

Figure 16

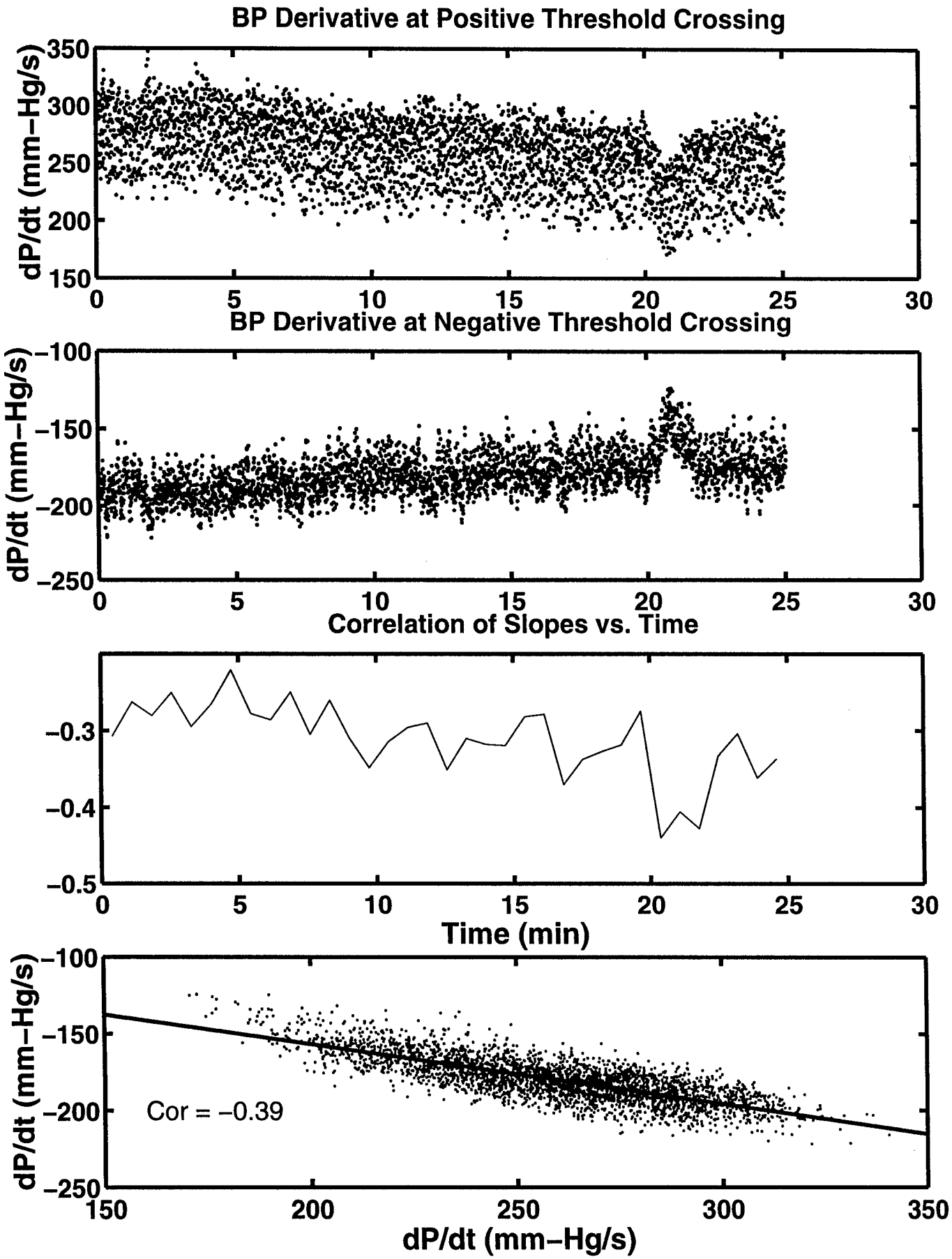
BP Derivative at Positive Threshold Crossing
dP/dt (mm–Hg/s)
350
300
250
200
150
0
5
10
15
20
25
30
BP Derivative at Negative Threshold Crossing
dP/dt (mm–Hg/s)
–100
–150
–200
–250
0
5
10
15
20
25
30
Correlation of Slopes vs. Time
–0.3
–0.4
–0.5
0
5
10
15
20
25
30
Time (min)
dP/dt (mm–Hg/s)
–100
–150
–200
–250
Cor = –0.39
150
200
250
300
350
dP/dt (mm–Hg/s)

Figure 17

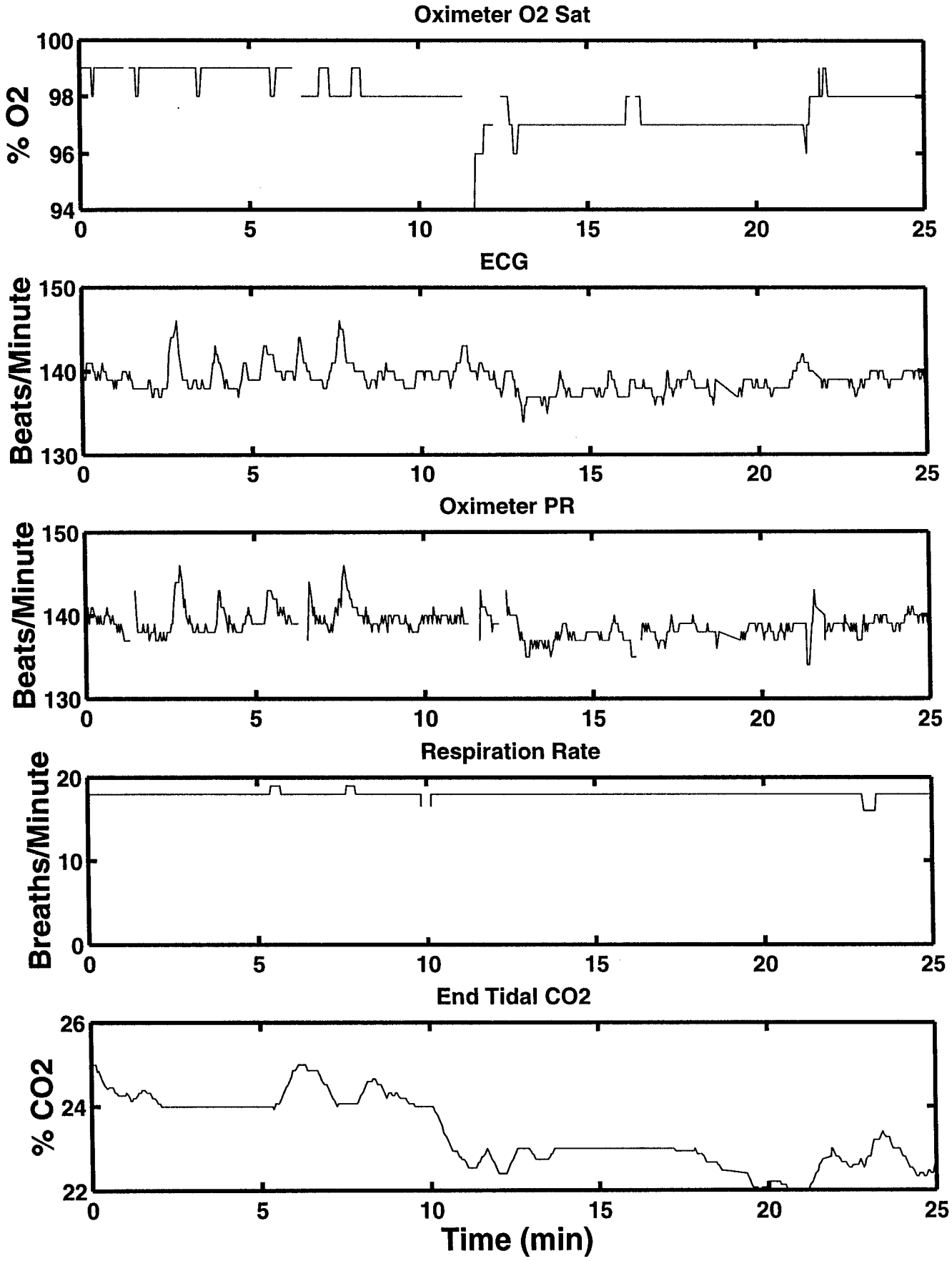
Oximeter O2 Sat
% O2
100
98
96
94
0
5
10
15
20
25
ECG
Beats/Minute
150
140
130
0
5
10
15
20
25
Oximeter PR
Beats/Minute
150
140
130
0
5
10
15
20
25
Respiration Rate
Breaths/Minute
20
10
0
0
5
10
15
20
25
End Tidal CO2
% CO2
26
24
22
0
5
10
15
20
25
Time (min)

Figure 18

indicate that very small trends in blood pressure, pulse rate, and respiration can be detected with the A-line data.

Finally, the A-line data was highly useful in establishing meaningful averaging, fitting, and smoothing intervals for the determination of systolic blood pressure trends. Figure 19 illustrates a reasonable set of parameter values selected for the trending of a 95-minute data segment. The first 25 minutes of observations (samples 0 through 5660) were used in the A-line analyses described above. The mean of the systolic blood pressure is represented by a dark, thick line in the upper panel. It was obtained by averaging 100 consecutive measurements and then fitting ten of the averaged values to a straight line. A moving fit is employed in that the most recent average value replaces the oldest average in the 10-point fitting routine to yield one smoothed value for every averaged value. The slopes of the fitted values are presented in the bottom panel. Two methods for processing the slopes are illustrated. In one case the calculated slopes are digitally filtered over a 15 point interval, while in the second case the data were fit over 15 points to obtain the average slope. Both cases generate slowly varying rates of change that are not influenced by rapid, clinically insignificant fluctuations in blood pressure. The rate of change is expressed in units of mmHg per 100 points or equivalently mmHg change per 36-s interval.

6. Inference Engines and Decision-Making Software

As part of this research program, Geospace Research, Inc. performed an extensive survey of inference engines currently on the market and carefully investigated their relevance to the present project. There are more than two hundred professional expert system products in the commercial marketplace, but only a few notable inference engines. The inference engine is usually a purchased program that resides on the main computer system. However, the knowledge base which invokes the inference engine is a program that is developed by the user (e.g., GRI). The knowledge base contains all of the rules, variables, attributes, and procedures necessary to make informed medical decisions. The inference engines considered for this project include "G2" from Gensym Corporation, XpertRule from Attar Software, and Haley Enterprise's "Eclipse." Eclipse uses the Rete algorithm to support both forward and backward chaining; it includes a programming interface for ANSI C and Visual Basic. Both Gensym and Attar have user-friendly developmental interfaces, and all three incorporate fuzzy logic (a necessary requirement for medical decision-making) into the inference engine. Our experience in the

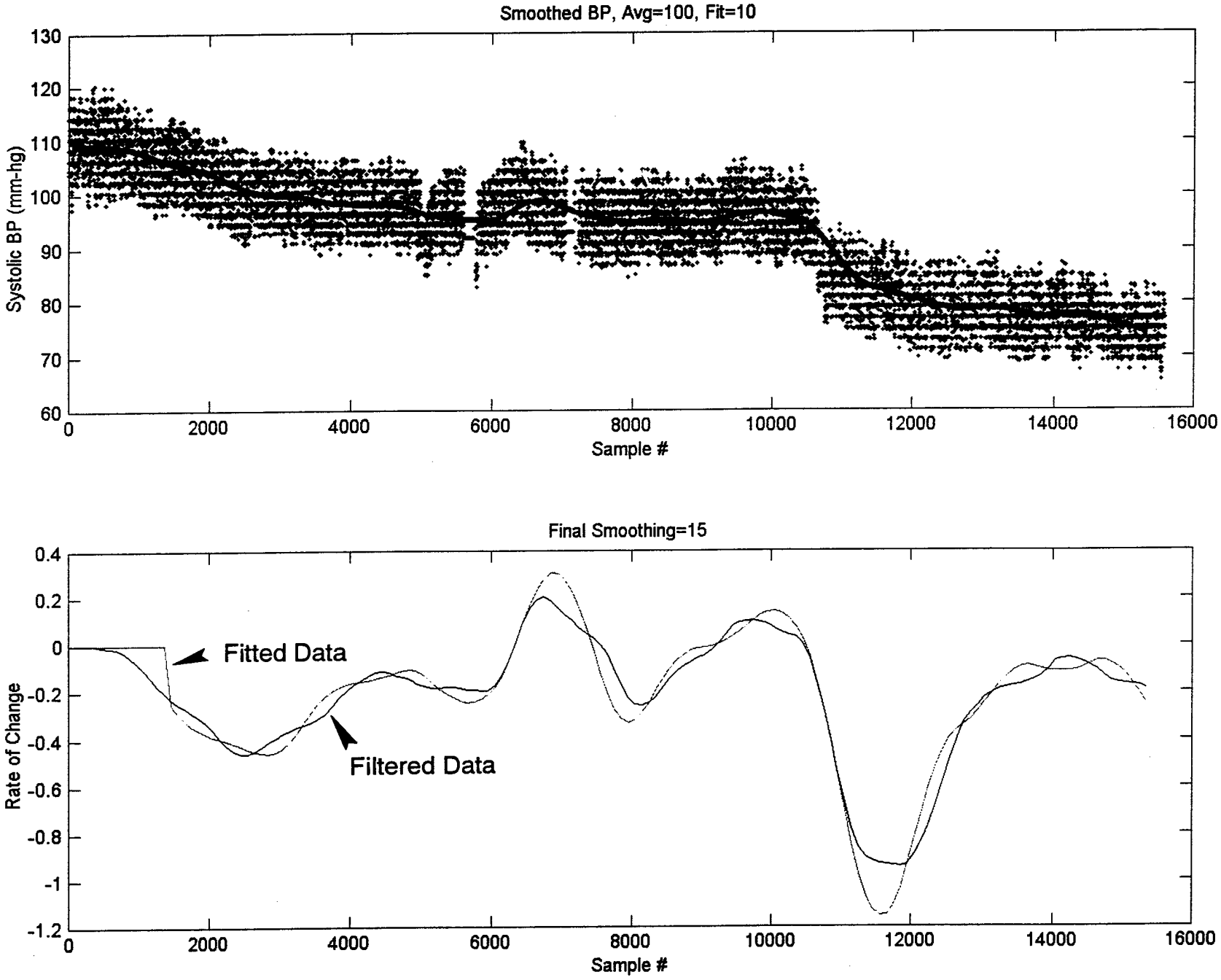
Smoothed BP, Avg=100, Fit=10
Systolic BP (mm-hg)
Sample #
Final Smoothing=15
Rate of Change
Fitted Data
Filtered Data
Sample #

Figure 19

Phase 1 study indicated that a developmental interface dramatically reduces programming time and allows the user to focus on developing an accurate and complete knowledge base.

XpertRule was initially selected for use in this project. XpertRule is a compact knowledge-based development program with an embedded Graphical User Interface (GUI). Both G2 and XpertRule implement efficient forward and backward chaining, rule confidence estimates, system confidence reporting, rule priority assignments, as well as a choice of inference strategies. However, XpertRule allows the backward and forward chaining to be controlled and mapped, which is not the case with G2. A chaining map is provided as a menu item in XpertRule. A particular task may be chained backwards or forwards to find a missing attribute, or the particular operation may be left unchained. Because the chaining path is limited to the rules and tasks prescribed, the chaining process does not encompass the entire knowledge base. Thus, the user is in complete control of the chaining process. Although XpertRule does not prevent a user from using chaining loops it considers illegal, it does "red line" such loops in the chaining map.

As in the case of Gensym's G2/GDA, XpertRule makes fuzzy logic available as part of the inference process. XpertRule is not unlike Gensym GDA in that it restricts the user to classical trapezoidal membership functions within the Fuzzy Logic Editor.

We encountered difficulties in implementing Attar's XpertRun ActiveX with high-level programs such as National Instruments' LabVIEW. XpertRule expects a detailed (low-level) programming interface to be present. For example, the interfaces available with Visual Basic or Visual C are acceptable to XpertRun ActiveX, but programs such as LabVIEW are not. As a result, ActiveX does not represent a viable means for data exchange and communications among programs used in the diagnostic and treatment display unit. However, this was resolved by using external semaphores (timing routines) and Windows NT system calls to the kernel.

Nevertheless, we found that XpertRule program execution times were far too slow and consumed too many system resources when interfaced with the complete data acquisition and data-processing system. Recall that a key goal was to operate the knowledge-based system from a high-performance laptop, and that all programs must run simultaneously. We also used G2/GDA for several trial runs and found that it was also too slow and consumed too much memory. Most expert system engines are developed under the assumption that all computer system resources will be made available to the program. This is not the case in the current

project. Data must be acquired and parsed from many medical sensors and the data from each sensor has to be processed and analyzed in real-time. Although mathematical calculations can be performed within an expert system, this code is interpreted rather than compiled. Moreover, we have included an analog-to-digital acquisition card in the system so that data from prototype sensors can readily be interfaced to the system. This put additional demands on computer resources, but it is essential if one is to accommodate newly emerging medical sensors.

The immediate solution was to write a decision-making kernal in the C programming language and make it part of a Windows NT library. This is referred to as the Decision-Making Module (DMM). This greatly improved program speed and allowed the decision-making software to co-exist with all other programs. At the same time, we left the program interface to XpertRule in place. XpertRule may become viable as processor speeds increase and/or after a new version of XpertRule is introduced (in 2001) with a new ActiveX interface. A technical description of the setup and implementation of the Windows NT library functions within LabVIEW is provided in Appendix A.

7. Knowledge-Based Software Developed Under This Program

In this section, the full version of the software program developed as part of this project is described. Various elements of this program can be readily omitted giving rise to a more compact program. The objective of this section is to describe all of the features currently available with this program. The software package developed by Geospace Research, Inc. is referred to as Trauma Evaluation and Analysis, or TREA for short. TREA is designed to work under the Windows NT operating system.

As noted earlier, several different program modules are run simultaneously so that physiological sensor data can be acquired, parsed, processed, and analyzed. The results are sent to the decision-making module which constantly examines the patient and determines how severe the injuries are or are about to become. Changes in patient status are continuously examined and re-examined over short (~ 2 min), medium (~ 10 min), and long (~ 60 min) time scales. Warnings are issued as "severity indices" increase. (This rating system is discussed in detail below.) If a patient is determined to have a critical diagnosis, the program will not tolerate any instability in the trauma victim's physiological parameters; it will automatically issue a critical warning requesting that an attending physician or physician's assistant re-examine the patient. At

the same time, trends in biomedical parameters are calculated and examined within the context of the diagnosis presented to the program. If the program determines that the changes in physiological parameters are inconsistent with the suggested diagnosis, a warning of a diagnosis mismatch is issued.

7.1 Overview

From a software architecture standpoint, the knowledge-based program begins with several setup routines which allow the user to select various sensor combinations for analysis, input observational data related to the trauma victim's medical status, indicate wound locations and pathophysiologic assessments, and select the primary injury to be tracked. The Setup module consists of 16 subroutines used to gather user input and initialize data-acquisition subsystems. Additionally, data storage files are opened and all other program modules are initialized. As part of the setup process, either the standard real time mode or a demo mode can be selected. The demo mode allows the user to run the program with one of three patient data sets. The demo mode allows the user to become accustomed to the program interface and program operations without having to insert valid physiologic data streams into the computer's serial-line and/or PCMCIA inputs.

Once the setup is completed, the program becomes operational. The program can readily be terminated by clicking the stop button on the real-time sensor display. Except in the case of the demo mode, the program acquires sensor data in real time, immediately parses and processes these data, then writes both the processed data and the original binary sensor data to disk, and finally plots the time histories of the unanalyzed sensor data on a large display. When demo mode is invoked, raw sensor data is read from a binary file and processed in exactly the same manner as in the real-time mode and the processed data is written to the hard disk. However, a second binary file containing the raw sensor data is not generated in demo mode. The data acquisition and storage tasks described above are performed with the aid of LabVIEW 5.0, which also serves as the graphical user interface. This portion of the program is referred to as the data acquisition/processing module (DAPM). The data is analyzed in real time with the aid of an NT library written in the C language. This is referred to as the real-time analysis module (RTAM). Finally, analyzed results are passed on to the decision-making module (DMM) for examination. DMM also takes the form of an NT library and like the RTAM is written in C. Details

concerning specialized library functions developed as part of this project are provided in Appendix A.

7.2 Real-Time Data Analyses

Data are simultaneously acquired by several different sensors, usually at varying rates. Figure 20 illustrates the data reduction process for a single physiological parameter measured with a sensor. This analysis process is reproduced for each medical parameter available. Thus, typically 10-15 parameters are being analyzed in parallel. The first stage of the data reduction screens the sensor input for properly formatted numbers. An incorrectly formatted number in the digital data stream is commonly referred to as Not a Number (NaN) and is automatically discarded by the program. The mean and standard deviation of the points in the data stream are calculated for each sensor. Points falling too far from the mean are rejected as outliers and are not included in the analysis.

7.3 Outlier Screening

The screening algorithm for outliers is outlined in Figure 21. The screening is intended to remove artifacts from the data such as those generated by sensor movement or disconnection of the sensor from the patient. In addition, the program must be able to eliminate artifacts generated by such events as randomly timed instrument calibrations and the administration of IV boluses (which typically leads to impulsive increases in blood pressure). If the current data point is greater than a specified number of standard deviations above the mean, the point is removed from the fitting process. This threshold limit is a user input. A viable value derived from detailed studies of patient data is ~2.75 sigma. The FIFO used to determine the mean value for the screening process and the current standard deviation is altered depending on whether or not the point is greater than 1.5 sigma above the mean. If it is not, this point is stored in the FIFOs used to calculate the current mean and standard deviation. The rationale is that points that are only 1.5 standard deviations above the mean are not readily distinguishable from the statistical population as a whole. If all such points were eliminated, the statistical distribution will be altered. Moreover, by keeping all of these points, one allows the mean and standard deviation to grow slowly in response to a changing statistical distribution of data points.

Points greater than 1.5 standard deviations must be processed in a different manner to avoid the large instantaneous impact of the outlier. The outlier value is replaced by the current

Data Reduction Process

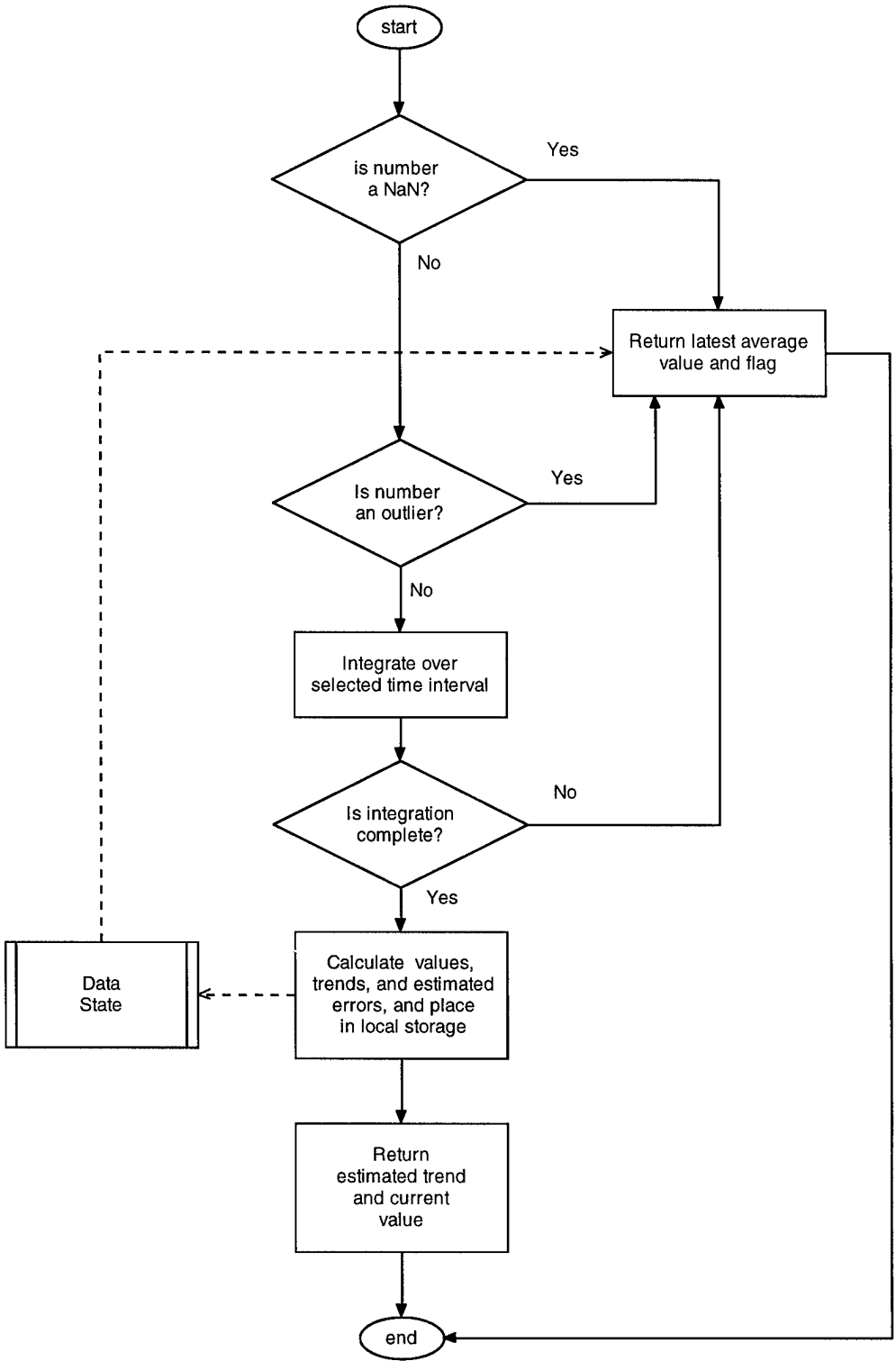

Figure 20

Outlier Screening Process

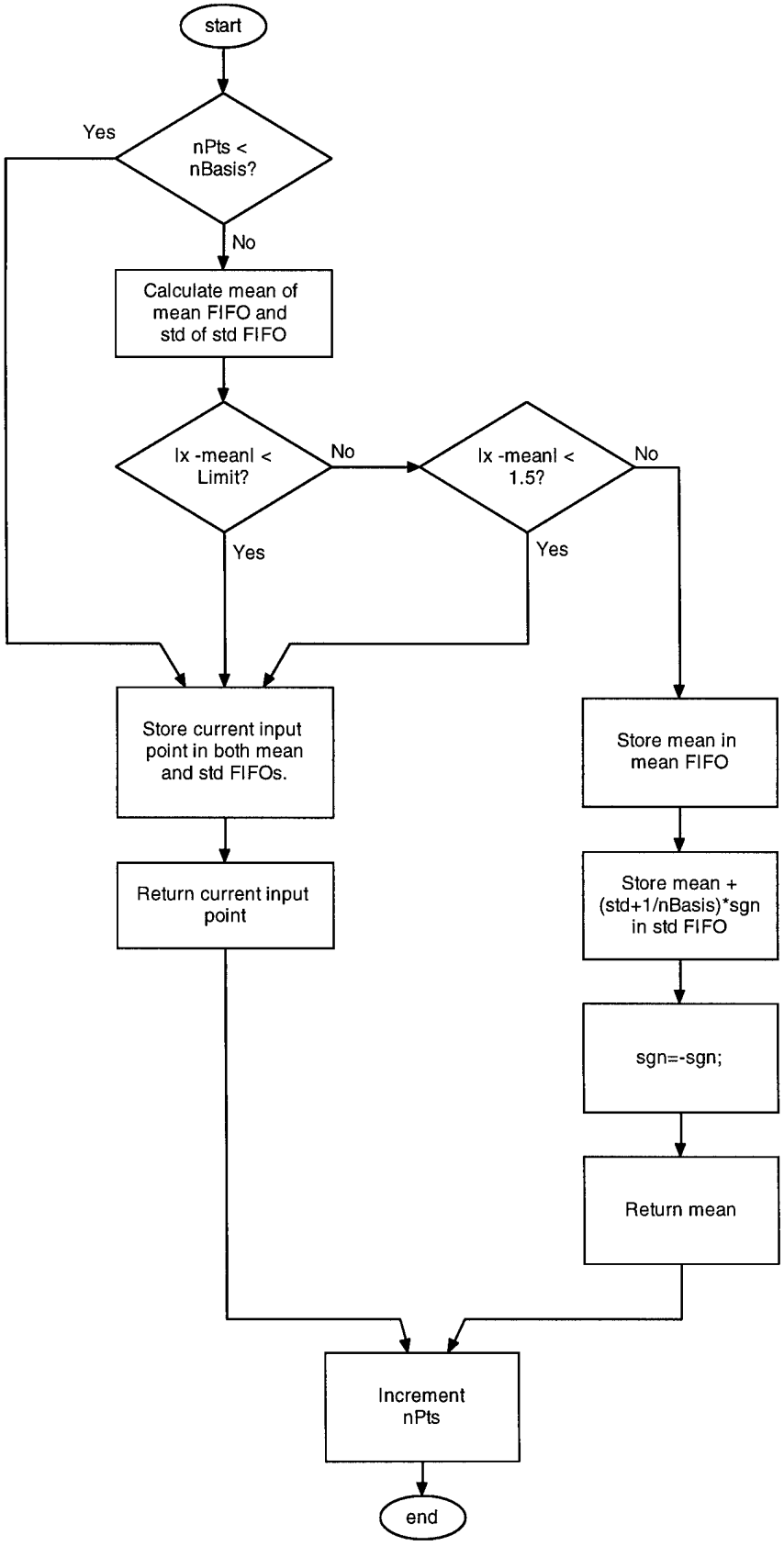

Figure 21

mean value in the data FIFO used to calculate the mean for the screening process. In the standard deviation FIFO, the outlier is replaced by a value equal to the mean ± (1 + 1/Nbasis) standard deviations, where Nbasis is the number of points used as the statistical basis for excluding outliers. The sign of the artificially added fluctuation is reversed for every other outlier to avoid generating a bias in the distribution function. The strategy of synthesizing points in the outlier screen buffer allows the standard deviation to slowly grow to admit larger statistical fluctuations as might be necessary if the fluctuation level of the data were increasing. Note that the screening buffer points are not used by any other element of the analysis program; it is used only in the screening routine. The threshold of 1.5 standard deviations was arrived at through extensive analyses of patient data. The granularity of this study was 0.1 standard deviations. Thus, 1.5 is optimized relative to 1.4 or 1.6 standard deviations. If outlier points were simply eliminated from the screening standard deviation buffers, the standard deviation of the screening data could dwindle over time until all data points are rejected because of the very small standard deviations that develop.

After the outlier screening process (Figure 20), the data is integrated over a predetermined time period (not for a specific number of points) and the variance is calculated. A typical integration period is 10 to 30 seconds, depending on the sensor parameter. The integrated data point serves as an input for least-squares fitting to a straight line; each data point is weighted by its calculated variance. The number of points to be fitted to a straight line is selectable, but typical values range between 5 and 10. The fitting is performed every time a new data point becomes available. The most recent point is added to the FIFO stack and the oldest point is dropped. Average data values and their first derivative (trend) are obtained from the fitting process. One-sigma error values are calculated for both the fitted data values and the trends.

7.4 Mapping of Sensors

Each sensor has its own data stream, and internal storage is maintained for each data stream, whether or not the sensor is enabled. This is necessary because medical sensors are typically activated in a step-wise fashion. Several different sensors may provide data relating to the same biomedical parameter. For instance, the patient's pulse rate/heart rate may be measured by the pulse oximeter, the ECG, and the tonometer. The tonometer itself produces pulse rate data with two temporal resolutions, one near 10 s and another near 1 s. Although all four data streams are

reduced and fitted, only one is used for monitoring patient status. In the current program, the sensors to be used for measurements of blood pressure and pulse rate are selected by the user. The mapping of sensors to biomedical parameters is depicted in Figure 22.

7.5 Early Detection of Downturns in Patient Status

It is not unusual for a patient who initially appears to be in a stable condition at the trauma site to suffer a major decline during transport to a regional trauma center. The current program is designed to alert trauma support personnel regarding a suspected downturn in patient status. An essential input to the DMM is the smoothed, analyzed data that yields the current value and trend of every measured parameter. As can be seen with the aid of Figure 19, the analysis process can detect very small trends in biomedical parameters and use these data as early warning indicators. The program is currently set up to monitor seven biomedical parameters: systolic blood pressure, diastolic blood pressure, pulse pressure, O_2 saturation, end-tidal CO_2, pulse rate, and respiration rate. It is anticipated that additional diagnostics will become available in the future and provisions for these additions have been made. The program tracks the stability of these parameters and generates a severity warning based on how rapidly the readings deteriorate. The deterioration in condition is viewed within the context of the preliminary diagnosis supplied by the user. Additional warnings may be generated if parameter trends are inconsistent with patient diagnosis or if the patient suffers a setback because of a developing critical injury (e.g., an undetected hemorrhage).

7.6 Severity Calculation

Consistent with triage guidelines at a battalion aid station, a patient is assumed to be in the stable state when initially attached to medical sensors. The patient is viewed as being hemodynamically stable, although he may not be hemodynamically normal. When a stable state prevails, data are displayed normally and no alarms are issued. A patient is deemed to be stable if all measured parameters are stable. A parameter is stable over a time period, t, if time-to-limit, t_L, is greater than t_{LIM}:

$t_L = t(\text{LIM}-x)/\text{sum}(t; dx/dt) > t_{LIM}$, where t_{LIM} is user specified but nominally set to ~60-90 minutes, x is the current value of the parameter and LIM is the limiting value of the parameter.

Mapping of Sensors to Biomedical Parameters

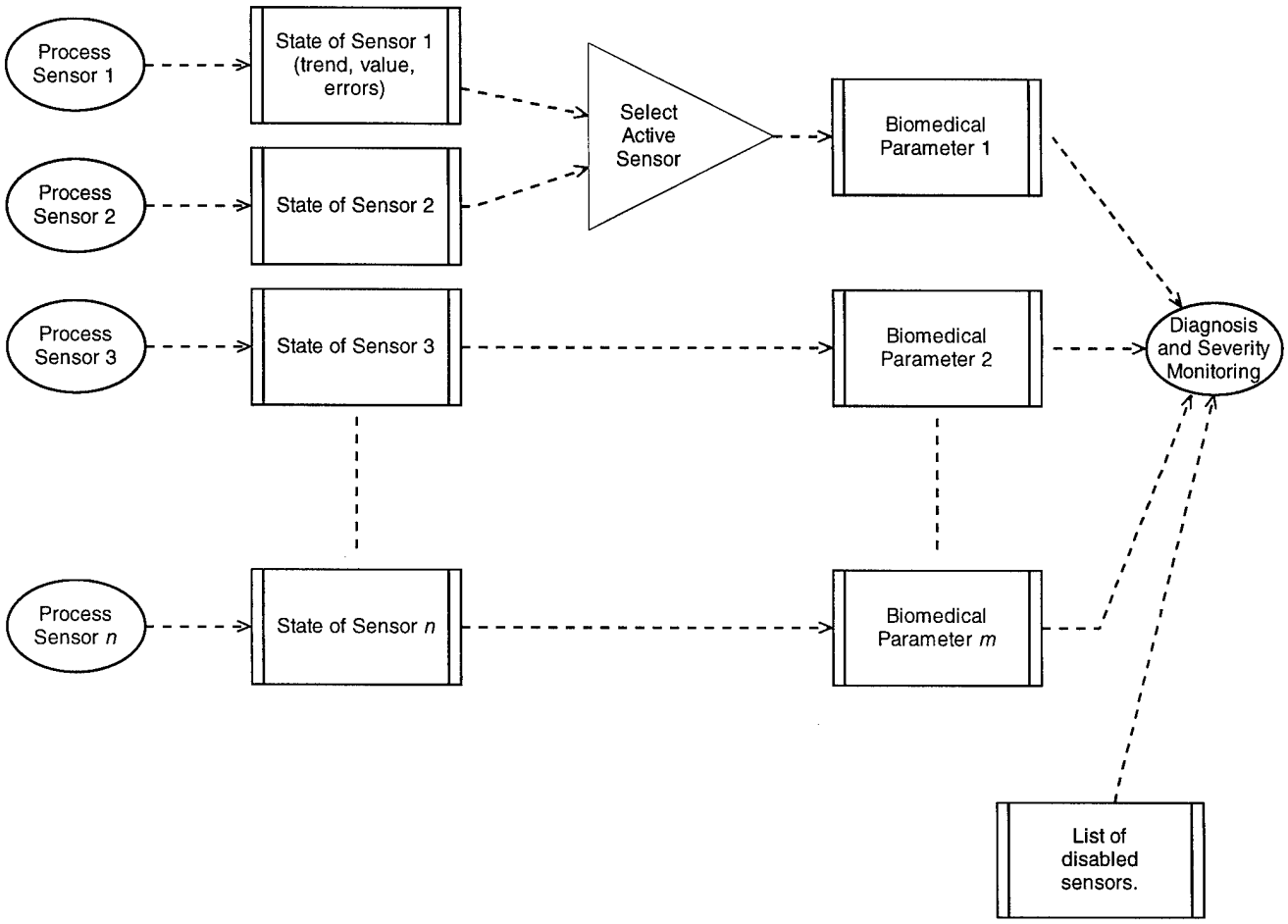

Figure 22

If one or more parameters do not fulfill the conditions for stability, the patient is deemed unstable. The instability is assigned a severity rating. The severity, s, is assigned as follows:

Set each t_L to t_{MAX} (nominally 60-90 min, but user selectable) for all stable parameters, otherwise use calculated t_Ls, where

$s = (\text{sqrt}(\text{sum}(t_L^{-2}))*K\text{-}1)*10$,

where K is calculated as $1 / \text{sqrt}(n/t^2_{MAX})$, n being the number of available biomedical parameters.

Examples of how the time to limits of six parameters combine to yield a severity rating are illustrated in the table below.

Table 4. Severity Parameter Calculated from Six Independent Bio-Medical Parameters

P1	P2	P3	P4	P5	P6	Severity
60	60	60	60	60	60	0
50	60	60	60	60	60	0.3602
40	60	60	60	60	60	0.9925
30	60	60	60	60	60	2.2475
20	60	60	60	60	60	5.2753
10	60	60	60	60	60	16.1408
5	60	60	60	60	60	39.8333
50	5	60	60	60	60	39.9068
40	5	60	60	60	60	40.0419
30	5	60	60	60	60	40.3324
20	5	60	60	60	60	41.1536
10	5	60	60	60	60	45.3777
5	5	60	60	60	60	59.7618
50	50	50	50	50	50	2.0001
40	40	40	40	40	40	5.0001
30	30	30	30	30	30	10.0001
20	20	20	20	20	20	20.0001
10	10	10	10	10	10	50.0003
5	5	5	5	5	5	110.0005

The severity index is used to provide an estimate of how unstable the trauma victim is. In general, severity indices ≤10 are considered mild, those in the range 10-25 are moderate, and those above 25 are severe. The GUI displays the severity indices calculated over short (2 min), medium (10 min), and long (60 min) time scales and uses indicator lights of green, yellow, and red for mild, moderate, and severe conditions, respectively.

7.7 Diagnoses

All possible diagnoses are not incorporated into this prototype system. However, the program is designed to be incrementally expandable in this area. Conditions addressed by the prototype system include: (1) ARDS, (2) hypovolemic shock, (3) hemo-pneumothorax, (4) cardiac tampanade, (5) head injury, (6) respiratory failure, and (7) neurogenic shock. Each condition is characterized in Section 3 above.

In Table 5 below, the trends of each biomedical parameter are characterized by direction (+ , -, or No Change, nc) and the magnitude of the trend (small S, medium M, large L). The designations of S, M, and L represent "fuzzy" attributes that characterize the trends in the DMM. A program flag is set when the trends of unstable biomedical parameters do not match the expectations shown in Table 5; this triggers an alarm in the display unit.

Table 5. Trends in systolic blood pressure (SBP), pulse pressure (PP), O_2 saturation (SaO2), end-tidal CO_2 (EtCO2), pulse rate (PR), and respiration rate (RR) for seven diagnoses.

Diagnosis	SBP	PP	SaO2	EtCO2	PR	RR
ARDS	- S	nc	- M	+ M	+ M	+ M
Tamponade	- M	+ M	- S	- S	+ M	- S
Head Injury	+ L	nc	- L	+ M	- M	- M
Hemo-pneumothorax	- L	nc	- L	+ L	+ L	+ L
Hypovolemic Shock	- M	- M	- M	+ M	+ L	+ M
Neurogenic Shock	- M	nc	- M	+ M	+ M	- M
Respiratory Failure	- S	nc	- L	+ L	+ M	- M

Figure 23 illustrates the manner in which the diagnosis and severity ratings enter into the decision-making process. Certain diagnoses can be considered critical while others are less demanding and termed normal. A critical diagnosis means that if certain measured parameters become unstable, the timeline to irrecoverable injury and death is very short. Examples include pneumothorax wherein an open pneumothorax may convert to a tension pneumothorax. Similarly, in the case of severe head injury, intracranial pressure (ICP) will increase dramatically once the point of compensation is reached on the ICP versus volume of mass curve. A quick response is needed to save the individual. The program knows that if a patient with a critical

Diagnosis & Severity Rating System

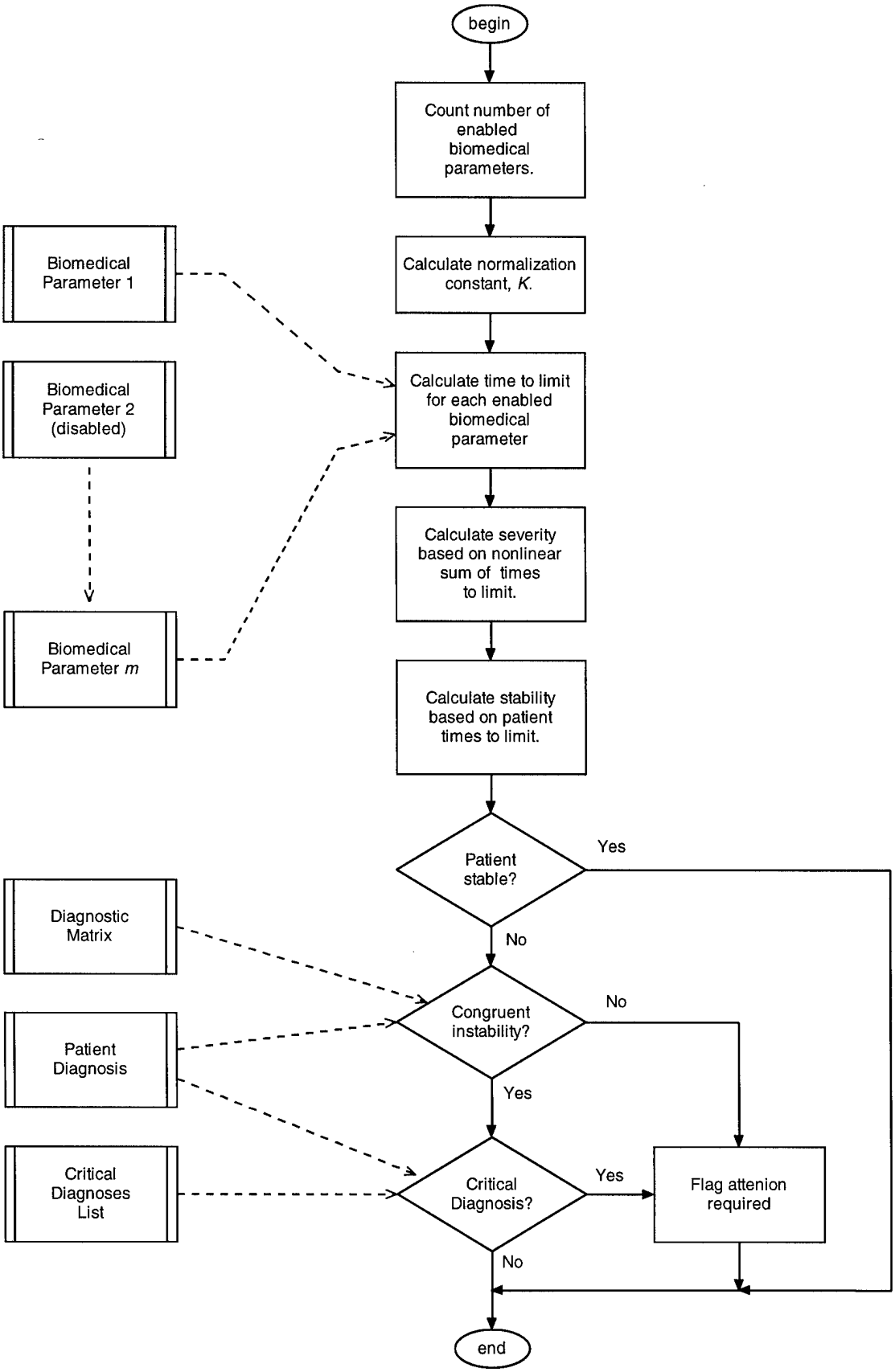

Figure 23

diagnosis becomes unstable, medical attention must immediately be summoned. For example, if a patient with a head injury or pneumothorax becomes unstable, this will also be flagged as a potentially critical event.

8. Operation of the Knowledge-Based Display and Diagnosis Software

The software written for this project was developed and implemented on a Toshiba Satellite 4030 CDT laptop computer. The program was also successfully tested on a more powerful Toshiba Tecra 8000 laptop. Both computers contain 366 MHz Intel Mobile Pentium II processors. The Satellite has 64 MB memory and 6.4 GB hard drive space, whereas the Tecra has 256 MB memory and an 8.2 GB hard drive. The additional memory of the Tecra facilitates certain real-time program activities such as the processing of incoming sensor data and the implementation of the decision-making software. The beat-to-beat data line from the Colin tonometer is inserted into serial port #1 at the back of the laptop. The second Colin data line containing the standard 2-second weighted output from the instrument suite is inserted into the serial I/O card which is inserted into one of the PCMCIA slots. The PCMCIA card is manufactured by Socket Communications (Model SL0707-078 Ruggedized Serial I/O Card). A-line data or other analog data is acquired with the aid of a DAQCard-500 data acquisition card from National Instruments. The DAQCard 500 occupies the second PCMCIA card slot. This unit has eight single-ended input channels, 12-bit resolution, and operates at a maximum data rate of 50 kilosamples per second.

As noted above, the name of the software package developed by Geospace Research, Inc. is Trauma Evaluation and Analysis (TREA). TREA is designed to work under the Windows NT operating system. The program encompasses 179 LabVIEW subroutines, an extensive NT analysis library, and a specialized decision-making module that also takes the form of an NT library.

8.1 Creation and Use of Data Files

As part of the program setup and subsequent program operation, data files are created to store medical observational inputs, wound locations, the trauma condition being tracked, raw and processed sensor data, notes generated by the attending physician or physician's assistant, and a debug file that documents all program activities. The latter is useful in the event that the program gives unexpected results. Data files are never overwritten; the program automatically

assigns a unique, usually sequential, name whenever it opens a new file. In some cases new folders are created at the same time.

The program also reads data from existing files on the hard drive. Examples of such files include patient data files used for the "live demo" mode of operation, a list of critical diagnoses, and DOS batch files called by LabVIEW. Table 6 below shows the default locations of files generated or used by the program.

Table 6. Default locations for program files.

Folder	Designated File Names, Data Type	Description
C:\external\patdat	demo_pat?_t2.dat, binary demo_pat?_tn.dat, binary demo_pat?.bin, binary	Colin averaged data, 2-s readouts Colin beat-to-beat data Raw A-line digitized data
C:\external\PFE	Program File Editor program files, various	Used to enter text notes related to the status of the patient during the operation of the program
D:\TREA\Diagnosis	Note??.txt, ASCII	Text notes documenting patient status
D:\TREA\Diagnosis\GSW\g??	head.dat, thorax_front.dat, thorax_back.dat, abdomen_front.dat, abdomen_back.dat, upper_extremity.dat, lower_extremity.dat, ASCII	Number and nature of wounds sustained
D:\TREA\Diagnosis\nonsensor\ns???	BloodLs.dat, CapRefill.dat, MotorResp.dat, PupilCond.dat, PupilResp.dat, RespEffort.dat, SkinColor.dat, SkinMoist.dat, SkinTemp.dat, VerbalRes.dat, ASCII	Nonsensor, observational inputs
D:\TREA\Diagnosis\Tracking\tk???	head.dat, thorax_front.dat, thorax_back.dat, abdomen_front.dat, abdomen_back.dat,	Specifies trauma condition tracked by the decision-making module

	upper_extremity.dat, lower_extremity.dat, ASCII	
D:\TREA\DS_DIR	Debug.log, ASCII Critical.dat, ASCII	Documents activities of the real-time analysis and decision-making software Input file containing list of critical diagnoses
D:\TREA\RawData\Aline\ binasc???	binasc???.txt, ASCII	A-line data processed in real-time by the TREA program
D:\TREA\RawData\Aline\ Pat???	Pat???.bin, binary	Raw voltage A-line data from which the systolic and diastolic blood pressures are deduced
D:\TREA\RawData\T2\ Pat???	cuffbp.dat, degC.dat, ecg.dat, gases.dat, N2O.dat, ox.dat, t2bp.dat, pat???.dat ASCII	Files used to record Colin 2-s measurements of cuff blood pressure, core temperature, ECG values, blood gases, N_2O, pulse oximetry, tonometer blood pressure, and all patient data accepted as valid by the program during the ??? run of the program (dat.pat???).
D:\TREA\RawData\T2\ raw???	raw???.dat binary	Raw data stream generated by the Colin T2 serial data line
D:\TREA\RawData\TN\ Pat???	pat???.dat ASCII	Contains beat-to-beat systolic and diastolic blood pressure measurements and pulse rate measurements accepted as valid by the program during the ??? run of the program
D:\TREA\RawData\TN\ raw???	raw???.dat binary	Contains raw pulse-by-pulse systolic and diastolic blood pressure and pulse rate generated by the Colin TN serial data line.
D:\TREA\XRule	Currently not in use	For the storage of XpertRule results once an improved version of the program becomes available in 2001
D:\TREA\Temp	AL_cur.dat, T2_cur.dat, TN_cur.dat ASCII	Temporary storage of the current sensor data for use by other programs.

D:\TREA\Batchfiles	*.bat ASCII	DOS batch files called by LabVIEW

The files D:\TREA\RawData\TN\raw???\raw???.dat, D:\TREA\RawData\T2\raw???\raw???.dat, and D:\TREA\RawData\Aline\Pat???\Pat???.dat contain records of the raw binary data furnished by the Colin beat-to-beat tonometer channel, the standard 2-second weighted data from the Colin Instrumentation Suite, and the output of the analog-to-digital converter used to acquire A-line data, respectively. These files are quite useful in that they can be read by the program in "Demo Mode" to replay the real-time data acquisition process.

8.2 Operation of the TREA Program

In this section, the full version of the TREA program is described. It is relatively easy to spin off versions of the program that are more streamlined and do not have the detailed menus of the full version. However, for completeness, the full version is described below.

8.2.1 Setup

To activate the program, double-click the TREA icon in the D: drive root directory. The menu entitled Setup System Parameters Figure 24 will appear. This allows the user to redefine the location of the data stored on the hard drive. The default directory is D:\TREA.

When the Continue button is clicked the Program Setup in Figure 24 appears. In the upper left panel, one can select among three types of analysis and processing: Decision-Making, Trending Graphs, and Display Raw Data. By choosing "Decision-making" mode, the user takes full advantage of all elements of TREA. This includes the decision-making module and real-time data analysis capability discussed above. When "Trending Graphs" is chosen, sensor data are processed and displayed in graphical format. This mode does not include any real-time analysis or decision-making capability. Its utility lies in the testing of sensor measurements; it is also a viable option when no real-time analysis is desired. Finally, "Display Raw Data" provides only the current numerical values that are output by the active sensors in the Colin instrumentation suite.

The display on the top right allows the user to turn on the A-line data acquisition and/or the beat-to-beat tonometer read-out and/or the standard two-second weighted data from the Colin instrumentation suite. The latter provides the best selection of vital signs. In most cases, tonometer and the vitals are selected. If A-line data is available, this item is chosen as well.

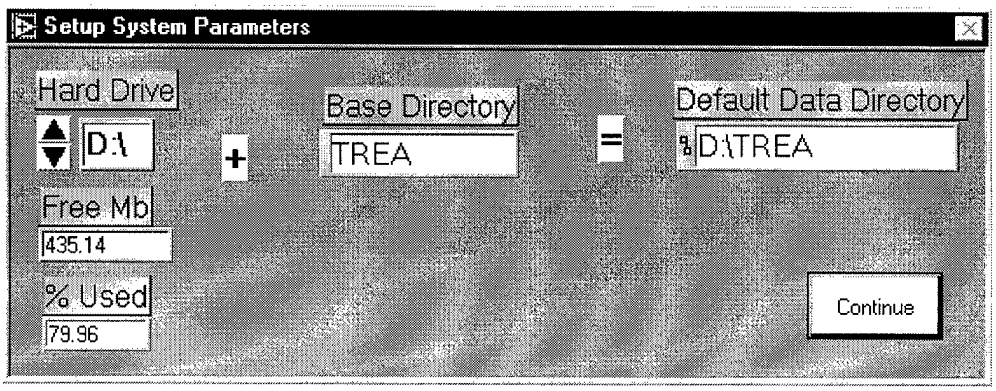

System Setup Menu

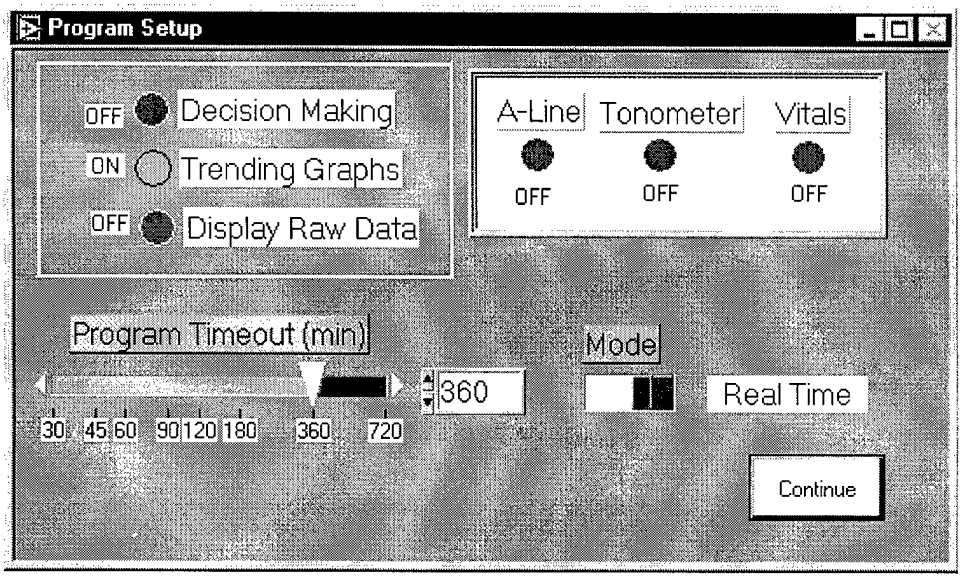

Program Setup Menu

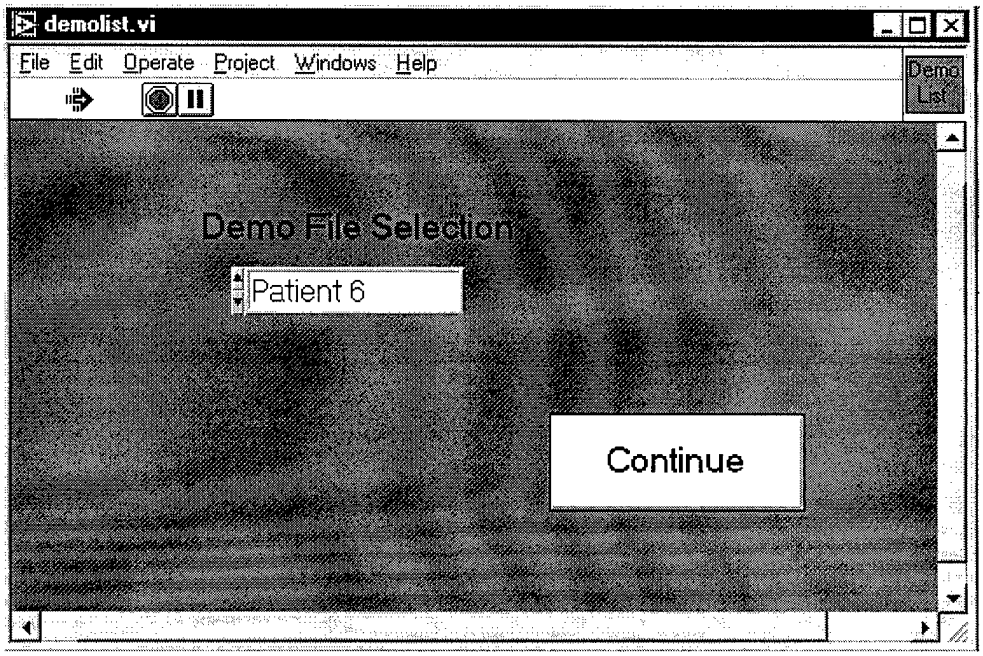

Demo File Menu

Figure 24

The program has an automatic timeout feature. This prevents the needless accumulation of useless data when the monitoring period concludes and the user fails to turn off the program. When the menu first appears, it is set at the default value of 360 minutes. The timeout period can be reset by either moving the sliding bar in the lower left portion of the menu, or by changing the digital indicator to the right of the sliding bar. The minimum timeout is 30 minutes, and the maximum is 720 minutes. Once the program is initiated in either the real-time or demo mode, the timer begins its count down. After the selected time period has expired, a timeout notice is displayed by the program. The user can either stop the program or reinitiate the counter. If the user does not respond to the notice within 10 minutes, the program automatically shuts down.

The mode switch in the bottom right allows the user to select either the real-time mode or the demo mode. When in demo mode, the program reads and processes data from an existing selection of data files, rather than directly from the medical instrumentation. When in demo mode, the TREA does not create raw binary data files for sensor data as it does when it is in real-time mode. This would be equivalent to creating a copy of the data file currently being used for the live demo. However, the processed ASCII data files are generated by the program when demo mode is selected.

When the Continue button is depressed in the Program Setup menu, different displays will appear depending on the selection. If either Trending Graphs or Display Raw Data is selected in the Program Setup Menu and Real-Time mode is chosen, the program will immediately start acquiring and processing data. If Demo Mode is selected, a warning will appear. The purpose of the warning is to make the user aware that real-time data is not being acquired. Click "OK" so that the program can proceed to the next menu. The Demo File Menu shown in Figure 24 will subsequently appear. Currently, there are three files in the selection list denoted as patient 6, 7, and 8. Select one of the patient files for the demo and depress Continue. Raw data will be read from the patient files and the usual processing of the sensor data will be performed.

Additional menus appear when "Decision-Making" is selected in the Program Setup Menu. A second Program Setup menu shown in Figure 25 appears. The user is asked to select the sensor for blood pressure monitoring by the decision-making module and the pulse rate/heart rate sensor. When continue is pressed, a menu to Enter Trauma Information appears as illustrated in Figure 25. Press Enter Data in the Observation Data category to enter non-sensor

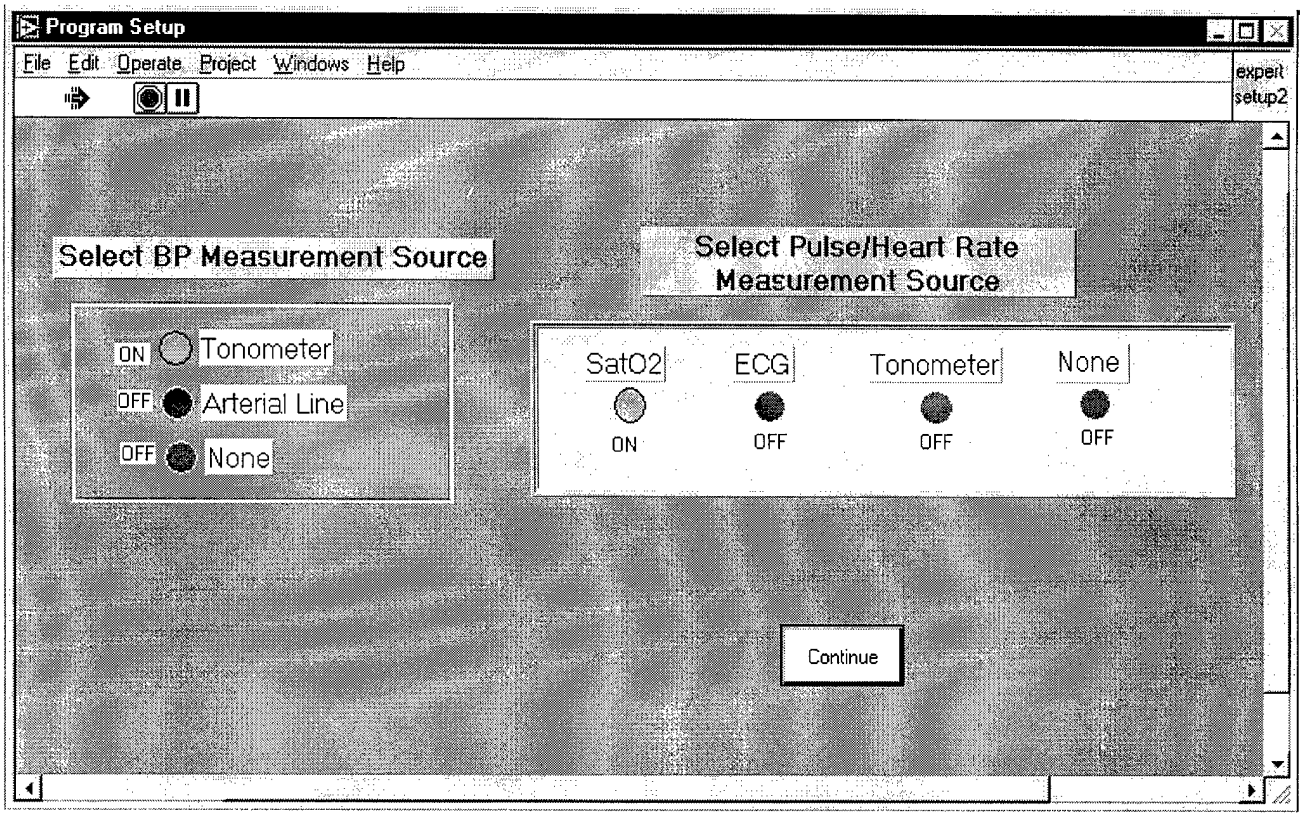

Program Setup Menu for the Decision-Making Software

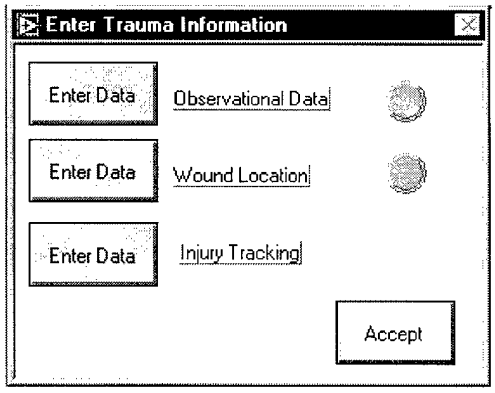

Trauma Menu Used to Guide the Decision-Making Process

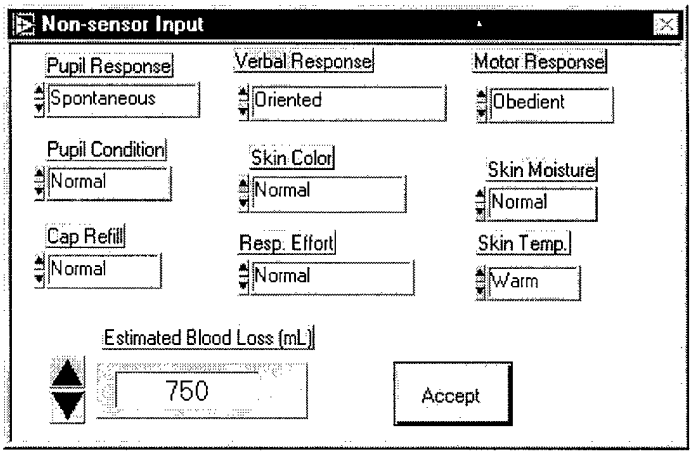

Menu for the Input of Observational Data

Figure 25

inputs. The Observational Data Menu shown in Figure 25 provides an opportunity for the user to report Pupil Response, Verbal Response, Motor Response, Pupil Condition, Skin Color, Skin Moisture, Capillary Refill, Respiration Rate, Skin Temperature, and Estimated Blood Loss. Default values of the parameters in the menu are those of a normal individual, except for the estimated blood loss item, which has a default value of 750 ml. Once these values are entered and accepted, the Enter Trauma Information reappears and requests information about Wound Location (and preliminary diagnosis).

Clicking Wound Location brings up the Trauma Identification Menu shown in Figure 26. The mouse can be pointed to any body location to open up sub-menus to describe the nature of the trauma sustained. For example, clicking on the head region brings up the submenu shown in Figure 27. One can select the type of wound present. The neurological state is estimated from the GCS score, which is derived from the non-sensor inputs. One can accept a selection or cancel it. If the latter is chosen any entries are automatically cleared. If Penetrating Wound is selected, the number of entrance and exit wounds are solicited. This is for documentation only; if this information is not needed, press cancel to return to the Trauma Identification menu. The submenus for trauma to the thorax, abdomen, and extremities are displayed in Figures 28-30. In the case of the front and back thorax, a secondary menu shown on the right appears when Penetrating Trauma is selected from the main menu on the left. Secondary menus are not used in the case of the abdomen or the extremities.

Upon exiting the Trauma Identification Menu, the program displays the Tracking Menu shown in Figure 31. The user is requested to select one wound area to be tracked by the decision-making module. At this point in the knowledge-based system development, multiple severe injuries in diverse areas of the body cannot be tracked. Once the tracking area is accepted, the program either asks the user to identify which demo file to run (if that option was selected) or begins operating in real-time mode.

8.2.2 Runtime Operations

Once TREA is running, a variety of data is made available in graphical and tabular form. The various displays are accessible by scrolling the side bar on the right up and down. If the decision-making module is active, the current patient status can be found in the top most portion of the graphical display. This is illustrated in Figure 32. In the upper left panel, messages

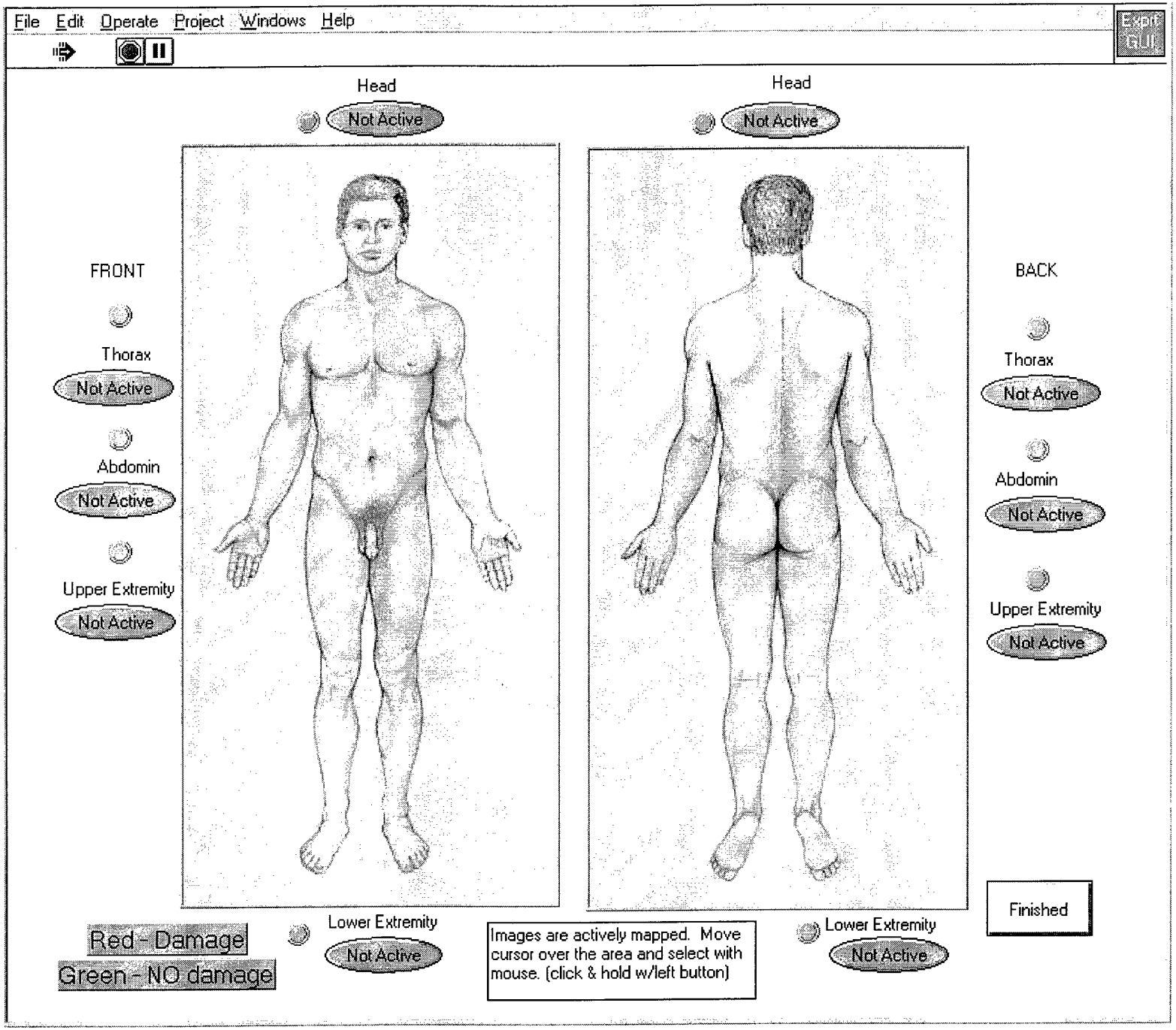

Figure 26. Trauma Identification Menu

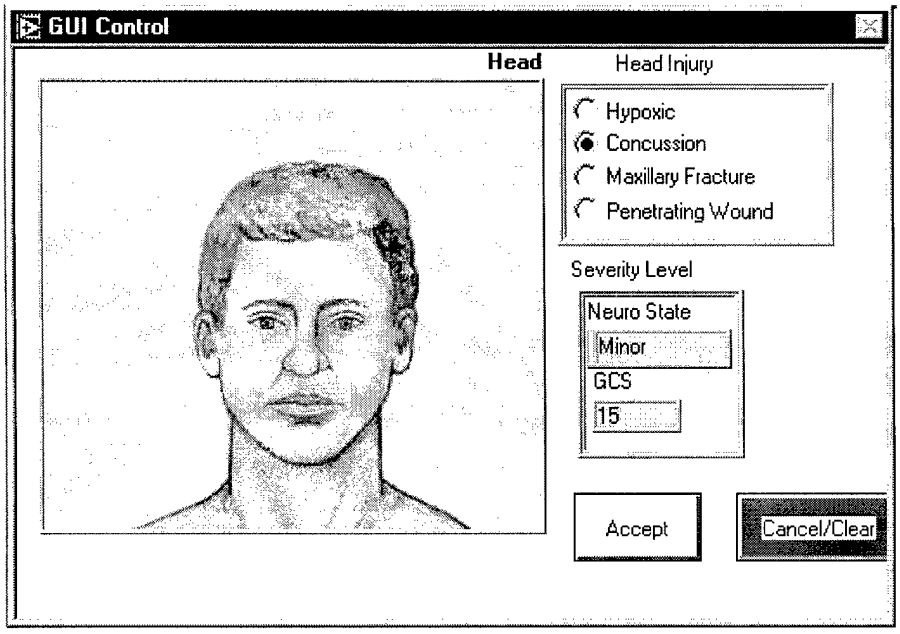

Head Injury Sub-Menu

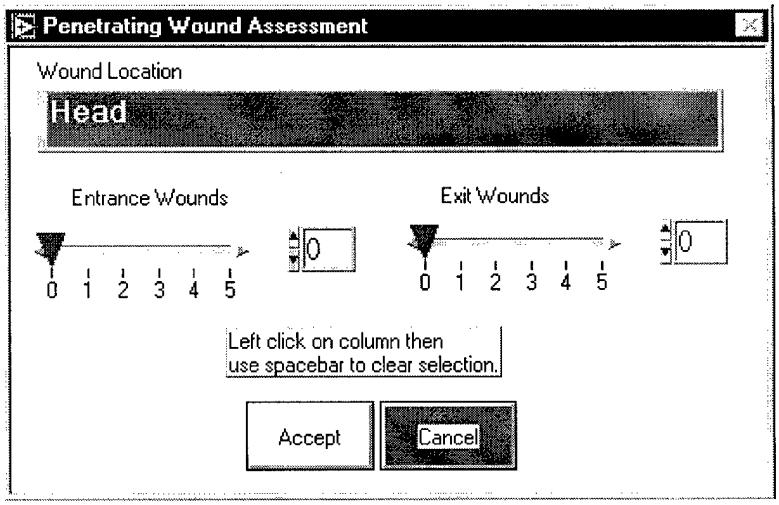

Wound Assessment Menu

Figure 27

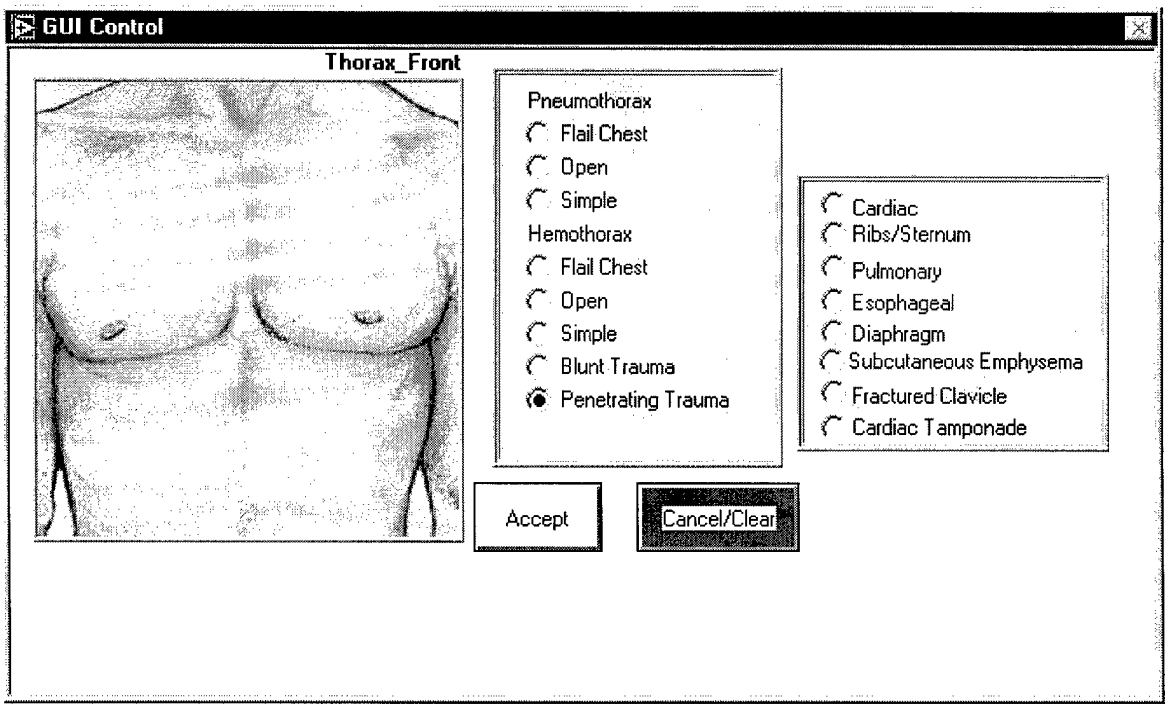

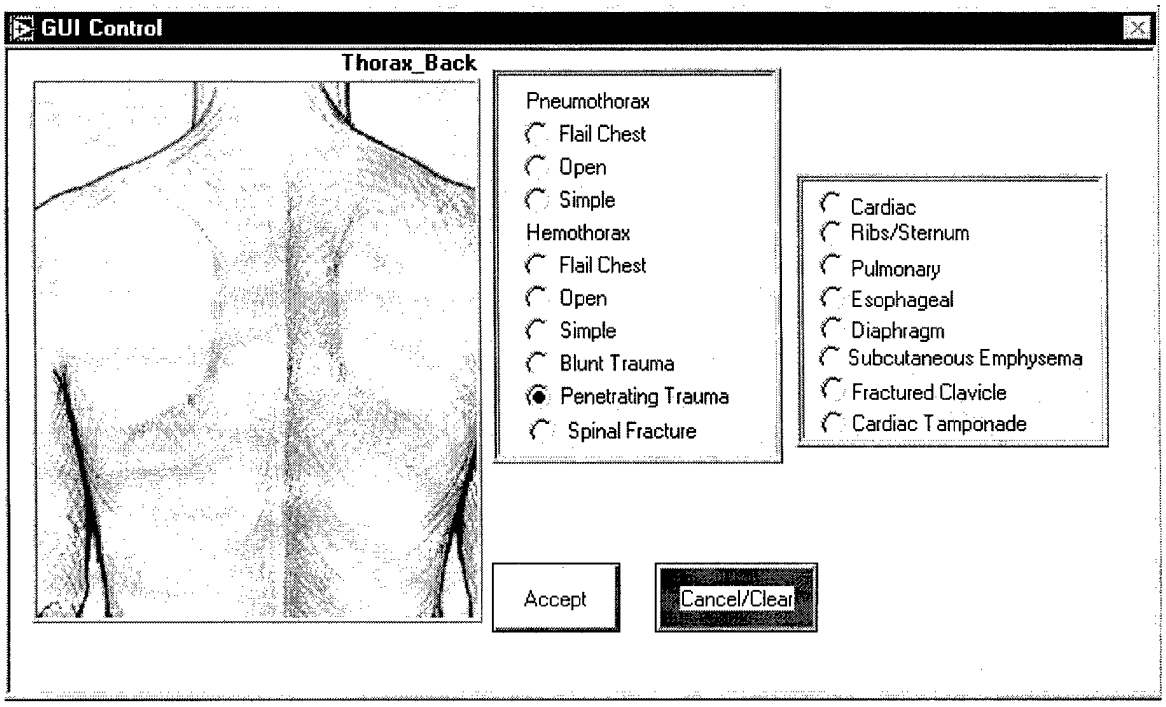

Figure 28. Sub-menus for thoracic trauma

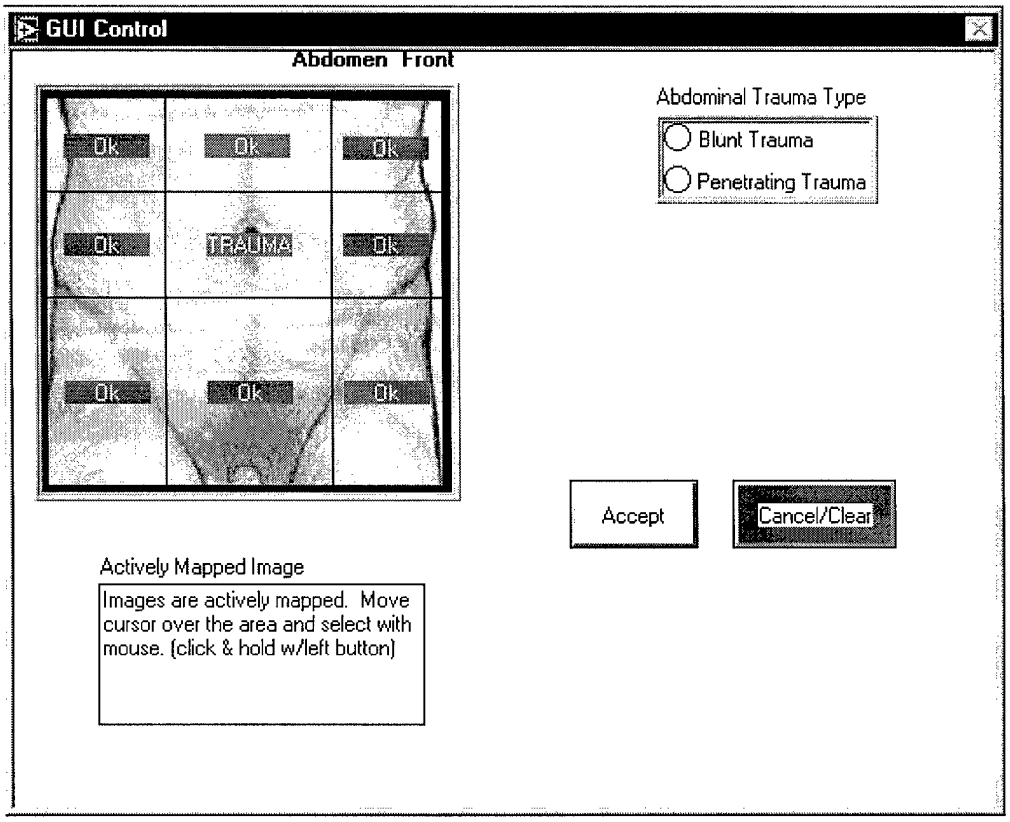

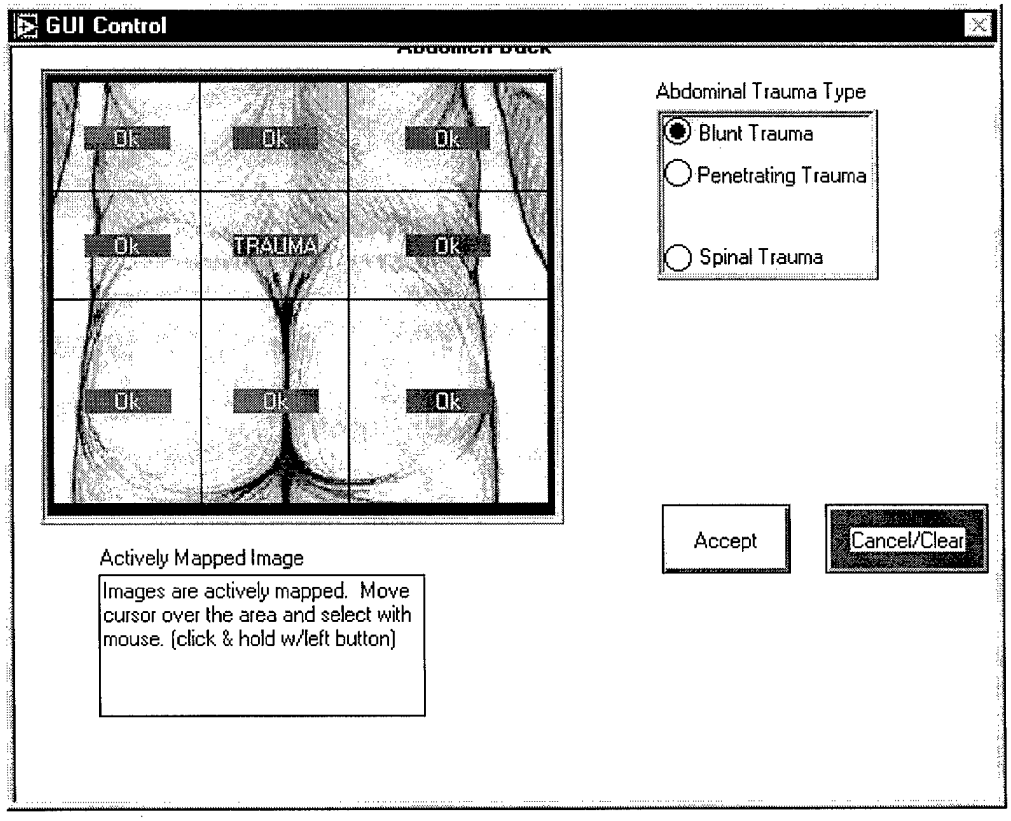

Figure 29. Sub-menus for abdominal trauma

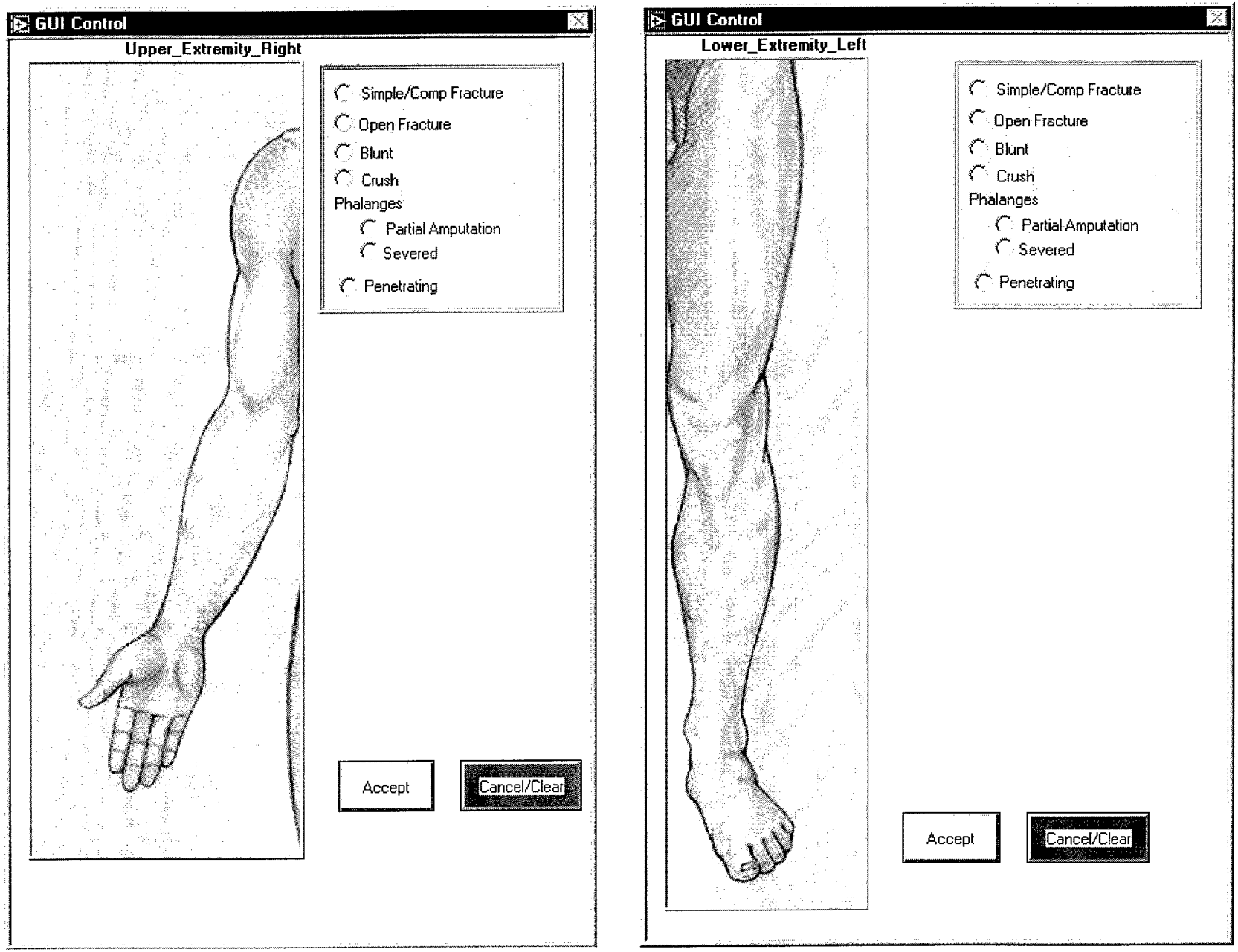

Figure 30. Sub-menus for extremity trauma

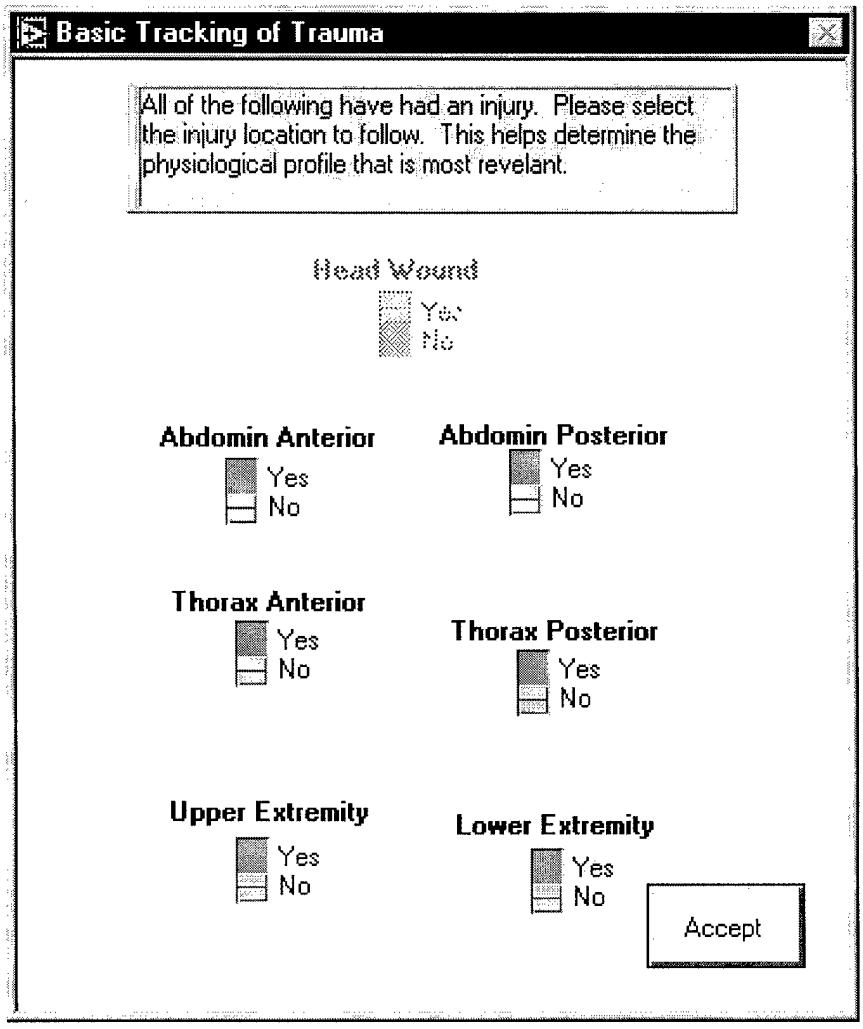

Figure 31. Selection menu for injury tracking

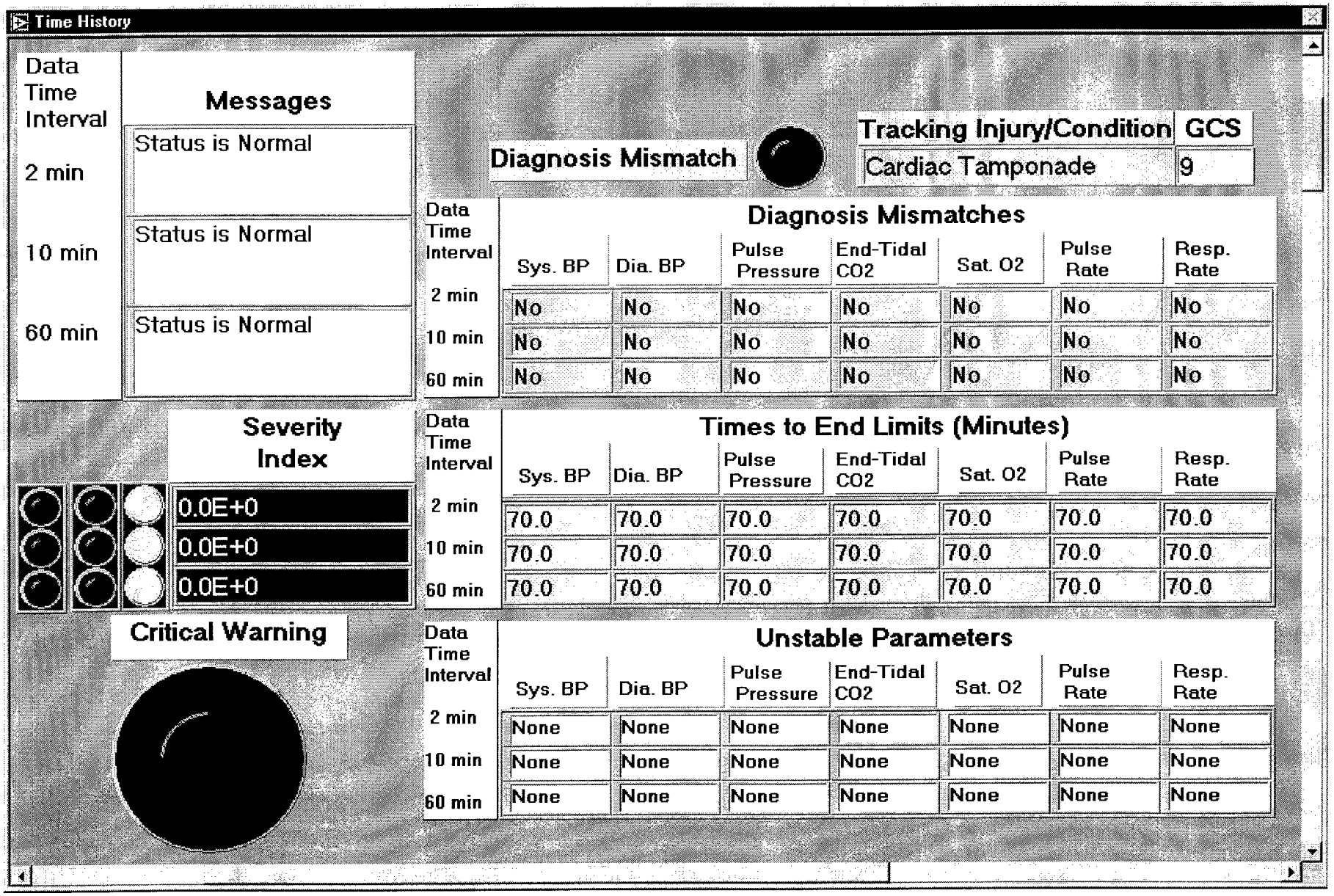

Figure 32. Data display used for the decision-making module

indicate the overall patient assessment based on sensor measurements recorded for 2 min, 10 min, and 60 min. One of the five messages shown below appears in each message box.

Patient Status Window Messages
Status is Normal
Diagnosis Mismatch
Critically Unstable
Critically Unstable and Diagnosis Mismatch

In addition, if the decision-making module determines that a trauma victim is critically unstable, the red Critical Warning light will light up. Similarly, the red diagnosis mismatch light is turned on when this situation is determined to exist.

At the top right the injury or trauma condition being tracked is listed along with the Glascow Coma Scale value obtained from non-sensor inputs during the program setup.

The diagnosis mismatch table is used to identify sensor parameters that do not agree with the diagnosis over the three measurement time scales. Individual values are either yes or no. Times to end limits are shown in the table below the diagnosis mismatch table, and on the left the associated severity index is provided. In the display of Figure 32, all of the times to end limits are set at the maximum time limit (70 min) indicating that the patient is stable. As the patient becomes unstable, the times to end limits decrease as indicated in Section 7 above. Next to the list of severity index values is a set of three lights for each time scale charted. The colors green, yellow, and red represent severity index ranges of $x < 10$, $10 \leq x < 25$, and $x \geq 25$, respectively. In the bottom table, parameters are listed according to whether they are stable or unstable; none indicates that a determination has yet to be made.

If one scrolls the bar on the right downward, the Time History graph shown in Figure 33 will appear. In this plot, processed results from all active sensors are displayed as a function of relative time. In addition, current sensor values are provided in digital form next to the legend at the top, right portion of the figure. The time window of the displayed results can be changed in real time by scrolling the indicator below the legend or by simply typing in a new value in the box. When the time values of the data points exceed the time limit of the window, the display is

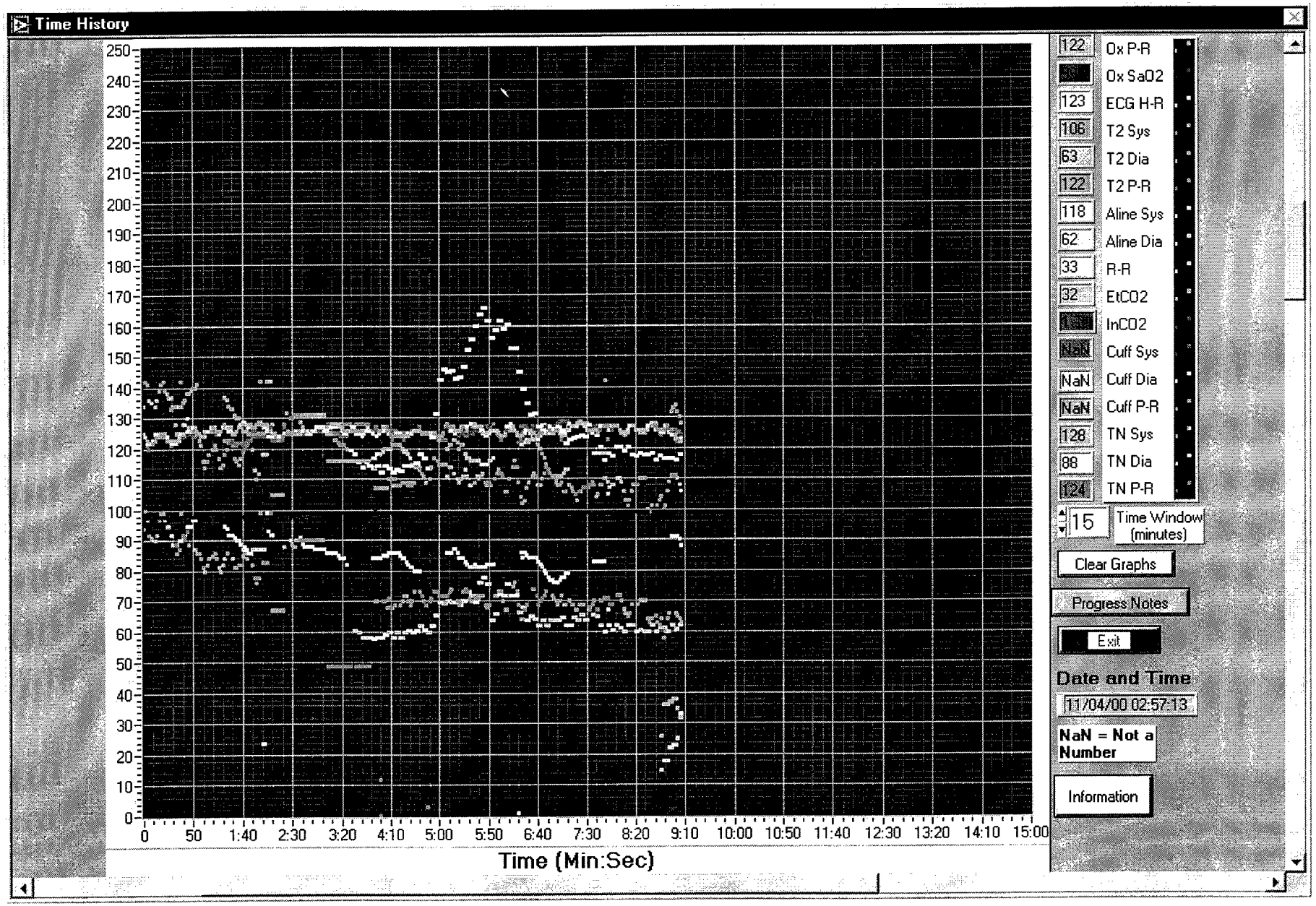

Figure 33. Temporal history of sensor values

cleared and points are plotted beginning at zero time on the left. One can manually clear the graph by clicking the Clear Graphs button.

The Progress Notes button calls up a text editor that allows the user to chart the status of the patient and enter information about drug administration, fluid therapies, procedures, etc. When the editor is active, the data acquisition and all program functions proceed as normal. Figure 34 shows the display that appears. The program automatically includes the time and date in the note and assigns a text file name to the entry.

The Exit button is located immediately below the Progress Notes button. When the Exit button is pressed, the program closes all files, terminates the analysis and decision-making modules, de-allocates all memory, and shuts the main program down.

The current date and time is displayed immediately below the Exit button. The Information button opens a window containing the program version, the C-code library build version, and the technical contacts for the project. This display can be closed manually by clicking the return button. It will automatically close after 60 s.

Below the time history plot are individual plots labeled Sat O_2 Pulse Rate, ECG Heart Rate, Tonometer Pulse Rate, $\%SaO_2$, Pulse-to-Pulse Tonometer Blood Pressure, Arterial-Line Blood Pressure, End-Tidal CO_2, and Respiration Rate. These are illustrated in Figures 35a-35c. The fully analyzed sensor data are shown in these figures. (See Section 7 above.) In each plot, the averaged sensor value is displayed along with its trend. Also included are the statistical error bars for all sensor parameters and their trends. In the case of systolic and diastolic pressure, the values of the trends represent the change in the blood pressure value per 2 min interval. In all other cases the trends correspond to changes over a 15 min interval, that is, the change in sensor value per 15-min time interval.

The temporal scale is referenced to the beginning of data acquisition and the maximum time scale will extend indefinitely into the data acquisition period. Fifteen minutes of data are displayed across the plot at any given time. Data acquired earlier or later can be examined by scrolling the horizontal bar at the bottom right of each plot. Thus, the user has graphical access to all of the data acquired during the monitoring period.

To the right of each graph are digital read-outs of the current sensor value and its trend. The Processing Status of the data is listed below this. One of the following messages listed below will appear in the status window.

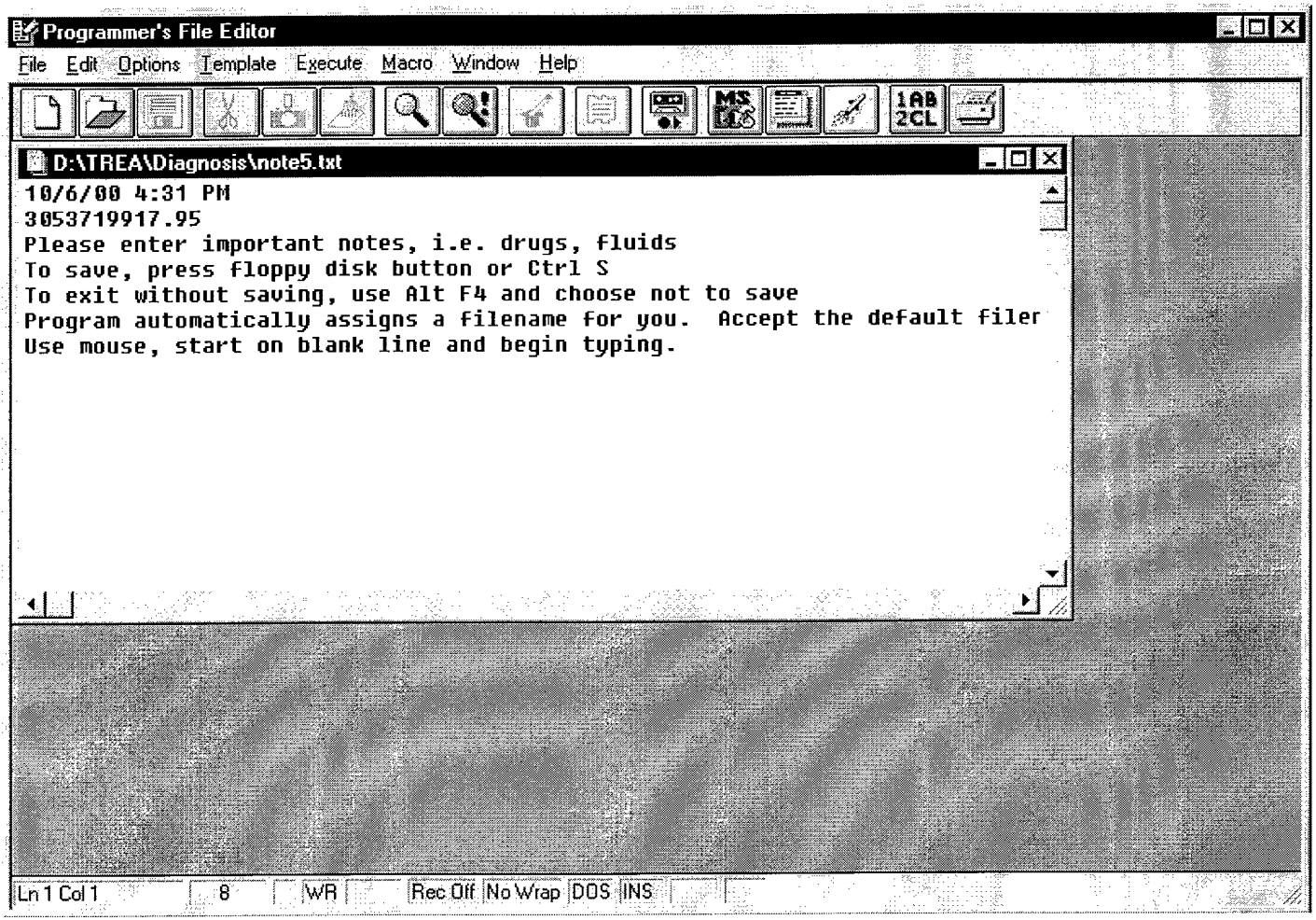

Figure 34. Display used for the entry of progress notes

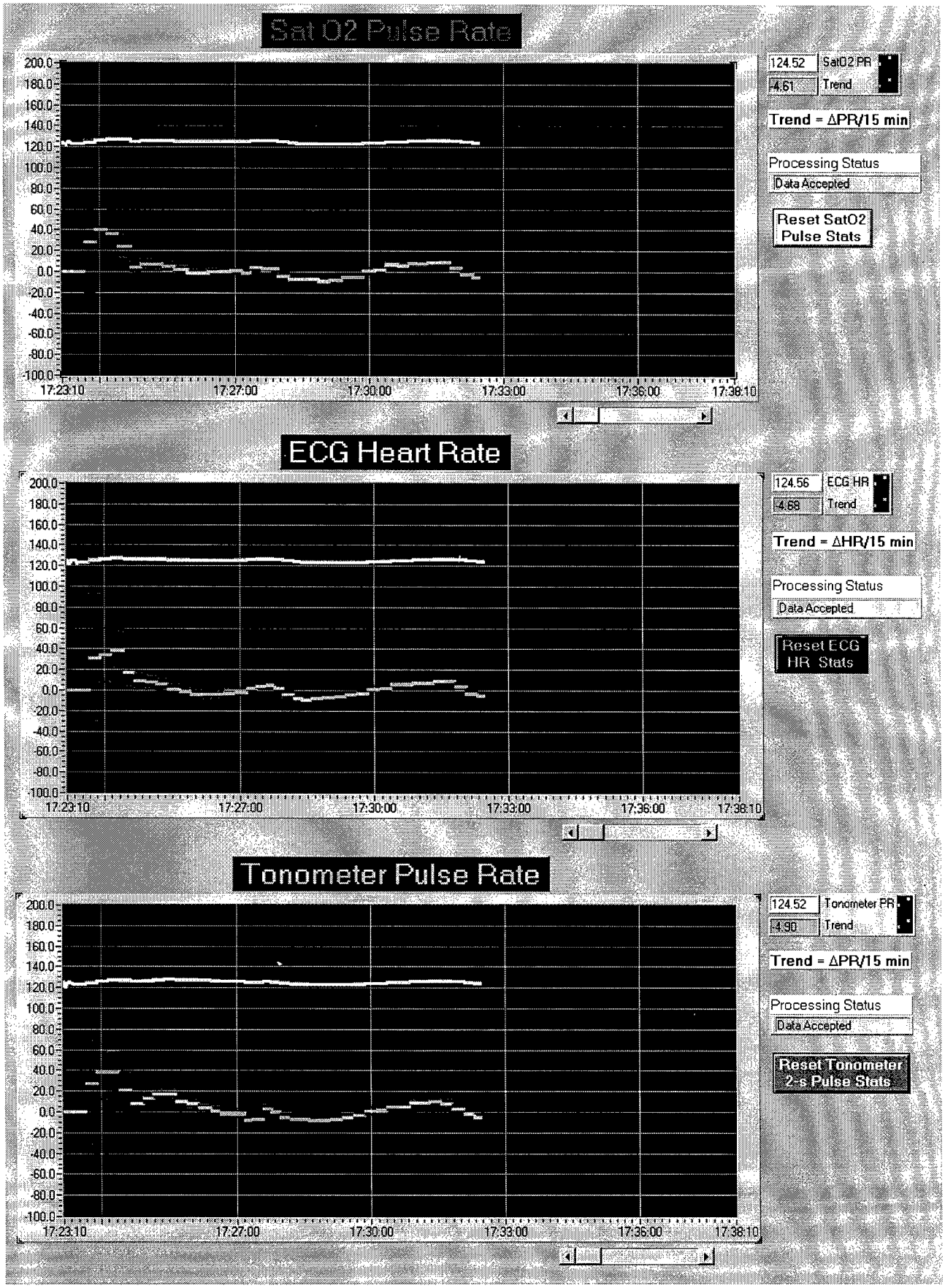

Figure 35a. Analyzed sensor values and their trends

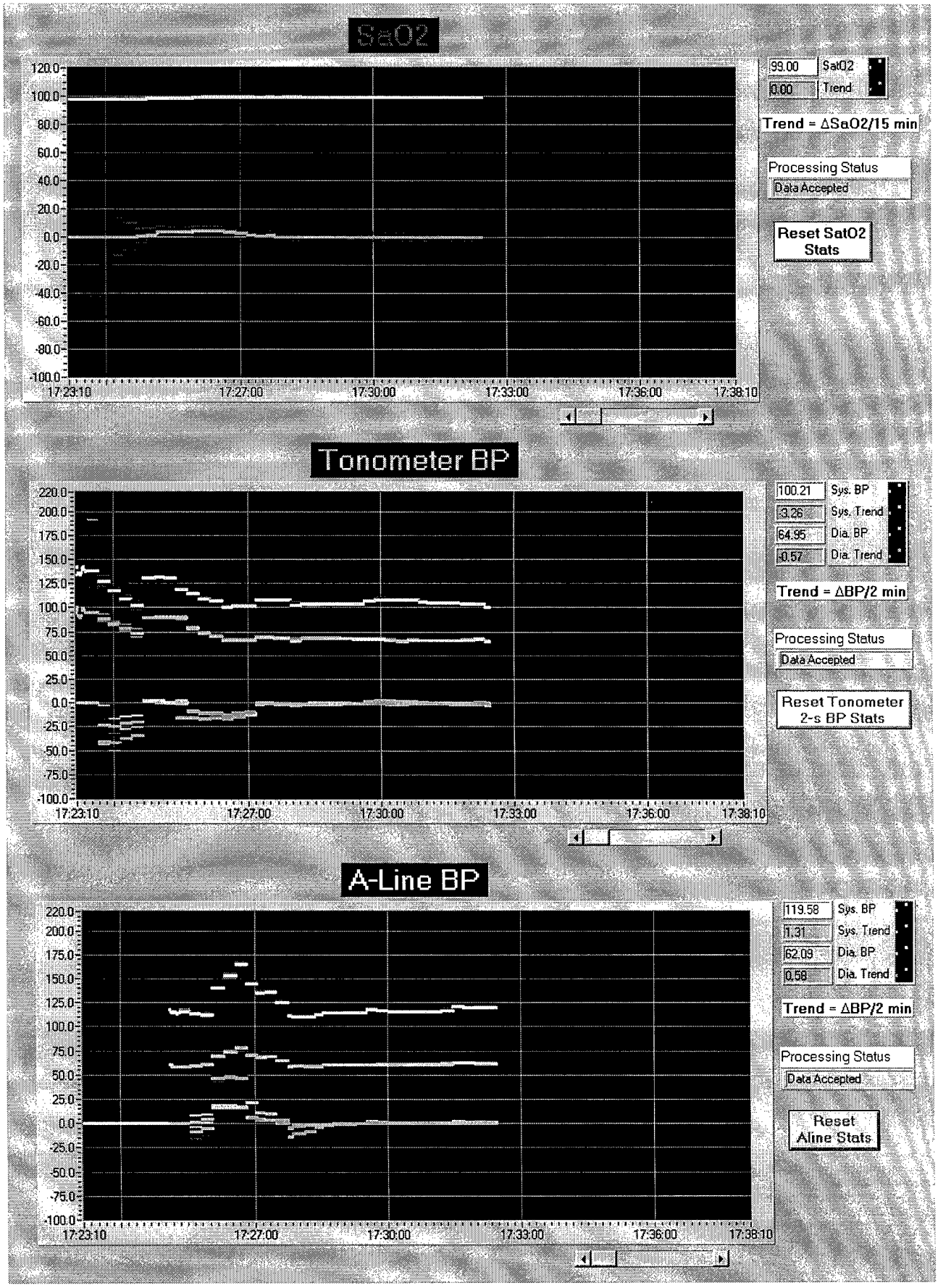

Figure 35b. Analyzed sensor values and their trends

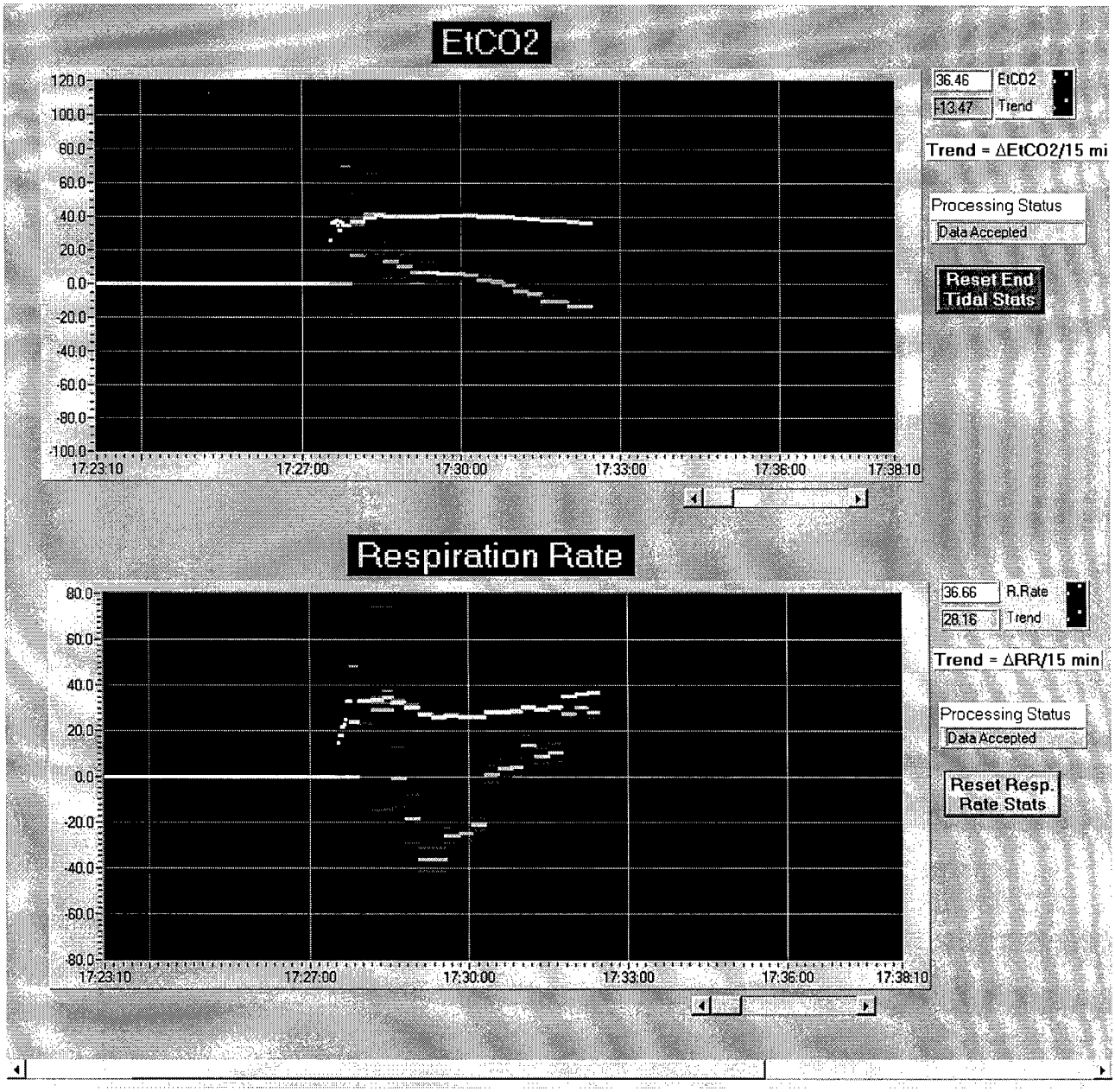

Figure 35c. Analyzed sensor values and their trends

Status Window Messages	Description
Data Accepted	The user will find that most data points are accepted.
Point is Not a Number (NaN)	Failure of the medical instrumentation to yield a numerical value after the data on the serial line is parsed will automatically give rise to rejected data. NaN errors can arise because of firmware errors in the Colin Medical Suite or as a result of a sensor being turned off.
Data Integration Complete	This indicates that the data analysis for another point in the display has been completed and that the new point has been added to the graph.
Point Statistically Rejected	When artifacts are detected by the software during the course of statistical analyses, the program will reject data points and issue this message.

Below the Processing Status indicator is a reset button, which is used to reset the statistics of all items plotted in the figure on the left. This is extremely useful in situations where sensor calibrations are performed or when the sensor is either removed from the patient or turned off for a short period. This avoids the adverse impacts of artifacts on the calculated statistical distribution functions. If the reset button is not pressed after the introduction of large amplitude artificial signals, it may take a considerable amount of time before the statistics re-normalize to proper values. One can use the scroll bar shown at the very bottom of Figure 35c to access the current error bar values. These are located to the right of the figure legends and are not displayed in Figures 35a-35c.

Finally, we restate an important item discussed earlier. One must click the Exit button in the bottom right area of the Time History plot to terminate the program in an orderly fashion. Turning off the computer or rebooting the computer in lieu of clicking the exit button may corrupt data files containing the sensor results. The two safe methods for program termination

entail either clicking the Exit button or allowing the shutoff function to close down the program automatically after a specified period of time.

9. References

Adams, S. L., and J. S. Greene, Absence of a tachycardic response to intraperitoneal hemorrhage, *J. Emerg. Med., 4*, 383, 1986.

Aduen, J., W. K. Bernstein, T. Khastgir, et al., The use and clinical importance of a substrate-specific electrode for rapid determination of blood lactate concentrations, *JAMA, 272*, 1678, 1994.

American College of Emergency Physicians, *Emergency Medicine: A Comprehensive Study Guide*, 4th ed., J. E. Tintinalli, E. Ruiz, R. L. Krome, eds., McGraw-Hill, New York, 1996.

American College of Surgeons, *Advanced Trauma Life Support Course*, p. 45, Chicago, 1981.

American College of Surgeons, *Advanced Trauma Life Support for Doctors*, 6th edition, 444 pp., 1997.

American College of Surgeons, *Advanced Trauma Life Support Reference Manual*, 396 pp., Chicago, 1994.

Arrowood, J. A., P. K. Mohanty, and M. D. Thames, Cardiovascular problems in the spinal cord injured patient, *Phys. Med. Rehabil. State of the Art Rev., 1*, 443, 1987.

Ballinger, W. F., et al., *The Management of Trauma*, W. B. Saunders, Philadelphia, 1968.

Barriot, P., and B. Riou, Hemorrhagic shock with paradoxical bradycardia, *Intensive Care Med., 13*, 203, 1987.

Bellamy, R. F., Causes of death in conventional land warfare, *Mil. Med., 149*, 55, 1984.

Benzel, E. C., W. T. Day, L. Kesterson, et al., Civilian craniocerebral gunshot wounds, *Neurosurgery, 29*, 67, 1991.

Berguer, R., R. L. Staerkel, E. E. Moore, et al., Warning: Fatal reaction to the use of fibrin glue in deep hepatic wounds. Case Reports, *J. Trauma, 31*, 408, 1991.

Caroline, N. L., *Emergency Care in the Streets*, fifth ed., 1087 pp., Little, Brown and Company, New York, 1995.

Champion, H. R., W. J. Sacco, A. J. Carnazzo, et al., The Trauma Score, *Crit. Care Med., 9*, 672, 1981.

Champion, H. R., W. J. Sacco, and T. Hunt, Trauma severity scoring to predict mortality, *World J. Surg., 7*, 4, 1983.

Champion, H. R., W. J. Sacco, Trauma risk assessment: Review of severity scales, Emerg. Med. Ann., Appleton-Century-Crofts, New York, 1983.

Champion, H. R., W. J. Sacco, W. S. Copes, D. S. Gann, T. A. Gennarelli, and M. E. Flanagan, A revision of the trauma score, *J. Trauma, 29*, 623, 1989.

Cohn, R., Nonpenetrating wounds of the lungs and bronchi, *Surg. Clinics N. America, 52,* 585, 1972.

Copass, M. K., R. G. Soper, and M. S. Eisenberg, *EMT Manual*, 2nd Ed., 326 pp., W. B. Saunders Company, Philadelphia, 1991.

Cormum, R., V. Gresham, M. MacPhee, et al., Use of the radical retropubic prostatectomy for evaluation of an absorbable fibrin adhesive bandage (AFAB) in the dog, *Intern. Symp. Thromb, Hemostas.*, in press, 1997.

Demetriades, D., L. S. Chan, P. Bhasin, T. V. Berne, E. Ramicone, F. Huicochea, G. Velmahos, E. E. Cornwell, H. Belzberg, J. Murray, and J. A. Asensio, Relative bradycardia in patients with traumatic hypotension, *J. Trauma, 45*, 534-539, 1998.

Desai, V. S., M. H. Weil, W. Tang, G. Yang, and J. Bisera, Gastric intramural PCO2 during peritonitis and shock, Chest, 104, 1254-1258, 1993.

Desai, V. S., M. H. Weil, W. Tang, R. Gazmuri, and J. Bisera, Hepatic, renal, and cerebral tissue hypercarbia during sepsis and shock in rats, J. Lab. Clin. Med., 125, 456-461, 1995.

Di Maio, V. J. M., Gunshot Wounds: Practical Aspects of Firearms, Ballistics, and Forensic Techniques, 331 pp., CRC Press, Ann Arbor, 1993.

Drzewiecki, G. M., J. Melbin, and A. Noordergraaf, Arterial tonometry: Review and analysis, *J. Biomech., 16*, 141, 1983.

Falk, J. L., E. C. Rackow, and M. H. Weil, End-tidal carbon dioxide concentration during cardiopulmonary resuscitation, *N. Eng. J. Med., 318*, 607-611, 1988.

Gazmuri, R. J., M. H. Weil, J. Bisera, and E. C. Rackow, End-tidal carbon dioxide tension as a monitor of native blood flow during resuscitation by extracorporeal circulation, *Cardiovasc. Surg., 101*, 984-988, 1991.

Gudipati, C. V., M. H. Weil, J. Bisera, H. G. Deshmukh, and E. C Rackow, Expired carbon dioxide: a noninvasive monitor of cardiopulmonary resuscitation, *Circulation, 77*, 234-239, 1988.

Hernesniemi, J., Penetrating craniocerebral gunshot wounds in civilians, *Acta Neurochir, 49*, 199, 1979.

Holcomb, J. B., A. E. Pusateri, J. R. Hess, et al., Implications of new dry fibrin sealant technology for trauma surgery, *Surg. Clinics N. America*, submitted, 1997a.

Holcomb, J. B., M. J. MacPhee, S. Hetz, et al., Efficacy of a dry fibrin sealant dressing for hemorrhage control following ballistic injury, *Arch. Surg.*, submitted, 1997b.

Jackson, M. R., S. A. Friedman, A. J. Carter, et al., Hemostatic efficacy of a fibrin sealant-based topical agent in a femoral artery injury model: A randomized, blinded, placebo controlled study, *J. Vasc. Surg.*, in press, 1997.

Johnsen, R. P. S., Relative bradycardia: A sign of acute intraperitoneal bleeding, *Aust. NZ Obstet. Gynecol., 18*, 206, 1978.

Johnson, B. A., and M. A. Weil, Redefining ischemia due to circulatory failure as dual defects of oxygen deficits and of carbon dioxide excesses, *Crit. Care Med.*, 1432-1438, *19*, 1991.

Kaufman, H. H., M. E. Makela, F. Lee, et al., Gunshot wounds to the head: a perspective, *Neurosurgery, 18*, 689, 1986.

Kirsh, M. M., et al., *Blunt Chest Trauma*, Little, Brown, Boston, 1977.

Kline, J. A., Shock, in *Emergency Medicine: Concepts and Clinical Practice*, 4th ed., pp. 86-106, Mosby, St. Louis, 1998.

Kruse, J. A., S. A. Zaidi, and R. W. Carlson, Significance of blood lactate levels in critically ill patients with liver disease, *Am. J. Med., 83*, 77, 1987.

Kuzu, A., S. Aydintug, K. Karayalcin, et al., Use of autologous fibrin glue in the treatment of splenic trauma: An experimental study, *J. R. Coll. Surg. Edinb., 37*, 162, 1992.

Larson, M. J., J. C. Bowersox, and R. C. Lim, Efficacy of a fibrin hemostatic bandage in controlling hemorrhage from experimental injuries, *Arch. Surg., 130*, 420, 1995.

MacPhee, M. J., Fibrin sealant based hemostatic devices for treatment of trauma in the field, *Intern. Symp. Thromb. Hemosta.*, in press, 1997.

Malik, A. B., and M. J. Horgan, Mechanisms of thrombin-induced vascular injury and edema, *Am. Rev. Resp. Dis., 136*, 467, 1987.

Malik, A. B., Thrombin-induced endothelial injury, *Semin. Thromb. Hemostas, 12*, 184, 1986.

Mannix, F. L., Hemorrhagic shock, in *Emergency Medicine*, p. 187, P. Rosen, ed., C. V. Mosby, St. Louis, 1988.

Mengert, T. J., M. S. Eisenberg, and M. K. Copass, *Emergency Medical Therapy*, 992 pp., W. B. Saunders Company, Philadelphia, 1996.

Millikan, I. S., E. E. Moore, E. L. Den, et al., Temporary cardiac pacing in traumatic arrest victims, *Ann. Emerg. Med., 9*, 591, 1980.

Minnera, F. L., D. Martin, L. Hill, et al., Lung morphological and permeability changes induced by intravascular coagulation in dogs, *Am. J. Physiol., 253*, H634, 1987.

Moore, E. E., T. H. Cogbill, G. J. Jurkovich, et al., Organ injury scaling: Spleen and liver (1994 revision), *J. Trauma, 38*, 323, 1995.

Nagib, M. G., G. L. Rockswold, R. S. Sherman, et al., Civilian gunshot wounds to the brain: prognosis and management, *Neurosurgery, 18*, 533, 1986.

Nakagawa, Y., M. H. Weil, W. Tang, S. Sun, H Yamaguchi, X. Jin, and J. Bisera, Sublingual capnometry for diagnosis and quantitation of circulatory shock, *Crit. Care Med.*, 157, 1838-1843, 1998.

Noordergraaf, A., *Circulatory System Dynamics*, Academic Press, New York, 1978.

Oberg, B., and P. Thoren, Increased activity in vagal cardiac afferents correlated to the appearance of reflex bradycardia during severe hemorrhage in cats, *Acta Physiol. Scand., 80*, 22A, 1970.

Pearce, F. J., W. P. Wiesmann, J. Hale, and J. R. Licina, Life support for trauma and transport (LSTAT): A NATO litter-based critical care transport platform, *AGARD Conf. Proc.* 599, 30-1 - 30-4, 1998.

Poggetti, R. S., E. E. Moore, F. A. Moore, et al., Balloon tamponade for bilobar transfixing hepatic gunshot wounds, *J. Trauma, 33*, 694, 1992.

Pressman, G. L., and P. M. Newgard, A transducer for the external measurement of arterial blood pressure, *IEEE Trans. Biomed. Electron., 10*, 73, 1963.

Rosen, P., and M. Murphy, Thoracic vascular pathologies, *Emerg. Med. Clin. N. America, 1*, 417, 1983.

Sacco, W. J., H. R. Champion, and M. Stega, Trauma Care Evaluation, University Park Press, Baltimore, 1984a.

Sacco, W. J., H. R. Champion, P. Gainer, et al., The Trauma Score as applied to penetrating trauma, *Ann. Emerg. Med., 13*, 415, 1984b.

Salvino, C. K., T. J. Esposito, D. K. Smith, et al., Laparoscopic injection of fibrin glue to arrest intraparenchymal abdominal hemorrhage: An experimental study, *J. Trauma, 35*, 762, 1993.

Sandler, H., B. Gerdin, and T. Saldeen, Studies on the role of thromboxane in thrombin-induced pulmonary insufficiency in the rat, *Thromb. Res., 42*, 165, 1986.

Sato, Y., M. Nishinaga, A. Kawamoto, T. Ozawa, and H. Takatsuji, Accuracy of a continuous blood pressure monitor based on arterial tonometry, *Hypertension, 21*, 866-874, 1993.

Sato, Y., M. H. Weil, W. Tang, S. Sun, J. Xie, J. Bisera, and H. Hosaka, Esophageal PCO_2 as a monitor of perfusion failure during hemorrhagic shock, *J. Appl. Physiol., 82*, 558-662, 1997.

Shabetal, R., Pericardial Disease, in *The Heart*, 7th ed., J. W. Hurst and R. C. Schlant (eds.), McGraw-Hill, New York, 1990.

Shaffrey, C. I., W. D. Spotnitz, M. E. Shaffrey, et al., Neurosurgical application of fibrin glue: Augmentation of dural closure in 134 patients, *Neurosurgery, 26*, 207, 1990.

Stacpoole, P. W., E. C. Wright, T. G. Baumgartner, et al., Natural history and course of acquired lactic acidosis in adults, *Am. J. Med., 97*, 47, 1994.

Stefik, M. *Introduction to Knowledge Systems*, 870 pp., Morgan Kaufman Publishers, San Francisco, 1995.

Tang, W. M., M. H. Weil, S. Sun, M. Noc, R. J. Gazmuri, and J. Bisera, Gastric intramural PCO_2 as a monitor of perfusion failure during hemorrhagic and anaphylactic shock, *J. Appl. Physiol., 76*, 572-577, 1994.

Thompson, D., Relative bradycardia in patients with isolated penetrating abdominal trauma and isolated extremity trauma, *Ann. Emerg. Med., 19*, 268, 1990.

Trevino, R. P., J. Bisera, M. H. Weil, E. C. Rackow, and W. G. Grundler, End tidal CO_2 as a guide to successful cardiopulmonary resuscitation: A preliminary report, *Crit. Care Med., 13*, 910-911, 1985.

Valadka, A. B., and R. K. Narayan, Emergency room management of the head injured patient, in *Neurotrauma*, R. K. Narayan, J. E. Wilberger, and J. T. Povlishock, eds., p. 120, McGraw-Hill, New York, 1996.

von Planta, M., I. von Planta, M. H. Weil, S. Bruno, J. Bisera, and E. C. Rackow, End tidal carbon dioxide as a haemodynamic determinant of cardiopulmonary resuscitation in the rat, *Cardiovasc. Res., 23*, 364-368, 1989.

Ward, J. D., A. H. Chisholm, V. T. Prince, et al., Penetrating head injury, *Crit. Care Nurse Q., 17*, 79, 1994.

Waxweiler, R. J., D. Thurman, J. Sniezek, et. al, Monitoring the impact of traumatic brain injury: a review and update, *J. Neurotrauma, 12*, 509, 1995.

Weil, M. H., J. Bisera, R. P. Trevino, et al., Cardiac output and end-tidal carbon dioxide, *Crit. Care Med., 13*, 907, 1985.

Weil, M. H., Y. Nakagawa, W. Tang, Y. Sato, et al., Sublingual capnometry: a new non-invasive measurement for diagnosis and quantitation of severity of circulatory shock, *Crit. Care Med., 27*, 1225-1229, 1998.

Weltman, G., The continuous measurement of pulse wave velocity, M.S. Thesis, University of California, Los Angeles, 1959.

White, R. J., and M. J. Likavec, The diagnosis and initial management of head injury, *N. Engl. J. Med., 327*, 1507, 1992.

Wiener, S. L., and J. Barrett, *Trauma Management for Civilian and Military Physicians*, 582 pp., W. B. Saunders Company, Philadelphia, 1986.

Wilson, R. F., Thoracic Trauma, in *Emergency Medicine*, 4th ed., J. E. Tintinalli, E. Ruiz, R. L. Krome, eds., pp. 1156-1182, McGraw-Hill, New York, 1996.

Wilson, R. F., D. Antonenko, and D. B. Gibson, Shock and acute respiratory failure after chest trauma, *J. Trauma, 17*, 697, 1977.

Zimmerman, G. A., T. M. McIntyre, and S. M. Prescott, Thrombin stimulates the adherence of neutrophils to human endothelial cells in vivo, *J. Clin. Invest., 76*, 2235, 1985.

Zorn, E. A., M. B. Wilson, J. J. Angel, J. Zanella, and B. S. Alpert, Validation of an automated arterial tonometry monitor using Association for the Advancement of Medical Instrumentation standards, *Blood Pressure Monitoring*, *2*, 185, 1997.

10. Appendix A - Interface between Windows NT Libraries and LabVIEW

10.1 Data Acquisition

Data acquisition is implemented in LabVIEW. LabVIEW delivers a stream of samples from each of six parameters: systolic blood pressure, diastolic blood pressure, end-tidal CO_2, O_2 saturation, respiration rate, and pulse rate. Each sample has an associated time-tag.

10.2 Data Analysis Module and Decision-Making Module

The data analysis and decision-making modules are implemented in a combined Dynamic Link Library (DLL) written in C. Details of the reduction algorithm and decision-making system are provided in Section 7 above. The code for all program alarms are contained in the particular DLL libraries that call the alarm.

10.3 Functions in the DLL

All functions return zero if no further processing is needed. A return value greater than zero indicates successful completion and that one or more parameters have new data available in them. A return value less than zero indicates that an error occurred. The DLL is called from LabVIEW using the Call Library Function. (See *LabVIEW G Programming Reference Manual*, Chapter 25, Calling Code from Other Languages.) Because Windows NT is a multithreaded system, multiple calls to the DLL can be made simultaneously. All DLL functions are accessed as *stdcall* functions. By default, all call library nodes run in the user interface thread. The name of the combined DLL is *ReductionLib.dll*.

10.3.1 Function Arguments

All *int* and *unsigned* variables are 32-bit. All *double* variable are 8-byte, 64-bit double precision. All *float* variables are 4-byte, 32-bit single precision. All strings are passed as "C" strings (zero-terminated). Any argument prefixed with an asterisk (*) is passed by reference, not value, *i.e.* it is a pointer.

10.3.2 DS_Query

```
char *DS_Query(void);
```

This function returns a string containing the time and date of the latest DLL build.

10.3.3 DS_Init

```
int DS_Init(double ttag, int diagnosis, unsigned nBasis, float nStd, float IntTime, unsigned nFit,
        float Tmax, char *pPath);
```

This function initializes the DLL, and must be called prior to any other DLL calls. It returns a negative value if an error occurred during initialization, a zero otherwise.

DS_Init Arguments

Argument Name	Argument Type	Argument Purpose
ttag	64-bit float (double)	Data acquisition start time. All times will be referenced to this value. Specified in the LabVIEW standard time format of seconds since some date in 1904.
diagnosis	32-bit integer	Negative one if no diagnosis available, otherwise numeric codes as per following table.
nBasis	32-bit unsigned integer	Number of points used for the statistical basis determining which data points are outliers to be excluded.
nStd	32-bit float	Number of standard deviations of data to keep. Points lying outside nStd standard deviations will be excluded from further processing.
IntTime	32-bit float	Number of seconds to integrate data.
nFit	32-bit unsigned int	Number of points to use in fits.
Tmax	32-bit float	Maximum Time to Limit (seconds)
pPath	C-type String	Base file path (without trailing '\')

Diagnosis Codes

Code	Can be Critical	Diagnosis
-1	No	Diagnosis unavailable
0	No	No Diagnosis
1	Yes	ARDS
2	Yes	Hypovolemic Shock
3	Yes	Hemo-pneumothorax
4	Yes	Cardiac Tampanade
5	Yes	Head Injury
6	Yes	Respiratory Failure
7	Yes	Neurogenic Shock
999	No	Other Diagnosis

10.3.4 DS_End

void DS_End(void);

This function allows the DLL to release any allocated memory and shut down. It must be called at termination.

10.3.5 DS_EtCO2

int DS_EtCO2(double *pTtag, double *etco2, double *etco2tr, double *etco2er, double *etco2trer);

int DS_EtCO2Rst(int flag, double ttag);

DS_ EtCO2 Arguments

Argument Name	Argument Type	Argument Purpose
pTtag	pointer to double (64-bit float)	time of observation
etco2	pointer to double (64-bit float)	end-tidal CO_2 value
etco2tr	pointer to double (64-bit float)	end-tidal CO_2 trend (/sec)
etco2er	pointer to double (64-bit float)	error bar for end-tidal CO_2
etco2trer	pointer to double (64-bit float)	error bar for trend
flag	32-bit integer	if non-zero, will reset the statistics for the end-tidal CO_2 calculations.
ttag	double (64-bit float)	Time to begin new integration after reset.

DS_EtCO2 gives the diagnostic system the value for end-tidal CO_2 (etco2) at time ttag. If the return value is positive, the function has filled all the parameters with reduced values. A negative return value indicates that the point was rejected, either because it was a NaN (-1) or statistically invalid (-2). A return value of zero indicates that the data points were accepted but integration was not yet complete.

DS_EtCO2Rst resets the statistics. A non-zero flag will cause the statistics to be reset and a non-zero return value. Setting the flag to zero only consumes processor cycles. The ttag variable indicates the current time in LabVIEW format. This is used to reset integration periods.

10.3.6 DS_SaO2

int DS_SaO2(double *pTtag, double *sao2, double *sao2tr, double *sao2er, double *sao2trer);

int DS_SaO2Rst(int flag, double ttag);

The argument description for O_2 saturation (SaO2) is the same as DS_EtCO2 above.

10.3.7 DS_RR

int DS_RR(double *pTtag, double *rr, double *rrtr, double *rrer, double *rrtrer);

int DS_RRRst(int flag, double ttag);

The argument description for respiration rate (RR) is the same as DS_EtCO2 above.

10.3.8 DS_PR*x*

int DS_PR1(double *pTtag, double *pr, double *prtr, double *prer, double *prtrer);

int DS_PR1Rst(int flag, double ttag);

int DS_PR2(double *pTtag, double *pr, double *prtr, double *prer, double *prtrer);

int DS_PR2Rst(int flag, double ttag);

int DS_PR3(double *pTtag, double *pr, double *prtr, double *prer, double *prtrer);

int DS_PR3Rst(int flag, double ttag);

int DS_PR4(double *pTtag, double *pr, double *prtr, double *prer, double *prtrer);

int DS_PR4Rst(int flag, double ttag);

The argument description for pulse rate is similar to DS_EtCO2 above.

Pulse Rate Designations

Designation	Pulse Rate Source
PR1	O_2 Saturation
PR2	ECG
PR3	Tonometer
PR4	Reserved

10.3.9 DS_ALine

int DS_ALine(double *pTtag, double *sys, double *systr, double *syser, double *systrer, double *dia, double *diatr, double *diaer, double *diatrer, double *pp, double *pptr, double *pper, double *pptrer);

int DS_ALineRst(int flag, double ttag);

DS_Aline Arguments

Argument Name	Argument Type	Argument Purpose
pTtag	pointer to double (64-bit float)	time of observation
sys	pointer to double (64-bit float)	The systolic blood pressure (mm-Hg)
systr	pointer to double (64-bit float)	Trend in the systolic BP (mm-Hg/sec)
syser	pointer to double (64-bit float)	Error bar for systolic BP
systrer	pointer to double (64-bit float)	Error bar for systolic trend
dia	pointer to double (64-bit float)	The diastolic blood pressure (mm-Hg)
diatr	pointer to double (64-bit float)	Trend in the diasolic BP (mm-Hg/sec)
diaer	pointer to double (64-bit float)	Error bar for diastolic BP
diatrer	pointer to double (64-bit float)	Error Bar for diastolic trend
pp	pointer to double (64-bit float)	Pulse pressure (mm-Hg)
pptr	pointer to double (64-bit float)	Trend in pulse pressure (mm-Hg/s
pper	pointer to double (64-bit float)	Pulse pressure error bar
pptrer	pointer to double (64-bit float)	Pulse pressure trend error bar
flag	32-bit integer	if non-zero, will reset the statistics for the end-tidal CO_2 calculations.
ttag	double (64-bit float)	Time to begin new integration after reset.

DS_ALine gives the diagnostic system the values for blood pressure (systolic, diastolic pulse-pressure). If the return value is positive, the function has filled all the parameters with reduced values. A negative return value indicates that the point was rejected, either because it was a NaN (-1) or statistically invalid (-2). A return value of zero indicates that the data points were accepted but integration was not yet complete.

DS_ALineRst resets the statistics. A non-zero flag will cause the statistics to be reset and a non-zero return value. Setting the flag to zero only consumes processor cycles. The ttag variable indicates the current time in LabVIEW format. This is used to reset the data integration buffer.

10.3.10 DS_Tono

int DS_Tono(double *pTtag, double *sys, double *systr, double *syser, double *systrer, double *dia, double *diatr, double *diaer, double *diatrer, double *pp, double *pptr, double *pper, double *pptrer);

int DS_TonoRst(int flag, double ttag);

The argument description for tonometer blood pressure is the same as that for DS_Aline above.

10.3.11 DS_SelectBP

int DS_SelectBP(unsigned nBpSource);

This function selects the blood pressure source according to the table provided below. The absolute value of the returned value indicates the number of the previously selected source. nBpSource is a signed 32-bit integer, passed by value. A negative return value indicates that nBpSource was invalid and that no change has been made. In order to find the currently selected source without making any changes, call the function with nBpSource set to –1.

Blood Pressure Source Nomenclature

nBpSource	Source
0	None
1	Arterial Line
2	Tonometer

10.3.12 DS_SelectPR

int DS_SelectPR(unsigned nPrSource);

Selects the pulse rate source, as indicated by the following table. The absolute value of the returned value indicates the number of the previously selected source. nPrSource is a signed 32-bit integer, passed by value. A negative return value indicates that nPrSource was invalid and that no change has been made. In order to find the currently selected source without making any changes, call the function with nPrSource set to –1.

Pulse Rate Source Nomenclature

nBpSource	Source
0	None
1	PR1 (O_2 Saturation)
2	PR2 (ECG)
3	PR3 (Tonometer)
4	PR4 (reserved)

10.3.13 DS_SetLimits and DS_GetLimits

void DS_SetLimits(double Upper[7], double Lower[7]);

void DS_GetLimits(double Upper[7], double Lower[7]);

Sets/gets limits for each biomedical parameter. Each argument is a seven-element array of double precision floating point numbers. The table below indicates the element ordering. This function must not be called before DS_Init, which sets default limits.

Vector Ordering for DS_SetLimits and DS_GetLimits

Index	Parameter
1	Systolic BP
2	Diastolic BP
3	Pulse Pressure
4	End-tidal CO_2
5	O_2 Saturation
6	Pulse Rate
7	Respiration Rate

10.3.14 DS_MsgInst, DS_MstMed, and DS_MsgLong

int DS_MsgInst(double *Severity, double TTL[7], int flag[7]);

int DS_MsgMed(double *Severity, double TTL[7], int flag[7]);

int DS_MsgLong(double *Severity, double TTL[7], int flag[7]);

DS_Msg*xxx* functions return a message code that indicates patient status. The codes are listed on in the following table:

Message Codes for DS_Msg*xxx*

Code	Message
0	No Message (Error)
1	Severity Level Available
2	Diagnosis Mismatch
4	Critical Injury Unstable
6	Diagnosis Mismatch & Critical Injury Unstable

Function Arguments for DS_Msg*xxx*

Argument Name	Argument Type	Argument Function
Severity	pointer to double (64-bit float)	Indicates the severity level of the patient
TTL	7 element array of double (64-bit float)	Time to limit for each of the 7 biomedical parameters. See table in DS_SetLimits() for indexing. The limits are set in DS_SetLimits.
flag	7 element array of signed integers (32-bit)	Flags, one for each of the 7 biomedical parameters. See table in DS_SetLimits() for indexing. The flags are further defined in the following table

Meaning of Flags for DS_Msg*xxx*

Msg Code	Flag Value	Meaning
0	–	N/A
1	–	N/A
2	0	Parameter is consistent with diagnosis
	1	Parameter is inconsistent with diagnosis
4	0	Parameter is stable
	1	Parameter is unstable
6	0	Parameter is stable
	1	Parameter is unstable, but consistent with diagnosis
	2	Parameter is unstable and inconsistent with diagnosis

10.3.15 DS_EnAble and DS_Abled

int DS_EnAble(int nSensor, int State);

int DS_Abled(int nSensor);

DS_Enabled will set the sensor indicated by nSensor to the value of State. State equal to 0 disables monitoring the chosen sensor. State equal to 1 enables monitoring the chosen sensor. If an invalid sensor number is entered, an error code of 1 will be returned. If a state is set for a sensor which has been deselected (DS_Select function), an error code of 2 will be returned, otherwise a value of zero is returned.

DS_Abled returns zero if the sensor is enabled, 1 if it is disabled, and –1 if it is deselected. It returns an error code of –2 if the sensor number is invalid.

Sensor Designation for DS_EnAble and DS_Abled

Sensor Number	Sensor Name
0	No Sensor
1	O_2 Saturation Derived Pulse Rate
2	ECG Derived Pulse Rate
3	Tonometer Derived Pulse Rate
4	O_2 Saturation
5	Tonometer Systolic BP
6	Tonometer Diastolic BP
7	A-Line Systolic BP
8	A-Line Diastolic BP
9	End-tidal CO_2
10	Respiration Rate

10.3.16 DS_SetCritical and DS_GetCritical

void DS_SetCritical(int fCritical[7]);

void DS_GetCritical(int fCritical[7]);

These functions determine which diagnoses are considered critical and which are considered normal. A "critical diagnosis" tolerates no instability. If a patient with a critical diagnosis becomes unstable, medical attention must immediately be summoned. Each of the seven array elements is a flag. A one in a flag position sets/indicates that diagnosis is critical, a

zero sets/indicates that diagnosis is non-critical. The Set function sets the flags, the Get function reads the flags. Diagnostic code numbers are listed below the DS_Init function description.

Two critical diagnoses are hardwired into the code: head injury and pneumothorax. The function DS_Init checks for the existence of the file *DefaultPath*\DS_DIR\CRITICAL.DAT. If that file exists and is readable, the set of critical diagnoses is cleared. CRITICAL.DAT is a simple ASCII file. Each line contains the code of a diagnostic condition (using the same codes as DS_Set/GetCritical). All diagnostic conditions listed will be considered critical diagnoses.